北京大学, 2008年4月11日

Density Functional Theory and its Applications I

王恩哥

中国科学院物理所

Density Functional Theory

Ab initio

First Principles

Material properties

$$\{Z_\mu, \vec{R}_\mu\} \rightarrow P = P(\{Z_\mu, \vec{R}_\mu\})$$

is a function of atom type and position.

$\mu = 1, ..., 10^{23}$
$Z_\mu = 1, ..., 94$
$\vec{R}_\mu \in R^3$

Infinite degree of freedom !

Energy Function

$$E = E(\{Z_\mu, \vec{R}_\mu\})$$

Ground States

$$E(\{Z_\mu, \vec{R}_\mu\}_0) = \min E(\{Z_\mu, \vec{R}_\mu\})$$

Low Excitation States

$$E(\{Z_\mu, \vec{R}_\mu\}_L) < E(\{Z_\mu, \vec{R}_\mu\}_0) + \Delta$$

Motion of Atoms - Newton's Law

$$\frac{d^2\vec{R}_\mu}{dt^2} = -\frac{1}{M_\mu}\frac{\partial E(\{Z_\mu, \vec{R}_\mu\})}{\partial \vec{R}_\mu}$$

Atomic motion dt = 10^{-15} second versus

Material life = 3600*24*365*100=3 $\times$ 10^9 seconds

Infinite time span !

Challenges

Precise and explicit energy function $E(\{Z_\mu, \vec{R}_\mu\})$?

Minimize $E(\{Z_\mu, \vec{R}_\mu\})$ over infinite degree of freedom ?

Integrate the motion of atoms over infinite time span ?

Expressions of specified properties $P = P(\{Z_\mu, \vec{R}_\mu\})$?

Challenge

Connection of atomistic and macroscopic scales

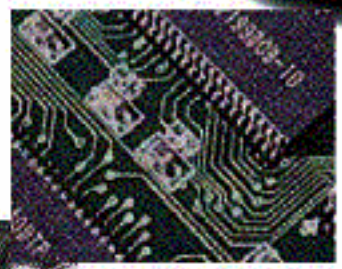

MACRO

10^{0}m, 10^{8}s

MICROSTRUCTURE

10^{-6}m, 10^{0}s

10 nm

ATOMS

10^{-9}m, 10^{-12}s

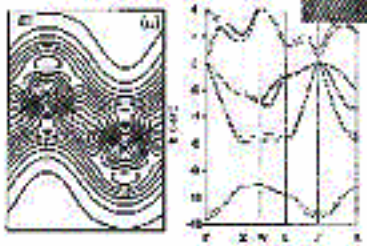

ELECTRONS

10^{-10}m, 10^{-15}s

Quantum Mechanical Energy Functional – First Principles Approach

Variables: $Z_\mu, \vec{R}_\mu, \psi(\{\vec{r}_i\}) \quad i = 1, 2, ... \sum_\mu Z_\mu$

$\rho(\vec{r}) = \sum_i \delta(\vec{r} - \vec{r}_i)|\psi(\{\vec{r}_i\})|^2$

$$
\begin{aligned}
&E(\{Z_\mu, \vec{R}_\mu\}, \psi(\{\vec{r}_i\}) \\
&\quad = -\frac{1}{2}\sum_i \int d\{\vec{r}_i\}|\nabla_i \psi(\{\vec{r}_i\})|^2 && : \text{Kinetic energy} \\
&\quad - \sum_\mu \int d\vec{r}\frac{\rho(\vec{r})Z_\mu}{|\vec{r}-\vec{R}_\mu|} + \frac{1}{2}\sum_{\mu\nu}\frac{Z_\mu Z_\nu}{|\vec{R}_\mu - \vec{R}_\nu|} && : \text{Z-e and Z-Z Coulomb} \\
&\quad + \frac{1}{2}\sum_{ij}\int d\{\vec{r}_i\}\frac{\psi^*(\{\vec{r}_i\})\psi(\{\vec{r}_i\})}{|\vec{r}_i - \vec{r}_j|} && : \text{e-e interaction}
\end{aligned}
$$

Energy depends on MANY-BODY electron wavefunction.

Early Optimistic Prediction

P.A.M.Dirac 1928:

Quantum mechanics will make chemistry merely a branch of computation mathematics.

Hartree Approximation

$$\psi(\{\vec{r}_i\}) = \Pi\psi_{l_i}(\vec{r}_i) \qquad : i = 1, 2, ... \sum_\mu Z_\mu$$

$$\rho(\vec{r}) = \sum_i \delta(\vec{r} - \vec{r}_i)|\psi(\{\vec{r}_i\})|^2 = \sum_l |\psi_l(\vec{r})|^2$$

$$E(\{Z_\mu, \vec{R}_\mu\}, \{\psi_l(\vec{r})\})$$

$$= -\frac{1}{2}\sum_l \int d\vec{r}|\nabla\psi_l(\vec{r})|^2 \qquad : \text{Kinetic energy}$$

$$-\sum_\mu \int d\vec{r}\frac{\rho(\vec{r})Z_\mu}{|\vec{r}-\vec{R}_\mu|} + \frac{1}{2}\sum_{\mu\nu}\frac{Z_\mu Z_\nu}{|\vec{R}_\mu - \vec{R}_\nu|} \qquad : \text{Z-e and Z-Z Coulomb}$$

$$+\frac{1}{2}\int d\vec{r}d\vec{r}'\frac{\rho(\vec{r})\rho(\vec{r}')}{|\vec{r}-\vec{r}'|} \qquad : \text{e-e Coulomb}$$

Wavefunctions independent; but E depends on $\rho(\vec{r})$.

Minimization: Independent Particle Equation

$$H = -\nabla^2 + V_c(\vec{r})$$

$$: \; V_c(\vec{r}) = -\sum_{\mu} \frac{Z_\mu}{|\vec{r}-\vec{R}_\mu|} + \int d\vec{r'} \frac{\rho(|\vec{r}-\vec{r'}|)}{|\vec{r}-\vec{r'}|}$$

$$H\psi_n(\vec{r}) = \epsilon_n \psi_n(\vec{r}) \quad \text{:Equation}$$

$$\psi_n(\vec{r}) = \sum_i \phi_i(\vec{r}) c_{in} \quad \text{:basis expansion}$$

$$\sum_j H_{ij} c_{jn} = E_n \sum_j S_{ij} c_{jn} \quad \text{:matrix eigen-problem}$$

$$H_{ij} = < \phi_i | H | \phi_j > \qquad S_{ij} = < \phi_i | \phi_j >$$

Self-consistency of $\rho(\vec{r})$ by Iterations

$$
\begin{array}{ccc}
 & & \text{Initial } \rho(\vec{r}) \\
 & & \downarrow \\
- \; -- \; \rightarrow \; -- & & \text{Input } \rho(\vec{r}) \\
\uparrow & & \downarrow \\
| & & \text{Minimization wrt each } \psi_l(\vec{r}) \\
| & & \downarrow \\
\uparrow & & \text{Output } \rho(\vec{r}) = \Sigma \left|\psi_l(\vec{r})\right|^2 \\
| & & \downarrow \\
| & & \text{If Output} = \text{Input}, \rightarrow \text{Physics} \\
\uparrow & & \downarrow \\
- \; -- \; \leftarrow \; -- & & \text{Input for next iteration}
\end{array}
$$

Hartree-Fock Approximation

$$\psi(\{\vec{r}_i\}) = \Delta(\{\psi_{l_i}\}, \{\vec{r}_i\}) \qquad : \text{Slater determinant}$$

$$\rho(\vec{r}) = \sum_l |\psi_l(\vec{r})|^2$$

$$E(\{Z_\mu, \vec{R}_\mu\}, \{\psi_l(\vec{r})\})$$

$$= -\frac{1}{2}\sum_l \int d\vec{r} |\nabla\psi_l(\vec{r})|^2 \qquad : \text{Kinetic energy}$$

$$-\sum_\mu \int d\vec{r} \frac{\rho(\vec{r}) Z_\mu}{|\vec{r}-\vec{R}_\mu|} + \frac{1}{2}\sum_{\mu\nu} \frac{Z_\mu Z_\nu}{|\vec{R}_\mu - \vec{R}_\nu|} \qquad : \text{Z-e and Z-Z Coulomb}$$

$$+\frac{1}{2}\int d\vec{r}\rho(\vec{r})V_c(\vec{r}) \qquad : \text{e-e} \quad V_c(\vec{r}) = \int d\vec{r}' \frac{\rho(\vec{r}')}{|\vec{r}-\vec{r}'|}$$

$$-\frac{1}{2}\sum_{lm} \int d\vec{r} d\vec{r}' \frac{\psi_l^*(\vec{r})\psi_m^*(\vec{r}')\psi_l(\vec{r}')\psi_m(\vec{r})}{|\vec{r}-\vec{r}'|} \qquad : \text{e-e Exchange}$$

Exchange makes wavefunctions NOT independent.

Exchange Energy in Slater Approximation

$$\psi_k(\vec{r}) = \frac{1}{\sqrt{V}} e^{i\vec{k}\cdot\vec{r}} \quad : \text{ Uniform electron gas}$$

$$-\frac{1}{2}\sum_{lm}\int d\vec{r}d\vec{r}'\frac{\psi_l^*(\vec{r})\psi_m^*(\vec{r}')\psi_l(\vec{r}')\psi_m(\vec{r})}{|\vec{r}-\vec{r}'|} \quad : \text{ Exchange energy}$$

$$= -\frac{3}{4}\left(\frac{6}{\pi}\right)^{1/3} V \sum_{\sigma} \rho_\sigma^{4/3}$$

Cautious Conclusion

F. Seitz, 1940:

To calculate the cohesive energy of all elemental crystals from the first principles is a difficult task, which may not be furnished forever.

Theorems of Density Functional Theory (DFT)

P. Hohenberg and W. Kohn, PR **136**, B864 (1964)

Theorem 1. For an arbitrary non-uniform electron system, all ground state properties are uniquely determined by its electron density, e.g., its total energy could be expressed as an unique functional of electron density, i.e.,

$$E = E(\{\rho(\vec{r})\})$$

Proof: if there are two systems, $H = T + U + V$, and $H' = T + U + V'$ with different ground state wavefunction ψ and ψ', but the same ground state electron density $\rho(\vec{r})$. So

$$E = <\psi|H|\psi> \quad < \quad <\psi'|H|\psi'> = E' + \int d\vec{r}(V - V')\rho$$

We have also

$$E' = <\psi'|H'|\psi'> \quad < \quad <\psi|H'|\psi> = E + \int d\vec{r}(V' - V)\rho$$

Add them together

$$E + E' \ < \ E' + E$$

Theorems of Density Functional Theory (DFT)

P. Hohenberg and W. Kohn, PR **136**, B864 (1964)

Theorem 2. Electron density at ground state of system $(T + U + V)$ gives minimum of energy functional

$$E_V[\rho(\vec{r})] = \int d\vec{r} V \rho + F[\rho(\vec{r})]$$

Proof: If there is another $\rho'(\vec{r})$, which corresponds to wavefunction $\psi'(\vec{r})$, so

$$\begin{aligned} E_V[\rho'] &= \int d\vec{r} V \rho' + F[\rho'] \\ &= \ < \psi' | T + U + V | \psi' > \\ &> \ < \psi | T + U + V | \psi > \\ &= \int d\vec{r} V \rho + F[\rho] \\ &= E_V[\rho] \end{aligned}$$

Quantum Energy Functional in DFT

W. Kohn and L. J. Sham, Phys. Rev. **140**, A1133 (1965)

$$\rho(\vec{r}) = \sum_i |\psi_i(\vec{r})|^2 \qquad : i = 1, 2, \ldots \sum_\mu Z_\mu$$

$$\begin{aligned}
&E(\{Z_\mu, \vec{R}_\mu\}, \{\rho(\vec{r})\}) \\
&= -\frac{1}{2}\sum_i \int d\vec{r} |\nabla\psi_i(\vec{r})|^2 && : \text{Kinetic energy} \\
&- \sum_\mu \int d\vec{r} \frac{\rho(\vec{r}) Z_\mu}{|\vec{r}-\vec{R}_\mu|} + \frac{1}{2}\sum_{\mu\nu} \frac{Z_\mu Z_\nu}{|\vec{R}_\mu - \vec{R}_\nu|} && : \text{Z-e and Z-Z Coulomb} \\
&+ \frac{1}{2}\int d\vec{r}\rho(\vec{r}) V_C(\vec{r}) && : \text{e-e} \quad V_C(\vec{r}) = \int d\vec{r}' \frac{\rho(\vec{r}')}{|\vec{r}-\vec{r}'|} \\
&+ \int d\vec{r} E_{xc}[\rho(\vec{r})] && : \text{e-e Exchange-correlation}
\end{aligned}$$

Energy functional depends ONLY on $\rho(\vec{r})$.
Particle wavefunctions are independent.
Challenge: Explicit exchange-correlation functional

Quantum Energy Functional in DFT

W. Kohn and L. J. Sham, Phys. Rev. **140**, A1133 (1965)

$$\rho(\vec{r}) = \sum_i |\psi_i(\vec{r})|^2 \qquad : i = 1, 2, \ldots \sum_\mu Z_\mu$$

$$\begin{aligned}
&E(\{Z_\mu, \vec{R}_\mu\}, \{\rho(\vec{r})\}) \\
&= -\frac{1}{2}\sum_i \int d\vec{r} |\nabla\psi_i(\vec{r})|^2 && : \text{Kinetic energy} \\
&- \sum_\mu \int d\vec{r} \frac{\rho(\vec{r}) Z_\mu}{|\vec{r}-\vec{R}_\mu|} + \frac{1}{2}\sum_{\mu\nu} \frac{Z_\mu Z_\nu}{|\vec{R}_\mu - \vec{R}_\nu|} && : \text{Z-e and Z-Z Coulomb} \\
&+ \frac{1}{2}\int d\vec{r}\rho(\vec{r}) V_c(\vec{r}) && : \text{e-e} \quad V_c(\vec{r}) = \int d\vec{r}' \frac{\rho(\vec{r}')}{|\vec{r}-\vec{r}'|} \\
&+ \int d\vec{r} E_{xc}[\rho(\vec{r})] && : \text{e-e Exchange-correlation}
\end{aligned}$$

Energy functional depends ONLY on $\rho(\vec{r})$.
Particle wavefunctions are independent.
Challenge: Explicit exchange-correlation functional

Kohn-Sham Local Density Approximation (LDA)

W. Kohn and L. J. Sham, Phys. Rev. **140**, A1133 (1965)

Local Density Approximation (LDA): Approximating exchange and correlation energy functional of non-uniform electron system by energy function of UNIFORM electron gas, $\bar{E}_{xc}(\rho)$

$$E_{xc}[\rho(\vec{r})] = E_{xc}(\vec{r}) = \bar{E}_{xc}(\rho = \rho(\vec{r}))$$

Exchange and correlation,

$$\psi(\{\vec{r}_i\}) = \Delta(\{\psi_{l_{i+}}\}, \{\vec{r}_{i+}\}) \times \Delta(\{\psi_{l_{i-}}\}, \{\vec{r}_{i-}\})$$

with mutual correlation between orbitals of two spins.

Ground State Energy of Uniform Electron Gas

'Solid State Theory', Li Zhen-Zhong, Ch.4

In Rydberg unit,

$$E_{xc} = \rho[-\frac{0.916}{r_s} - 0.094 + 0.062 lnr_s + O(r_s lnr_s)]$$

$$r_s = (\frac{4\pi\rho}{3})^{-1/3}$$

Parametrization of E_{xc} ($V_{xc} = \partial E_{xc}/\partial\rho$)

L. Hedin and B. Lundqvist (1971)

U. von Barth and L. Hedin, J. Phys. C5, 1629 (1972)

$$V_{xc}^{\pm} = -(\tfrac{3}{\pi}\rho)^{1/3}[A(\rho) \pm \tfrac{\rho^{+}-\rho^{-}}{3\rho} B(\rho)]$$

$$A(\rho) = 1 + C_p z ln(1 + 1/z)$$

$$B(\rho) = 1 + \frac{C_p}{2\times 2^{4/3}} z ln(1 + 2^{4/3}/z)$$

$$z = r_s/21.0 \quad \text{and} \quad C_p = 0.045$$

Theory


M. Planck


Louis de Broglie


E. Schrödinger


P. A. M. Dirac


D. Hartree


W. Kohn


J. Pople

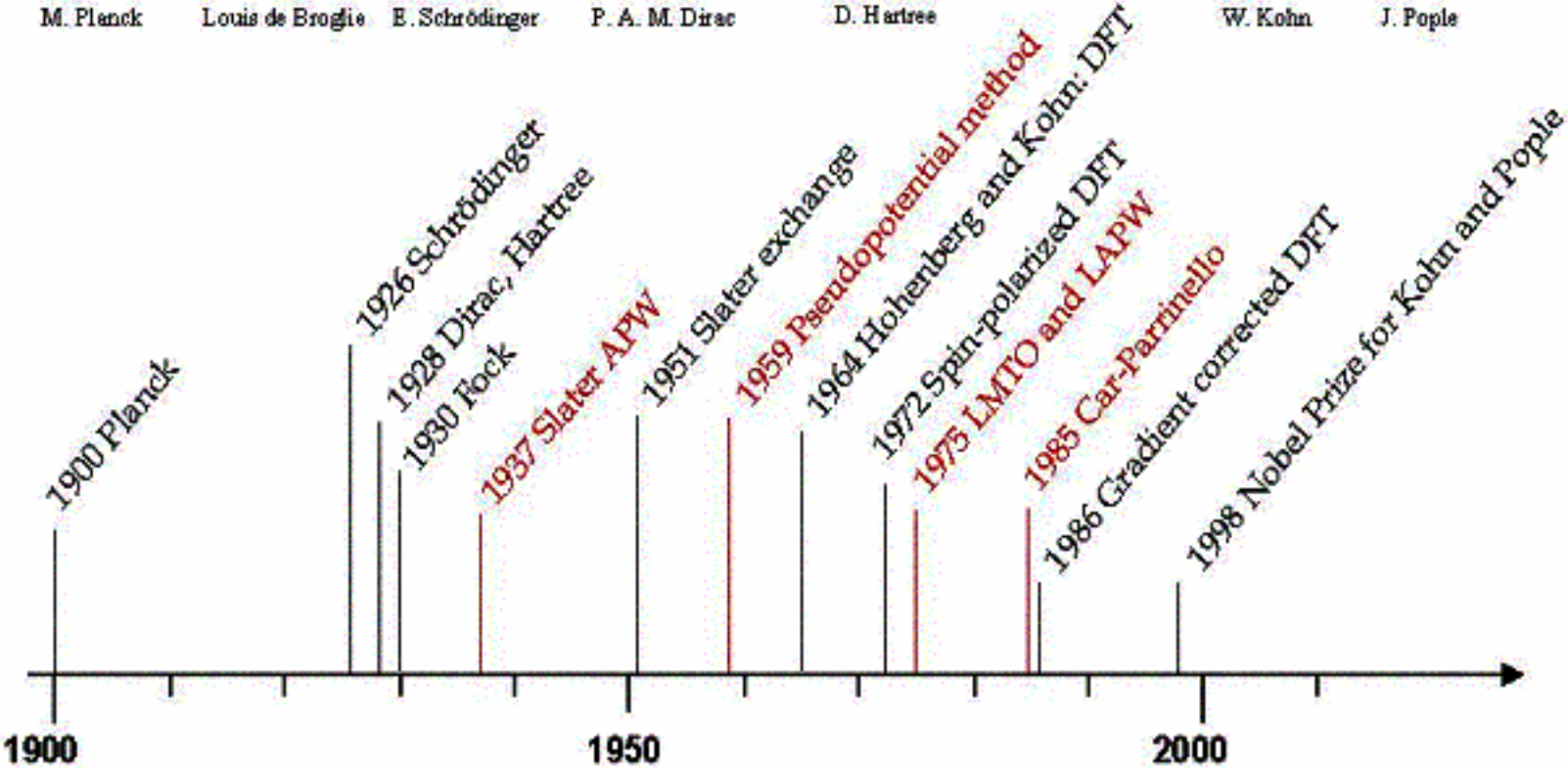

DFT Implementations

- self-consistent
- Harris functional
- all-electron full potential
- all-electron muffin-tin
- pseudopotential
- jellium
- beyond LDA
  - GW
  - model GW
  - sX-LDA
  - time-dependent DFT
  - optimized effective potentials (OEP)
  - LDA+U
  - self-interaction corrections (SIC)
- generalized gradient approximations (GGA)
- local density approximation (LDA)
- fully-relativistic
- semi-relativistic
- non-relativistic

$$\left[-\tfrac{1}{2}\nabla^2 + V(\mathbf{r}) + \mu_{xc}(\mathbf{r})\right]\psi_i^k = \varepsilon_i^k\,\psi_i^k$$

- non-periodic
- periodic
- symmetry
- non-spin-polarized
- spin-polarized
- atomic orbitals
  - Gaussians (GTO)
  - Slater type (STO)
  - numerical (DMol)
- plane waves
- augmentation
  - plane waves (FLAPW)
  - spherical waves (LMTO, ASW)
- fully numerical

Radial Electron Density of Atoms by LDA Calculation

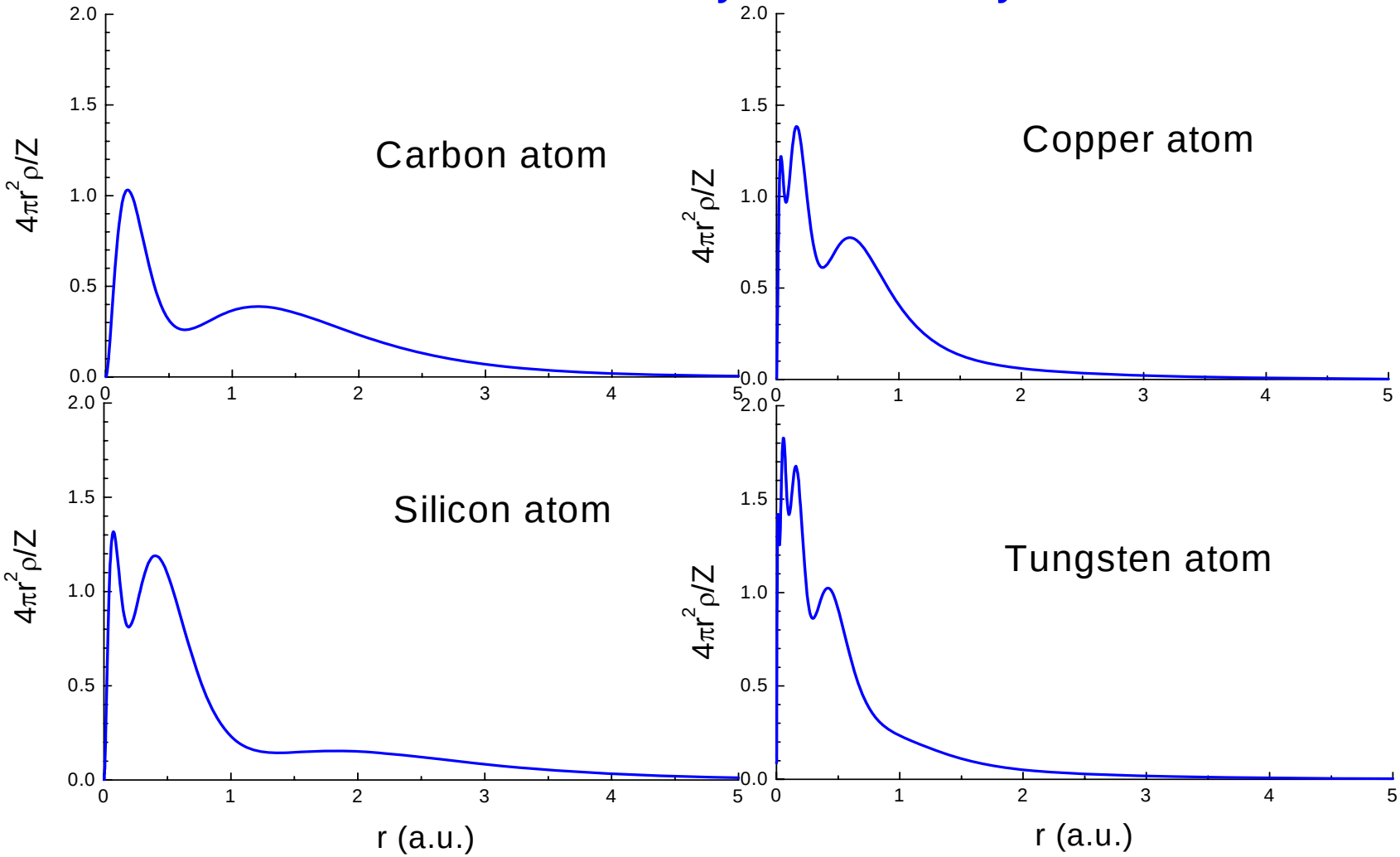

DFT Results of Molecule Bond Strength

		Atomization Energy (eV)			
Molecules	Bonds	Hartree-Fock	LSD	GGA	Experiment
H_2	1	3.63	4.89	4.55	4.75
C_2 (AF)	1	0.73	7.51	6.55	6.36
C_2H_2	3	13.00	20.02	18.09	17.69
C_2H_4	5	18.71	27.51	24.92	24.65
C_2H_6	7	24.16	34.48	31.24	31.22
C_6H_6	12	45.19	68.42	61.34	59.67
rms error/bond		2.40	0.68	0.13	

J.P.Perdew et al, Phys. Rev. B46, 6671 (1992)

Crystal Electronic Structure:

Isolated Atom: spherical symmetry reduces 3D to 1D

Crystal: translational symmetry

$$H(\vec{r}) = H(\vec{r} + \vec{T})$$

leads to Bloch theorem

$$\psi_l(\vec{r}) = \psi_{\vec{k}n}(\vec{r}) = e^{-i\vec{k}\cdot\vec{r}} u_{\vec{k}n}(\vec{r})$$

with translational periodic

$$u_{\vec{k}n}(\vec{r}) = u_{\vec{k}n}(\vec{r} + \vec{T})$$

Bloch theorem reduces infinite degrees of freedom to integration over Brillouin zone

Hard Core in Crystals

Bond length is about 1.4 - 4 Åfor all materials

Element	1s Diameter (Å)	Bond Length (Å)	Bond/Core
C	0.50	1.54	3.1
Si	0.20	2.35	11.8
Cu	0.093	2.56	27.5
W	0.032	2.74	85.6

Core is about 5 to 100 times smaller than bond length.

$(5\text{-}100)^3$ times denser mesh if describing 1s core properly.

Planewave Basis

The periodic function u is expanded as

$$u_{\vec{k}n}(\vec{r}) = \sum_G C_{\vec{k}n}(G)\phi_G(\vec{r})$$

by the planewave basis

$$\phi_{\vec{G}}(\vec{r}) = \frac{1}{\sqrt{V}} e^{-i\vec{G}\cdot\vec{r}}$$

Advantage: Basis is structureless and $\vec{k}$ independent.

Disadvantage: Large basis (>1000/atom) if including cores.

Scheme: 'Pseudopotentials that work from H to Pu'

G.B.Bachelet, D.R.Hamann, and M. Schluter, Phys. Rev. B26, 4199, 1982.

Atomic/Local Orbital Basis

The periodic function u is expanded

$$u_{\vec{k}n} = \sum_m C_{\vec{k}n}(m)\phi_{\vec{k}m}(\vec{r})$$

by atomic (Gaussian, MT etc) orbitals - LCAO (LCGO, MTO, etc)

$$\phi_{\vec{k}m}(\vec{r}) = \frac{1}{\sqrt{N}}\sum_\mu e^{-i\vec{k}\cdot(\vec{R}_\mu - \vec{r})}\phi_m(|\vec{r} - \vec{R}_\mu|)$$

Advantage: Minimum basis (10/atom) and exact cores.

Disadvantage: Basis depends on $\vec{k}$ and structure/potential, and approximation at far from nuclei.

Augmented Basis

The periodic function u is expanded

$$u_{\vec{k}n} = \sum_{\vec{G}} C_{\vec{k}n}(\vec{G})\phi_{\vec{G}}(\vec{r})$$

by atomic orbitals near atomic core, and augmented at region far from the cores. For example, augmented planewaves (APW) are, with $\vec{r}_\mu = \vec{r} - \vec{R}_\mu$),

$$\phi_{\vec{G}}(\vec{r}) = \begin{cases} \frac{1}{\sqrt{\Omega}} e^{-i\vec{G}\cdot\vec{r}} & \vec{r} \notin \text{MT} \\ \sum_L A_{L\mu}(\vec{G}) u_{l\mu}(|\vec{r}_\mu|) Y_L(\hat{\vec{r}}_\mu) & \vec{r} \in \text{MT}_\mu \end{cases}$$

Advantage: Acceptable basis ($<$ 100/atom) and exact over whole space.

Disadvantage: Basis depends on $\vec{k}$ and structure/potential.

Pseudopotential

- Frozen core approximation
- The valence electrons is important outside the core region.
- The nucleus and its core orbitals are replaced by a pseudo potential.

It should reproduce the exact valence orbitals outside the core region.

Schematic illustration of Pseudopotential

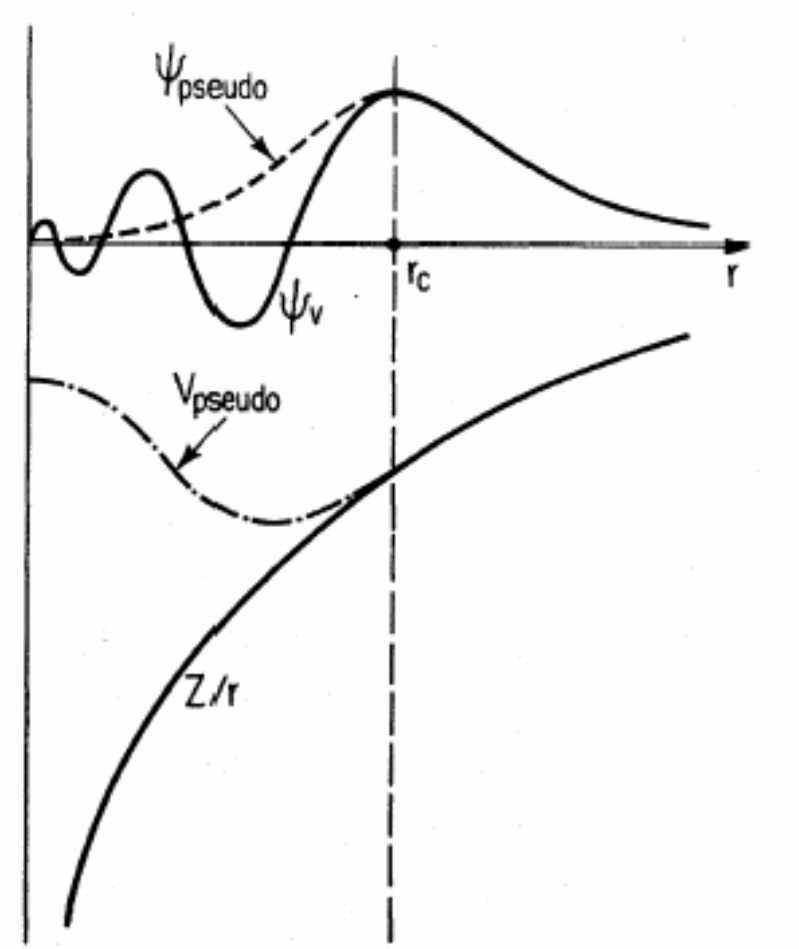

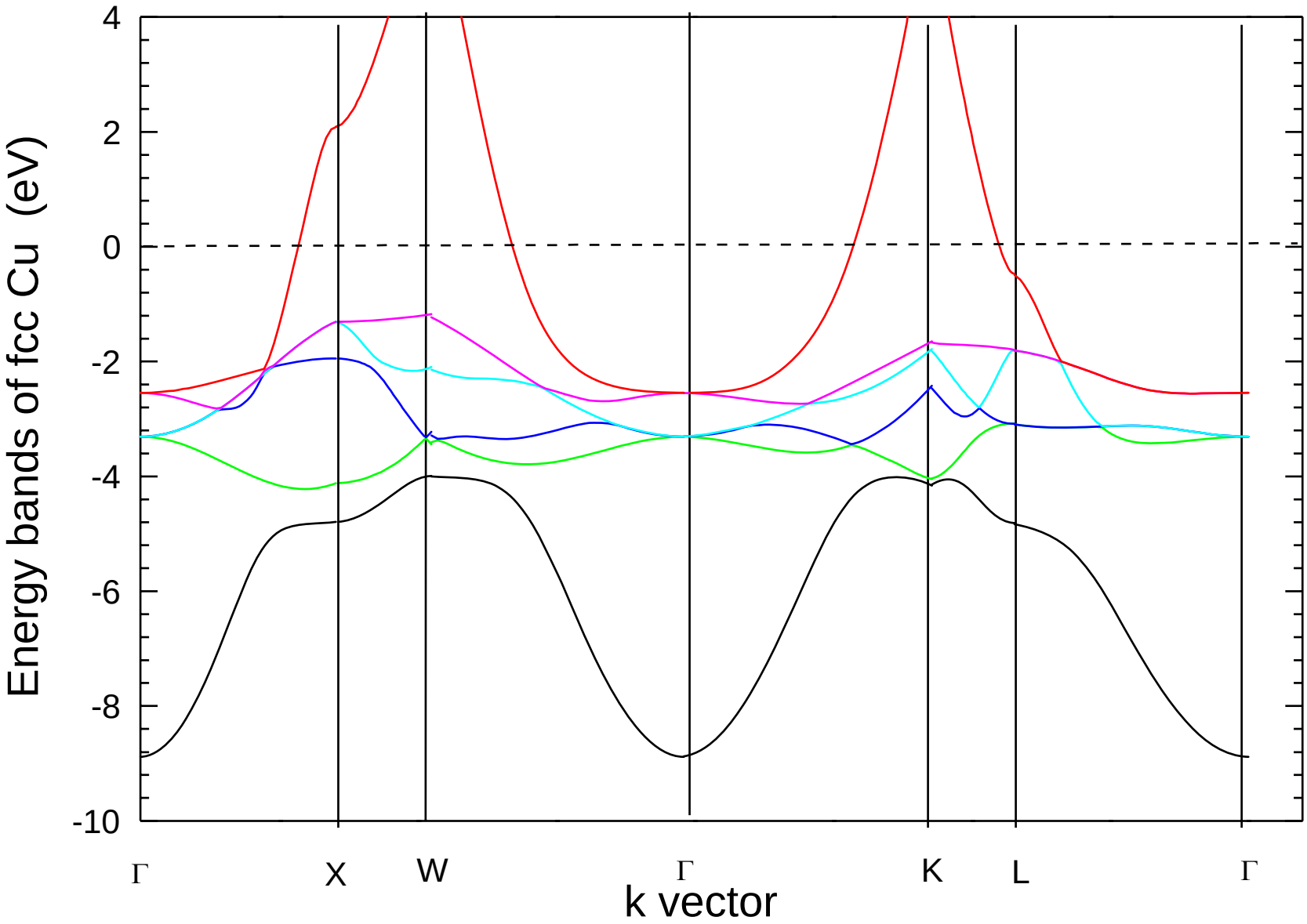
Energy bands of fcc Cu (eV)
4
2
0
-2
-4
-6
-8
-10
Γ
X
W
Γ
K
L
Γ
k vector

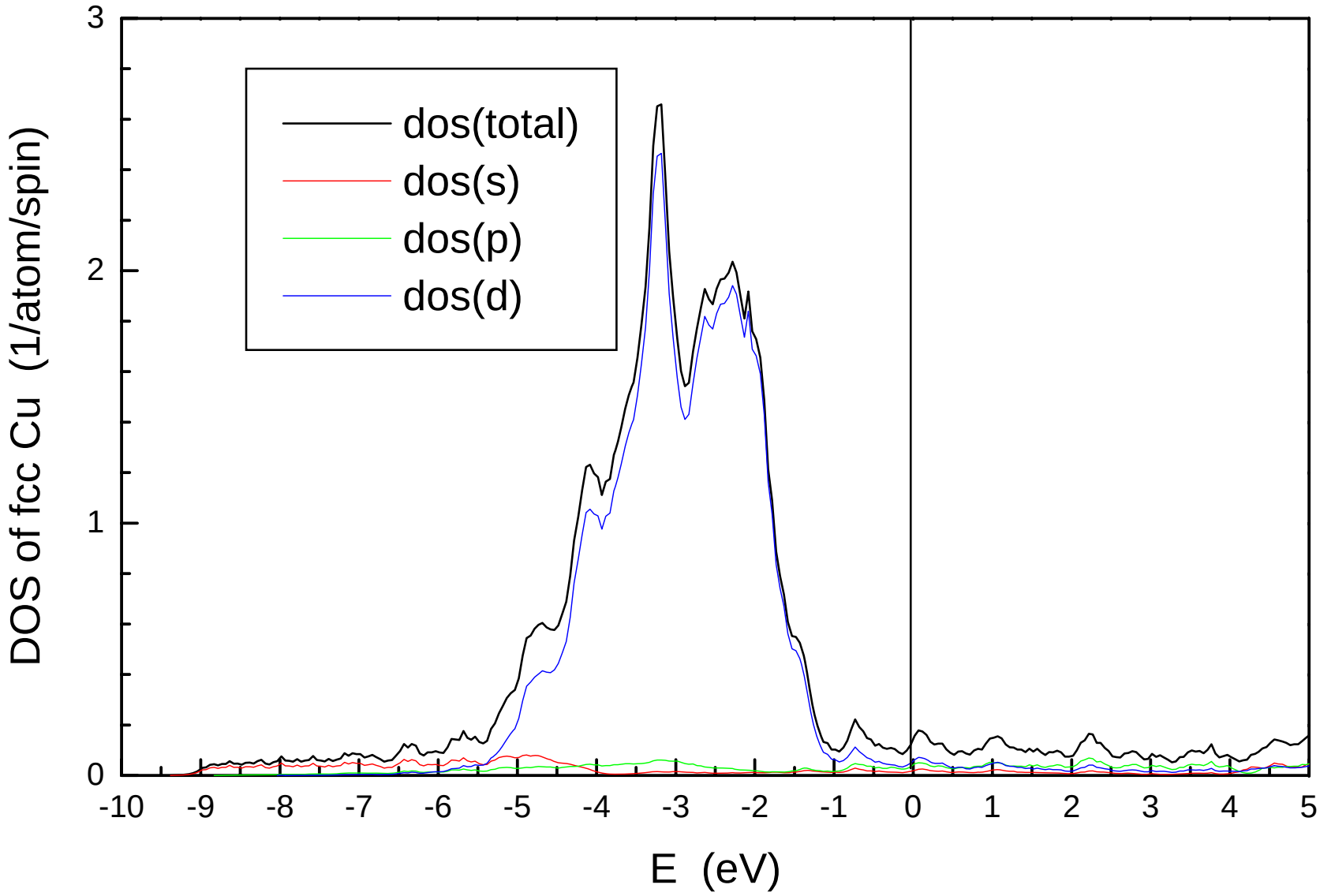
dos(total)
dos(s)
dos(p)
dos(d)
DOS of fcc Cu (1/atom/spin)
E (eV)
3
2
1
0
-10
-9
-8
-7
-6
-5
-4
-3
-2
-1
0
1
2
3
4
5

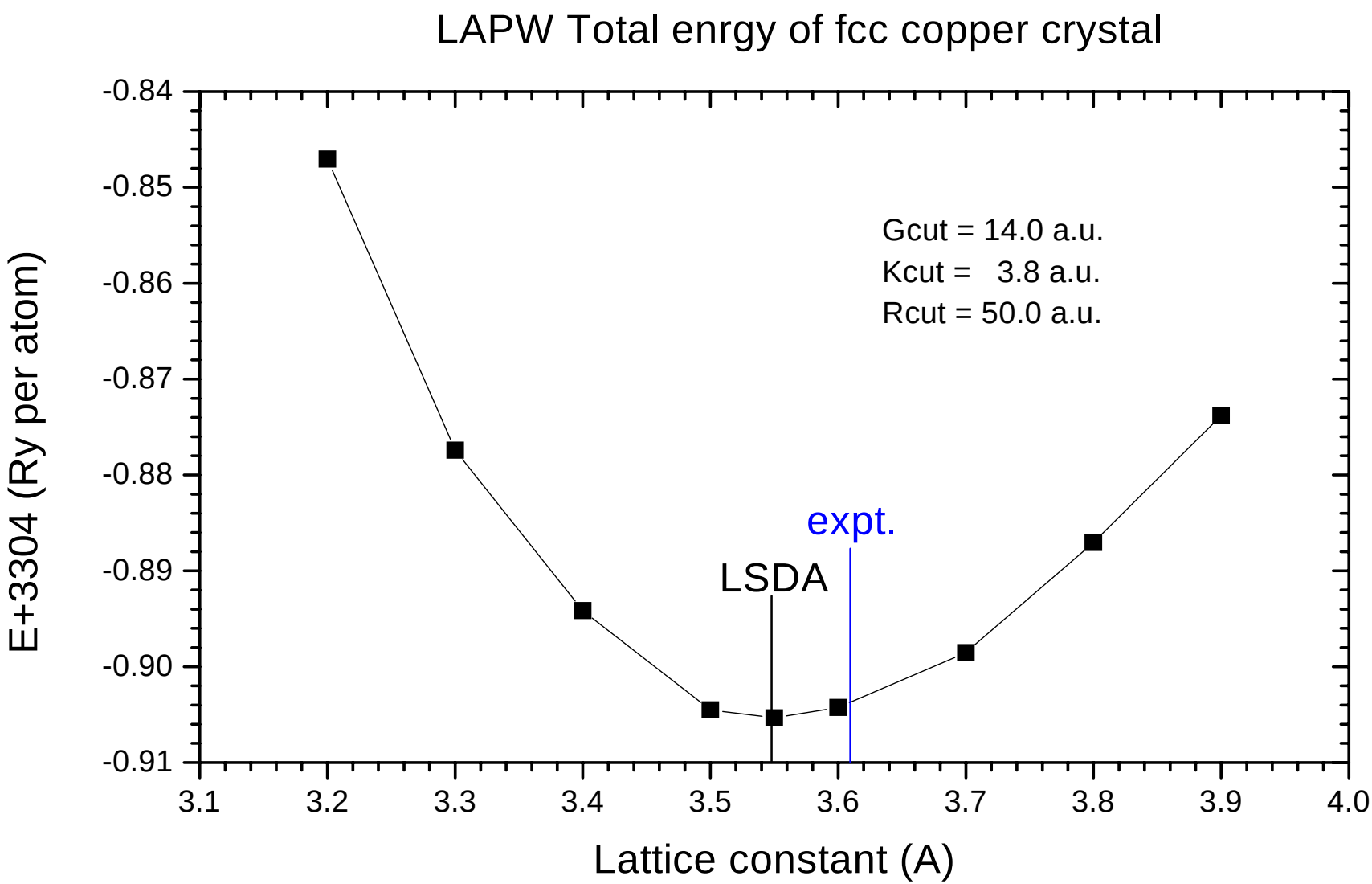
LAPW Total enrgy of fcc copper crystal
E+3304 (Ry per atom)
-0.84
-0.85
-0.86
-0.87
-0.88
-0.89
-0.90
-0.91
3.1
3.2
3.3
3.4
3.5
3.6
3.7
3.8
3.9
4.0
Lattice constant (A)
Gcut = 14.0 a.u.
Kcut = 3.8 a.u.
Rcut = 50.0 a.u.
expt.
LSDA

Joint Atomic/Electronic Energy Minimization

- Force Field Approach

$$
\begin{array}{lll}
 & \text{Initial } \{\ \vec{R}_\mu\ \},\ \rho(\vec{r}) & \\
 & \downarrow & \\
 & \text{Input } \{\ \vec{R}_\mu\ \},\ \rho(\vec{r}) - - \leftarrow & \vec{R}_\mu + \underline{\frac{1}{2}\frac{\vec{f}_\mu}{M_\mu}(\Delta t)^2} \\
| \rightarrow - & \downarrow & | \\
| & \text{min E wrt each } \psi_l(\vec{r}) & \uparrow \\
| & \text{Output } \rho(\vec{r}) = \Sigma\,|\psi_l(\vec{r})|^2 & \text{If } |\vec{f}_\mu| = 0 \quad \rightarrow \quad \text{Physics} \\
\uparrow & \downarrow & \uparrow \\
| & \text{If Output } \rho = \text{Input } \rho - \rightarrow & \text{Force Field } \vec{f}_\mu = -\frac{\partial E}{\partial \vec{R}_\mu} \\
\uparrow & \downarrow & \\
| \leftarrow - & \text{Input for next iteration} &
\end{array}
$$

Classical Molecular Dynamics - Newton's Law

$$L = \frac{1}{2}\sum_{\mu}\frac{1}{M_\mu}|\vec{p}_\mu|^2 - E(\{\vec{R}_\mu\}) \quad : \text{Lagrange}$$

$$\dot{\vec{R}}_\mu = \partial L/\partial\vec{p}_\mu = \frac{1}{M_\mu}\vec{p}_\mu \quad : \text{Canonical equation}$$

$$\dot{\vec{p}}_\mu = \partial L/\partial\vec{R}_\mu = -\partial E/\partial\vec{R}_\mu$$

$$M_\mu\frac{d^2\vec{R}_\mu}{dt^2} = -\frac{\partial E}{\partial\vec{R}_\mu} = \vec{f}_\mu \quad : \text{Newton's law}$$

First Principles Molecular Dynamics (CPMD)

R. Car and M. Parrinello, Phys. Rev. Lett 55, 2471 (1985)

Lagrange: $$L = \frac{1}{2}\sum_{\mu}\frac{1}{M_\mu}|\vec{p}_\mu|^2 - E(\{\vec{R}_\mu\},\{\psi_l(\vec{r})\}) + \frac{1}{2}\sum_i m_e|\dot{\psi}_l(\vec{r})|^2 + \sum_{ll'}\Lambda_{ll'}(\int d\vec{r}\psi_l^*(\vec{r})\psi_{l'}(\vec{r}) - \delta_{ll'})$$

Newton's law: $$M_\mu\frac{d^2\vec{R}_\mu}{dt^2} = -\frac{\partial E}{\partial \vec{R}_\mu} = \vec{f}_\mu$$

'Schrodinger' equation:

$$m_e d^2\psi_l(\vec{r})/dt^2 = -\partial E/\partial\psi_l(\vec{r}) + \sum_{ll'}\Lambda_{ll'}\psi_{l'}(\vec{r})$$
$$= \sum_{ll'}(- < \psi_l|H|\psi_{l'} > + \Lambda_{ll'})\psi_{l'}(\vec{r})$$

Joint Atomic/Electronic Energy Minimization

— First Principles Molecule Dynamics

$$
\begin{array}{lll}
 & & \text{Initial } \{\vec{R}_\mu\},\ \{\psi_l(\vec{r})\} \\
 & & \downarrow \\
|- & \rightarrow - & \text{Input } \{\vec{R}_\mu\},\ \{\psi_l(\vec{r})\} \\
| & & \rho(\vec{r}) = \Sigma\, |\psi_l(\vec{r})|^2 \\
| & & \vec{f}_\mu = -\dfrac{\partial E}{\partial \vec{R}_\mu}, \text{ and } H_{ll'} =< \psi_l|H|\psi_{l'} > \\
\uparrow & & \downarrow \\
| & & \text{If } \{\vec{f}_\mu\} = 0 \text{ and } H_{ll'} - \Lambda_{ll'} = 0, \quad \rightarrow \quad \text{Physics} \\
\uparrow & & \downarrow \\
| & & \vec{R}_\mu + \frac{1}{2M_\mu}(\Delta t)^2 \vec{f}_\mu \\
|- & \leftarrow - & \psi_l - \frac{1}{2m_e}(\Delta t)^2 \sum_{l'} (H_{ll'} - \Lambda_{ll'})\psi_{l'}
\end{array}
$$

DFT Application in Solid State Physics

1. Thermodynamic properties
   Cohesive energy, equilibrium structure
   Elastic moduli and phonon spectra
   Equation of state
   Molecular dynamics

2. Mechanical properties
   Energetics of finite strains
   Energetics in mechanical processes

DFT Application in Solid State Physics

1. Magnetism
   Moment, spin configuration, anisotropy
   Magnetic phase transition (T_C and T_N)
   Spin dynamics

2. Optical properties
   Energy (and density) of electron states
   Absorption spectra
   Linear and non-linear optical susceptibility
   Multi-photon absorption

Concluding Remarks

Precise and explicit energy function $E(\{Z_\mu, \vec{R}_\mu\})$ —

Direct extension, such as GGA, —
Atomic ionization energies: 0.1 eV within experiments
Bond energies: 0.13 eV/bond within experiments
Bond length: $\Delta a = 0.01$ Å

Orbital correlation still missing ?

Strong correlation doesn't treated properly ?

Concluding Remarks

Minimize $E(\{Z_\mu, \vec{R}_\mu\})$ over infinite degree of freedom —

If periodic, problem reduced by use of Bloch theorem.

Precise fast, $O(N)$, algorithm for intrinsic large system ?

Drop the electronic degrees of freedom properly ?

Concluding Remarks

Integrate the motion of atoms over infinitely long time span —

Accelerating algorithm, e.g., super-MD, exists with only limited success.

Dynamical vs statistical approaches ?

Concluding Remarks

Expressions for all properties $P = P(\{Z_\mu, \vec{R}_\mu\})$ —

Magnetic: orbital correlation, rare-earth elements, etc

Optical: band gap, spectra (excitation), etc

Structural: large scale systems, thermal behavior, etc

Post-LSDA era

- Accuracy: from physical to chemical, to bio
- System: type s-p-d to f
- System: size <100 to 100-10000 atoms
- System: few to statistical configurations
- Properties: ground to excited
- Properties: static to dynamics
- Properties: intrinsic to structure sensitive

Density functional theory

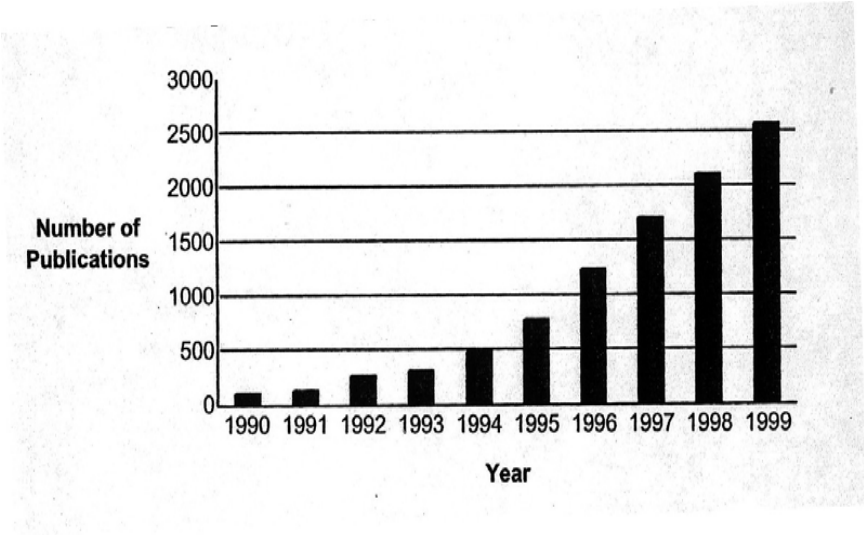

Axel D. Becke
10051
7539
1545

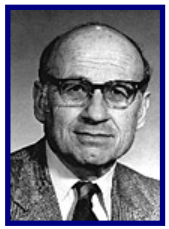

Walter Kohn (NP 1998)
9032
4116
1544

John P. Perdew
4643
3952
2541

What DFT can do

Some people applying DFT for real world problems

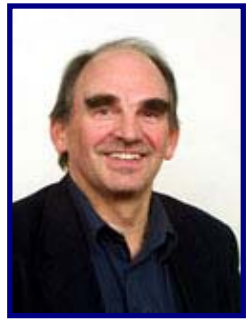

Bengt Lundqvist
Sweden
2381, 1856, 329
Materials
Surface theory

Michelle Parrinello
Italy - Switzerland
3192, 221, 205
Car-Parrinello Method;
Liquids and solutions;
Disordered materials.

Jens K. Norskov
Denmark
423, 289, 273
Surfaces;
Heterogeneous catalysis.

Georg Kresse
Austria
1145, 1103, 758
Liquids
Surfaces
Matallic systems

Matthias Scheffler
Germany
344, 259, 242
Surfaces;
First-principles Monte Carlo;
Heterogeneous catalysis.

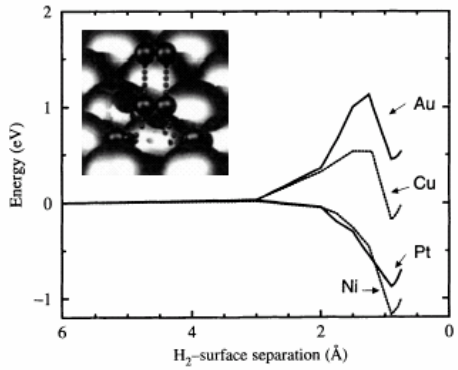

Why gold is the noblest of all metals?
B. Hammer and J. Norskov, Nature (1995);

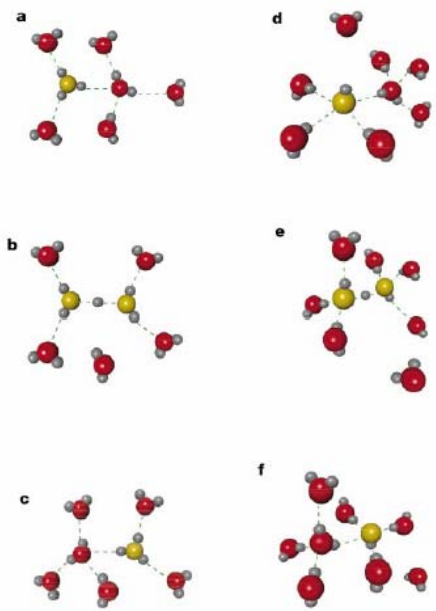

Diffusion of H30+ and OH- in water
M.E. Tuckerman et al, Nature (2002);

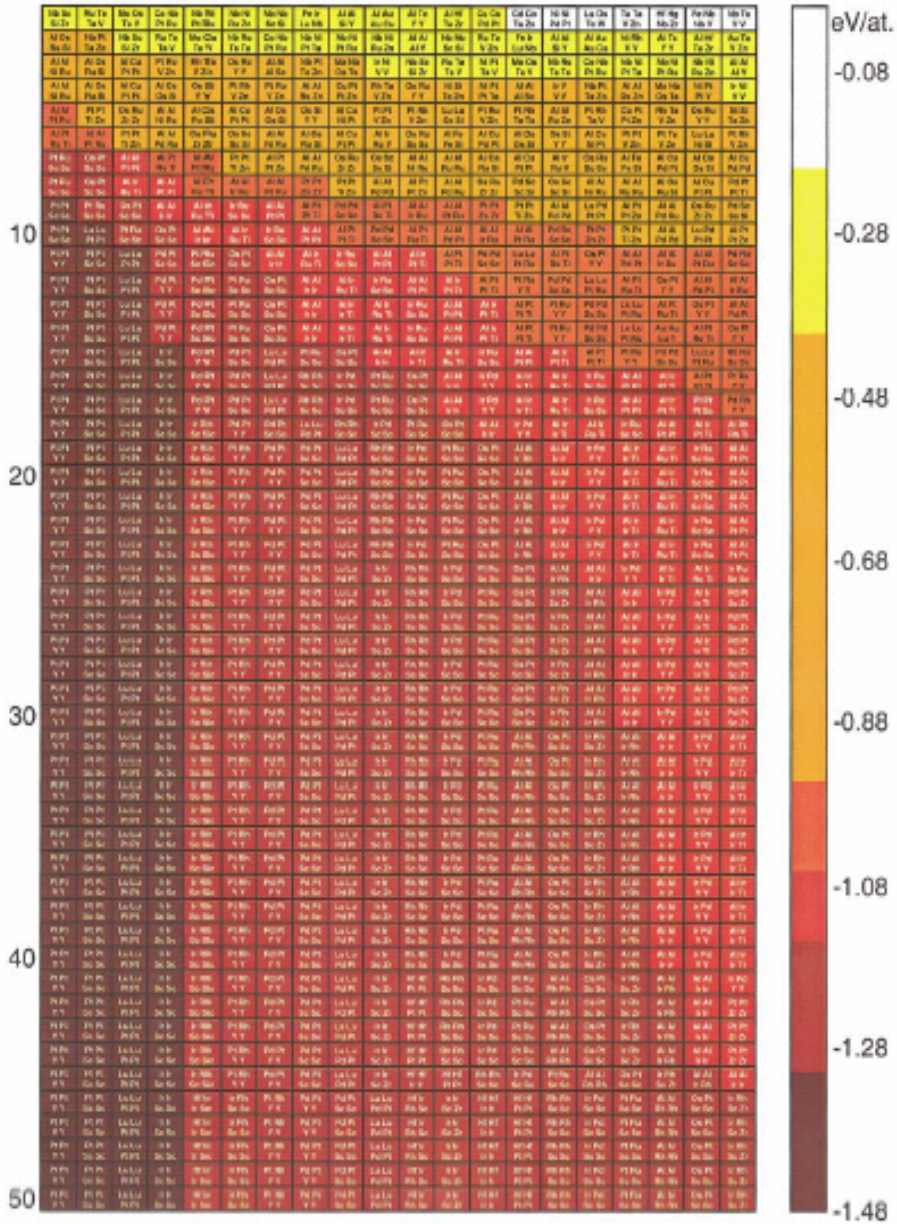

Search for the hardest material
G.H. Johanesson et al, PRL (2002);

Why noble metals are catalytically active?
W.X. Li et al., PRL (2003);

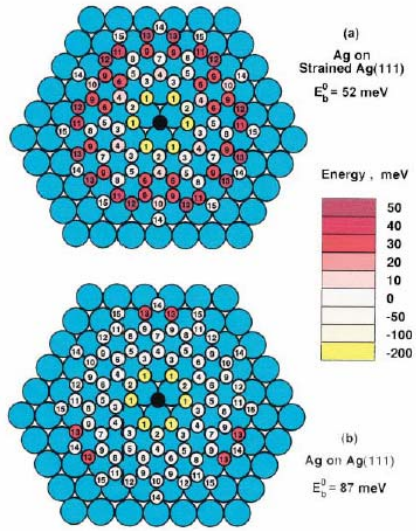

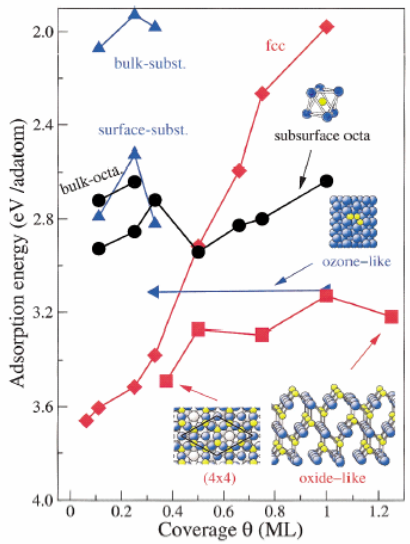

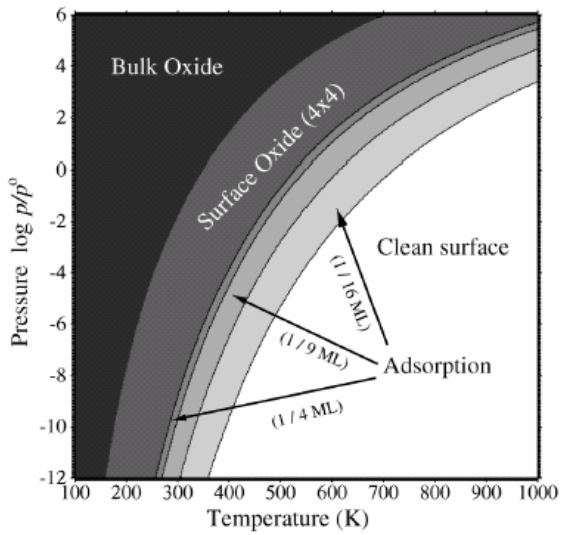

Long range interaction on surfaces
K. Fichthorn and M. Scheffler, PRL (2000);

Modifications

1. Free-energy density functional theory (Mermin)
2. Density matrix functional theory
3. Natural orbital functional theory (Geodecker & Umrigar)

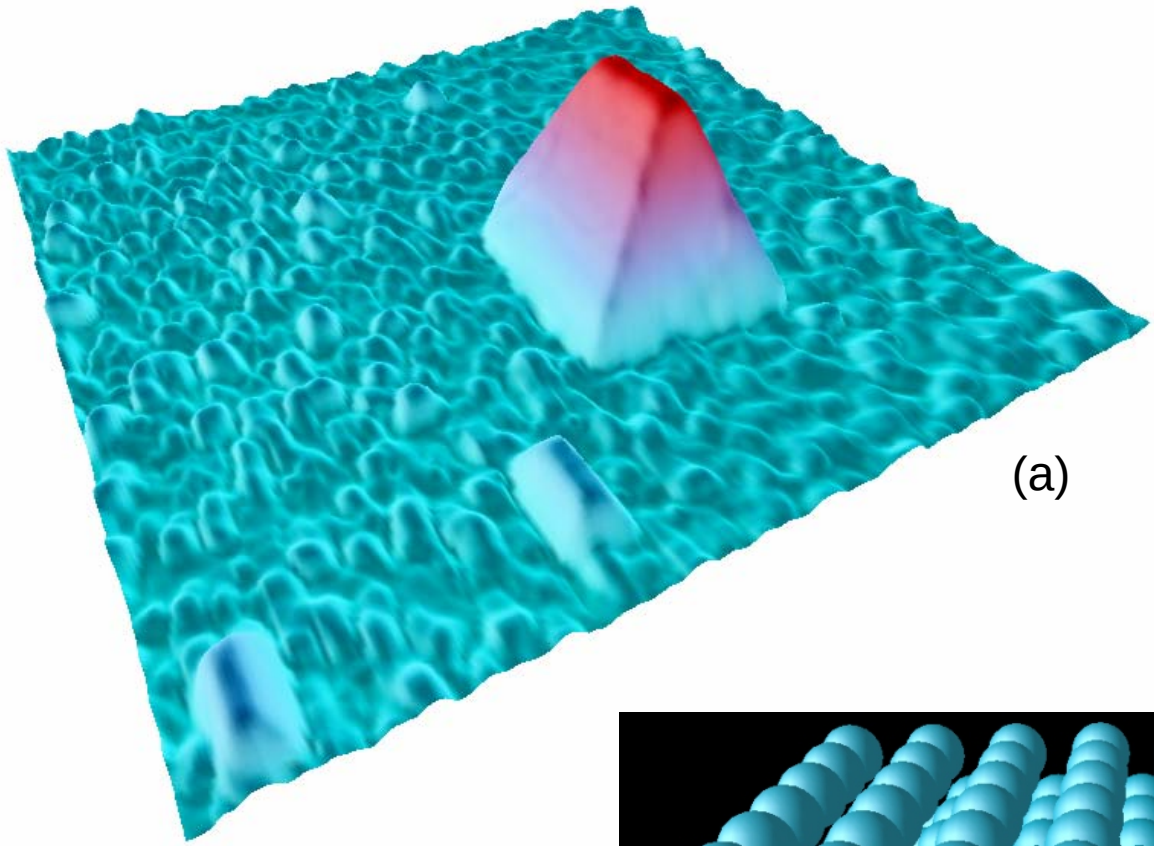

朱文光

Phys. Rev. Lett. 92, 106102(2004)
Phys. Rev. Lett. 91, 016102(2003)

Highlight
Phys. News Update 643, June 2003
Nature 429, 617(2004)

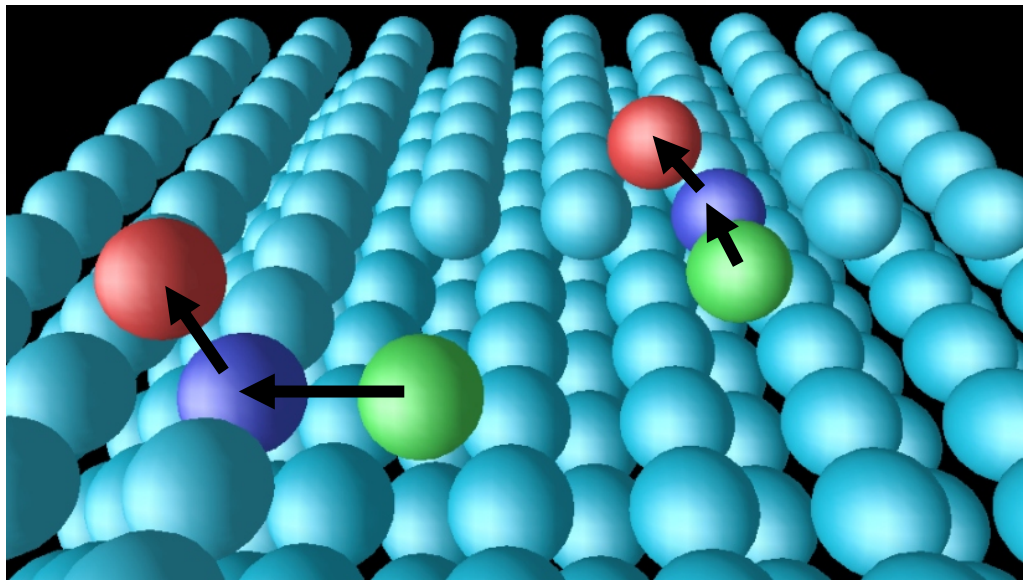

Wetting order

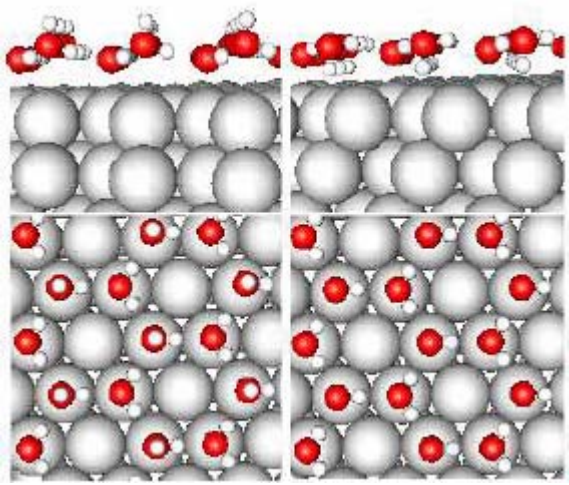

H-up H-down

孟 胜

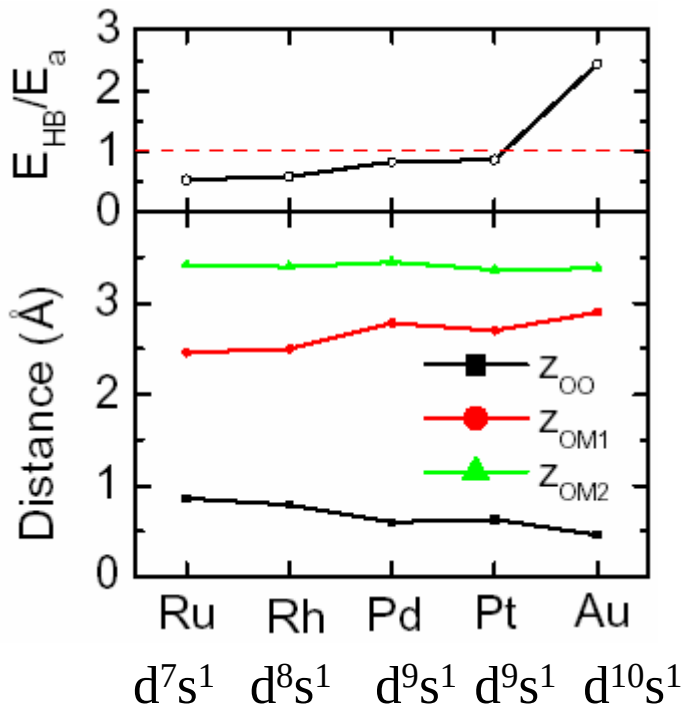

Wetting order:

Ru > Rh > Pd > Pt > Au

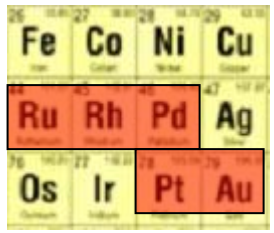

Phys. Rev. Lett. 89, 176104(2002); 91, 059602(2003)

Phys. Rev. B. 69, 195404(2004) ; *J. Chem. Phys.* 119, 7617(2003)

2D tessellation ice

杨健君

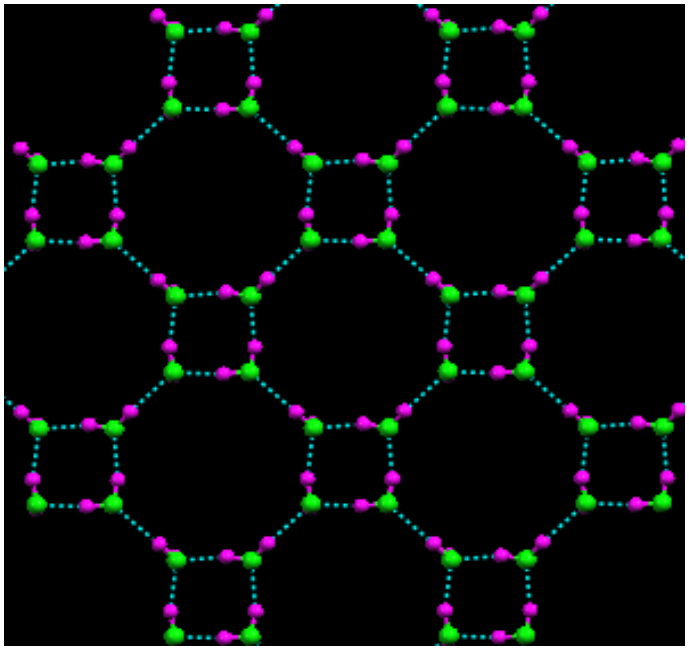

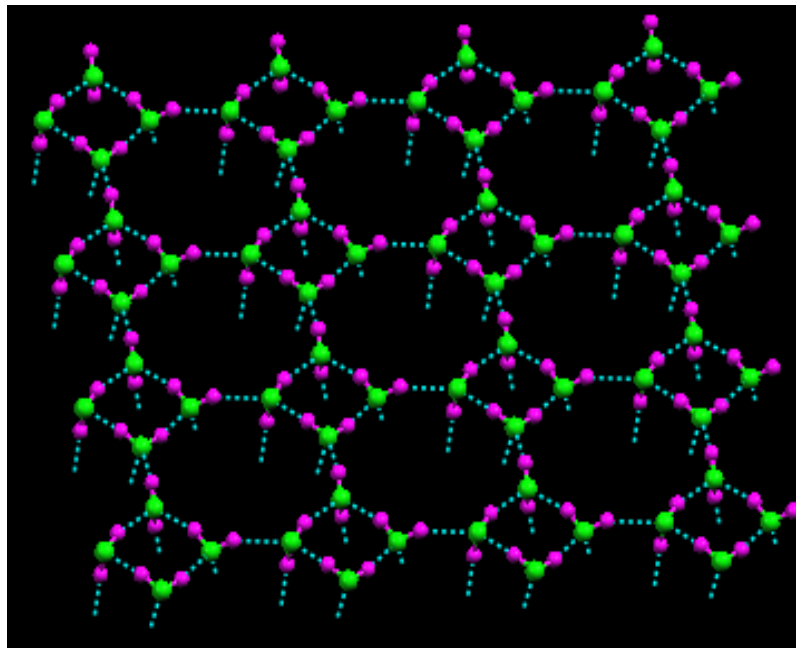

(110)

(110)

No free OH sticking out of the surface

Stable at 300K

Enge (E.G.) Wang's group in IOP/CAS, Beijing

(August, 2007)

Research in this group is focused on the study of the macroscopic property and microscopic behavior of surface-based nanostructures controlled by chemical and physical events. The approach is a combination of atomistic simulations and experiments. There are five staffs, E.G. Wang, Shuang Liu, Xuedong Bai, Wenlong Wang, and Wengang Lu. The areas of current interest include:

1) Novel formation and decay mechanism of nanostructures on surface;

2) Water in a confined condition, such as on surface, between interfaces, inside nanotube;

3) Covalently bonded light-element nanomaterials, such as the development of nanocones, polymerized carbon-nitrogen nanobells, aligned nanohelices and single-walled boron-carbon-nitrogen nanotubes.

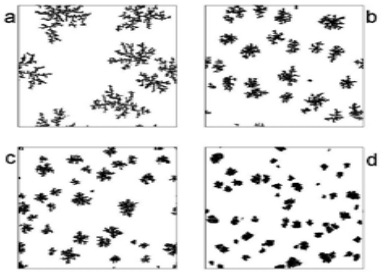

Surfactant-Mediated Epitaxy
Phys. Rev. Lett. (1999)
Phys. Rev. Lett. (2004)

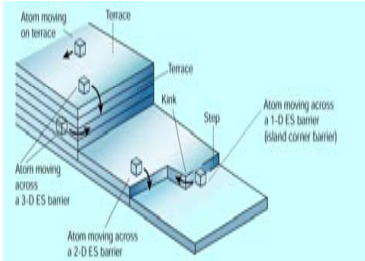

ES Barrier Controlled Growth
Phys. Rev. Lett. (2001)
Phys. Rev. Lett. (2002)
Science (2004)

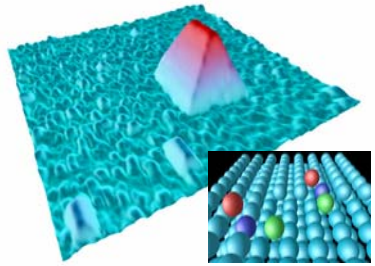

Adatom Upward Diffusion
Phys. Rev. Lett. (2003)
Phys. Rev. Lett. (2004)

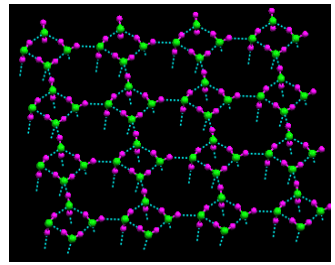

Ice Tessellation
Phys. Rev. Lett. (2004)
Phys. Rev. B (2005)

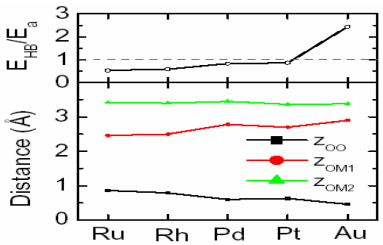

Hydrophilicity
J. Chem. Phys. (2003)
Phys. Rev. B (2004)
Phys. Rev. Lett. (2002)

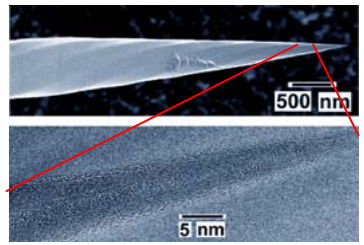

Nanocones
Science (2003)
Science (2004)
JACS (2006)

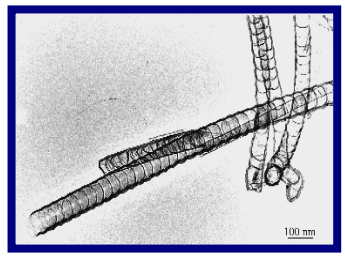

Nanobells
Appl. Phys. Lett. (1999)
Appl. Phys. Lett. (2000)
Appl. Phys. Lett. (2001)

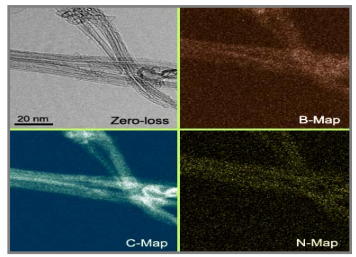

BCN SWNT
JACS (2006)
JACS (2007)

吴克辉 (Tohoku)

吴　静 (Maryland)

马旭村 (MPG)

郭建东(ORNL)

钟定永(Muenster)

李茂枝(Ames Lab)

张广宇 (Stanford)

支春义 (NIMS)

历建龙 (UT Austin)

肖文德 (EMPA)

许　智 (IoP)

朱文光 (Harvard)

张立新 (NREL)

孟　胜 (Harvard)

杨建君 (Saskatchewan)

于迎辉 (NIMS)

杨　勇 (Tohoku)

郑客飞 (Parma)

郭东辉 (Hokkaido)

江　颖 (UC Irvine)

北京大学, 2008年4月11日

Density Functional Theory and its Applications II

王恩哥

中国科学院物理所

A molecular view of water on surface

Outline

- Water adsorption on metal surface:
  Energetics and Kinetics
- Water adsorption on silica surface:
  Tessellation ice
- Hydrophilic and hydrophobic behavior
- Water interaction with NaCl:
  Adsorption, Dissolution and Nucleation

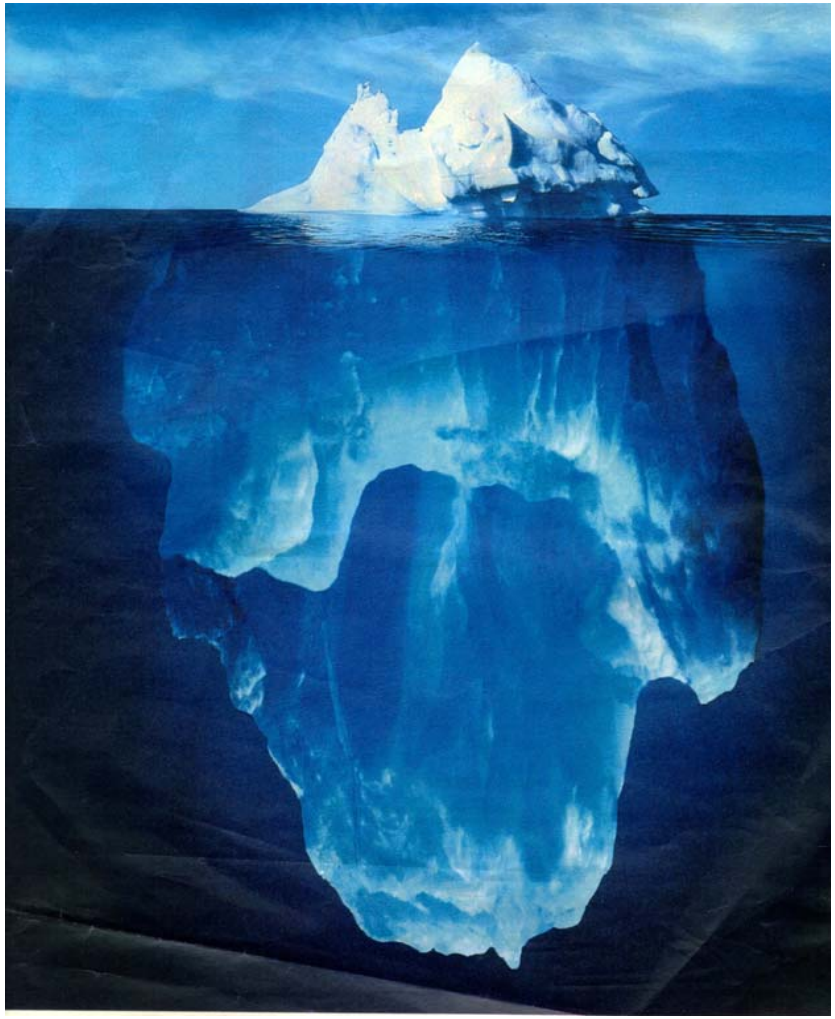

Exposed Water Ice Discovered near the South Pole of Mars

Timothy N. Titus,[1*] Hugh H. Kieffer,[1] Phillip R. Christensen[2]

The Mars Odyssey Thermal Emission Imaging System (THEMIS) has discovered water ice exposed near the edge of Mars' southern perennial polar cap. The surface H_2O ice was first observed by THEMIS as a region that was cooler than expected for dry soil at that latitude during the summer season. Diurnal and seasonal temperature trends derived from Mars Global Surveyor Thermal Emission Spectrometer observations indicate that there is H_2O ice at the surface. Viking observations, and the few other relevant THEMIS observations, indicate that surface H_2O ice may be widespread around and under the perennial CO_2 cap.

Determining the abundance and distribution of surface and near-surface H_2O ice is fundamental both for understanding the martian hydrological cycle and for the future exploration of Mars. H_2O ice, at or near the surface, is available for surface interactions and exchange with the atmosphere. H_2O ice that is buried a meter or more beneath the surface has a time constant for interaction with the atmosphere that is longer than a martian year and is thus relatively inactive (*1*). In addition, H_2O ice that is in the top few centimeters of soil will probably be accessible to future robotic probes and ultimately human exploration. Apart from the residual north polar cap, exposed H_2O ice may be limited to certain types of topographic features having spatial scales on the order of hundreds of meters rather than hundreds of kilometers.

The martian seasonal caps had been erroneously identified as H_2O (*2*) before modeling (*3*) indicated that CO_2 provided an excellent fit to the seasonal progression of the caps. The north polar perennial cap was then determined to be H_2O ice on the basis of observations of late summer surface temperatures (*4*) and associated atmospheric water vapor abundances (*5*). In late summer in the south polar area, when the seasonal CO_2 has retreated to its annual minimum extent, the only exposed volatile material to be identified has been CO_2 (*6*, *7*). Annual temperature observations of the north polar region also indicated the presence of ground H_2O ice (*8*), but no H_2O ice was identified in the southern hemisphere, although thermal modeling indicated that H_2O ice would be stable in the subsurface (*1*). The mean annual atmospheric H_2O saturation temperature is higher than the mean annual surface temperature in the south polar region, indicating that H_2O accumulation is inevitable. Thus, the extensive layered deposits in both polar regions have commonly been assumed to contain H_2O ice (*9*–*11*). Viking thermal observations indicated the difficulty of thermally detecting H_2O ice below a few centimeters of dust, and no positive identification of H_2O ice has previously been made in the southern hemisphere (*12*). Mod-

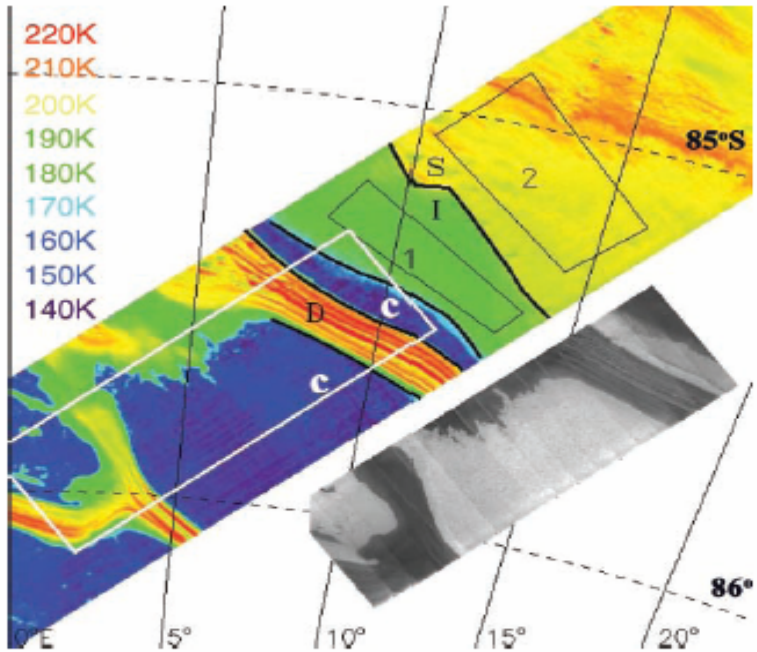

Fig. 1. Simultaneous THEMIS infrared (IR) and VIS images near the south polar cap at L_S = 334°; illumination is from the top. The false-color image is THEMIS IR image I00910002 (band 9, 12.6 μm). The darkest areas in the image are near 145 K, and the brightest, near 220 K; the strip is 32 km wide. The gray insert is THEMIS VIS image V00910003 (band 3, 654 nm). The thermal image is overlaid with a sketch of the individual thermal units: C, solid CO_2 on the surface; D, a dry, gently sloping unit that is dark and hot (the classic "dark lanes" through the perennial cap); I, the flat-lying unit of intermediate albedo and temperature (water ice); S, a warmer and darker flat-lying unit (soil). The numbered black rectangles are regions of interest (ROIs) used to accumulate seasonal data. The white rectangle outlines the position of the VIS image, shown to the right as the grayscale image.

[1]Branch of Astrogeology, U.S. Geological Survey, 2255 North Gemini Drive, Flagstaff, AZ 86001, USA. [2]Department of Geological Sciences, Arizona State University, Tempe, AZ 85287, USA.

*To whom correspondence should be addressed. E-mail: ttitus@usgs.gov

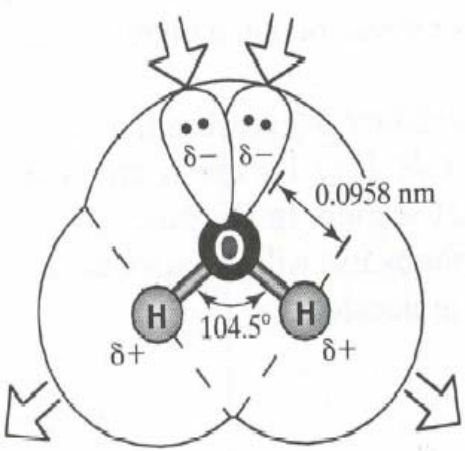
δ−
δ−
0.0958 nm
O
H
H
104.5°
δ+
δ+

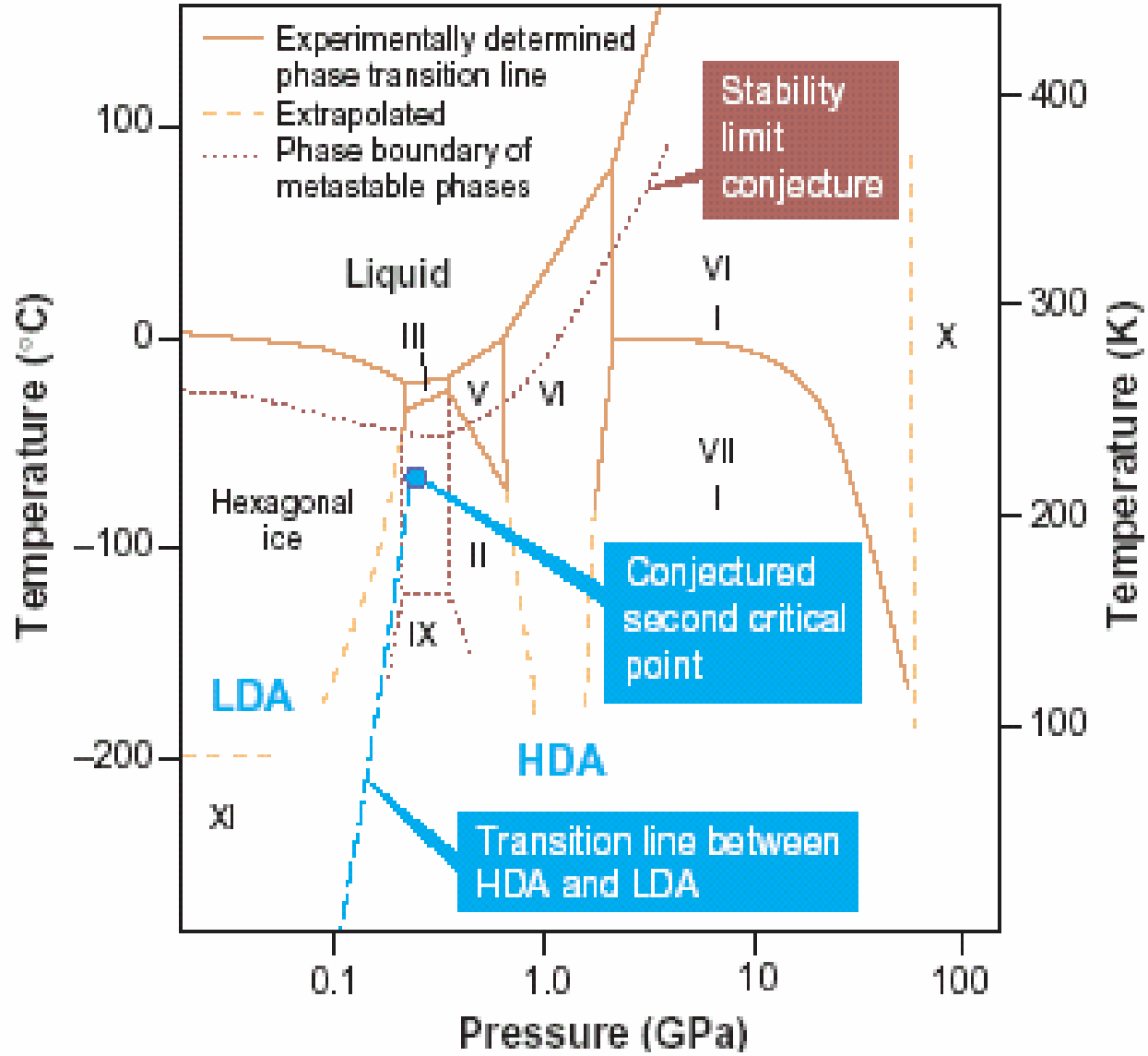
Experimentally determined phase transition line
Extrapolated
Phase boundary of metastable phases
Stability limit conjecture
Liquid
III
V
VI
VI
VII
X
Hexagonal ice
II
IX
XI
LDA
HDA
Conjectured second critical point
Transition line between HDA and LDA
100
0
−100
−200
400
300
200
100
0.1
1.0
10
100
Temperature (°C)
Temperature (K)
Pressure (GPa)

Free Water Clusters

Gregory *et al*. ***Science*** 275, 814 (1997)

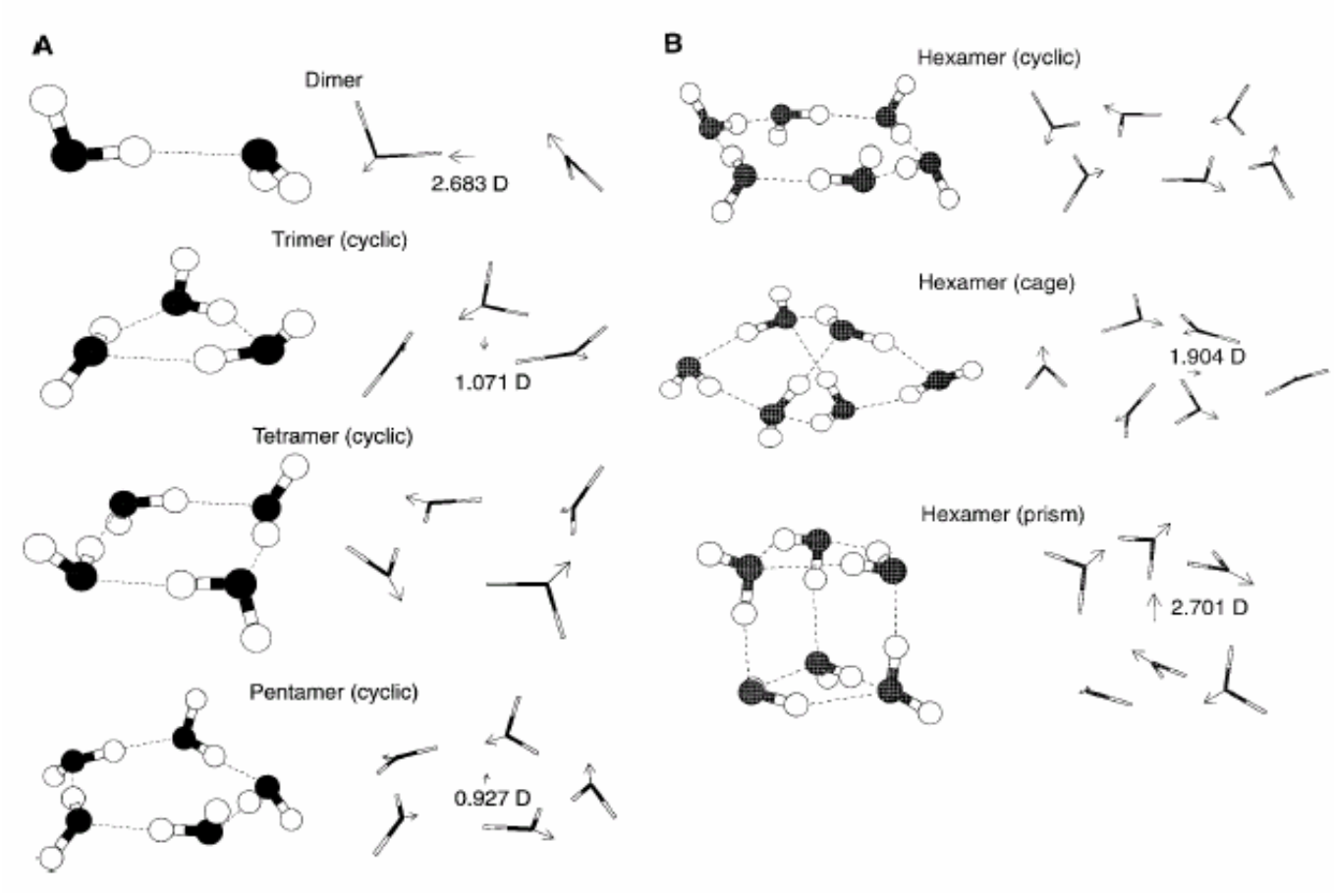

Water Adsorbate on Carbon Nanotubes

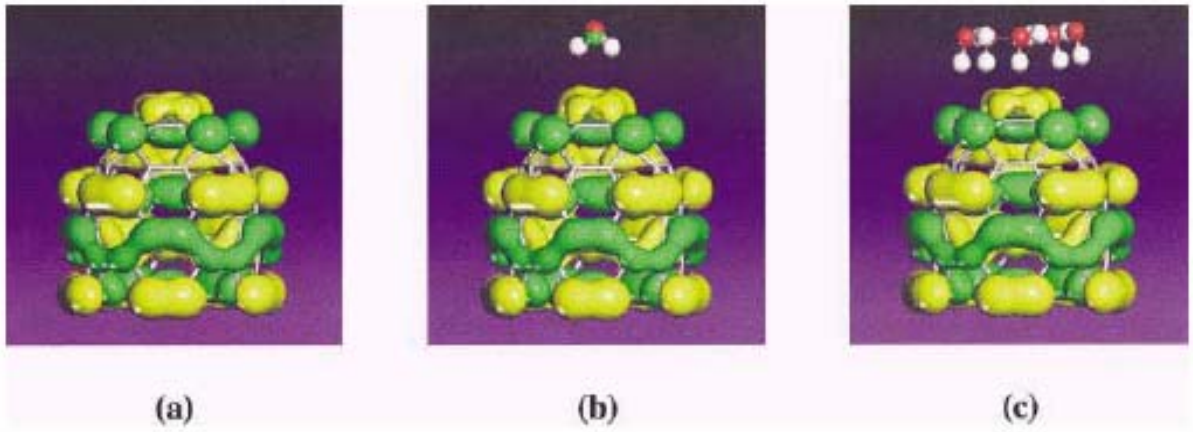

Maiti *et al.*, ***PRL*** 87, 155502 (2001)

Water in confined system

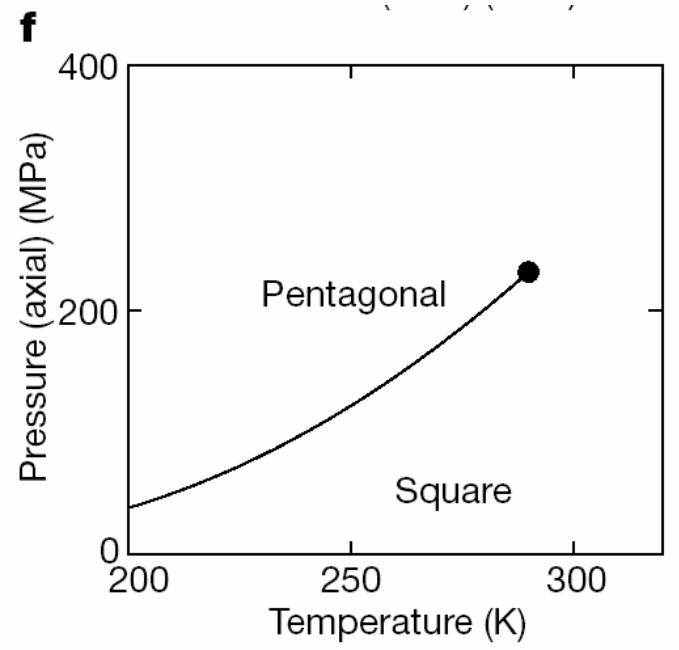

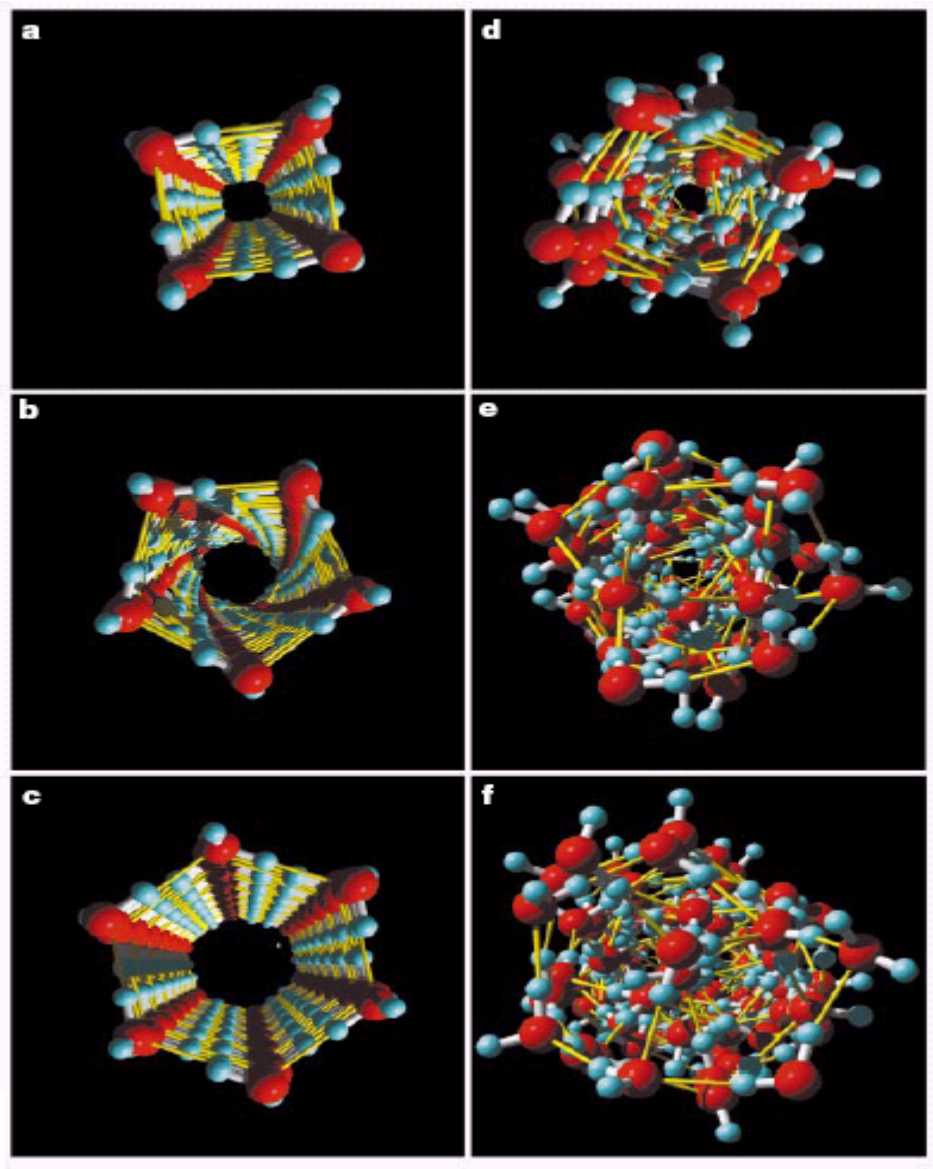

Koga *et al.*, ***Nature*** 412, 802 (2001)

Water on surface

H_2O/MgO

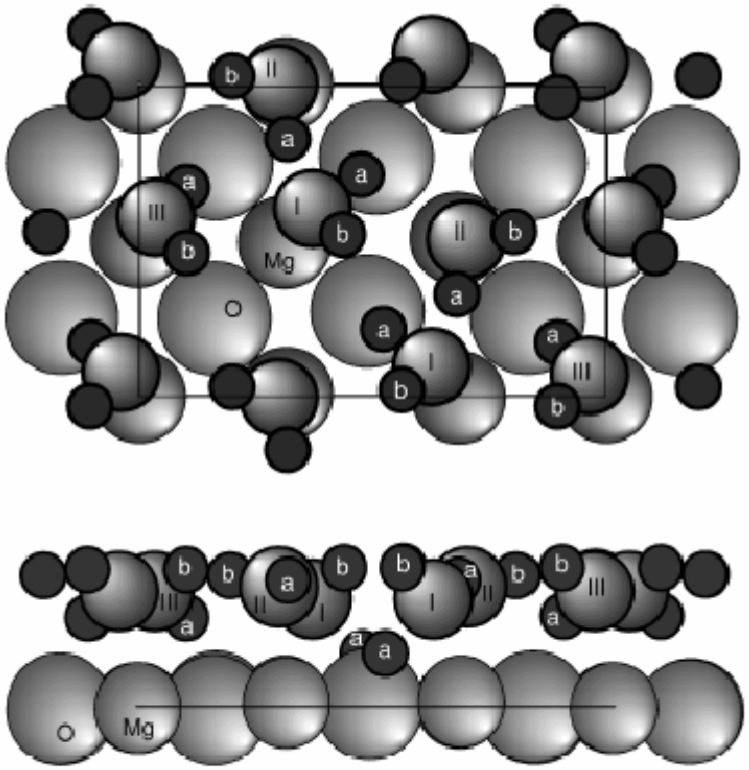

H_2O/MgO (100), Giordano *et al*, PRL 81, 1271 (1998)

Yu *et al*, PRB **68**, 115414 (2003)

H_2O/Ru

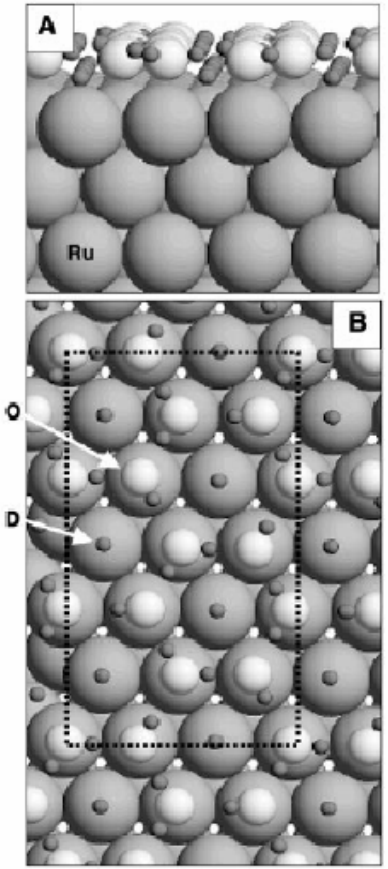

Feibelman, Science 295, 99 (2002)

- Water adsorption on
  Pt, Pd, Ru, Rh, Au surfaces

With Sheng Meng & Shiwu Gao

PRL 2002, 2003; PRB 2004; CPL 2005

Structure optimization and molecular dynamics

VASP code: US-PP (ultra-soft pseudo-potential) + GGA (generalized gradient approximation, PW91)

* Slab: 4 – 7 layers of metal with ~ 13Å vacuum;
* k-point: 3 X 3 X 1 or 5 X 5 X 1;
* Plan wave cutoff: 300 eV or 400 eV;
* Total energy convergence: 0.01 eV/atom;
* In MD, force on all relaxed atoms: < 0.05 eV/Å;
  a time step: 0.5 fs;
* In vibrational spectra, a 2 ps production run at 90-140K was performed after equilibrating the system for ~1 ps;
  (Also checked by higher energy cutoff (400 eV) and shorter time step (0.25 fs))

$H_2O/Pt(111)$

层数	E_{cut} (eV)	Top		Bridge		Hollow		d_{OH}	HOH	θ
		d_{OPt}	E_{ads}	d_{OPt}	E_{ads}	d_{OPt}	E_{ads}			
4	300	2.43	291	3.11	123	3.12	121	0.978	105.36	13
6	400	2.40	304	2.89	117	3.02	102	0.980	105.62	14

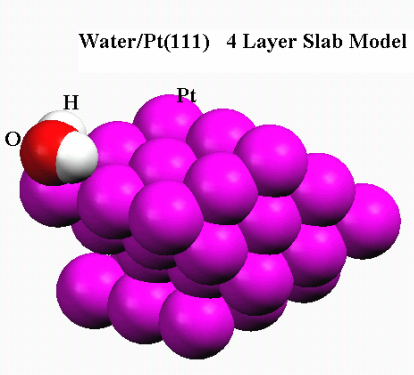

- Adsorption energy on top atom：~300 meV
- Flat on surface (13-14 °), freely rotates on the surface
- Rotational barrier： 140~190meV
- Charge transfor from O to Pt： 0.02e

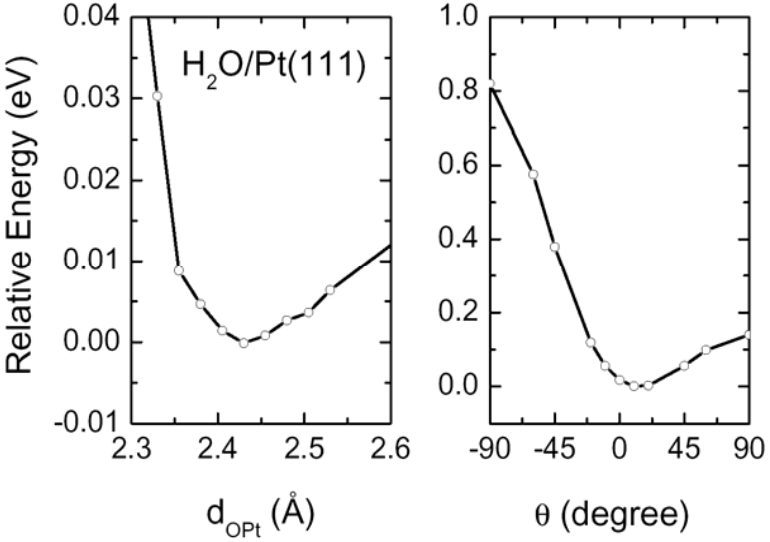

Small Clusters

304 meV 359 meV

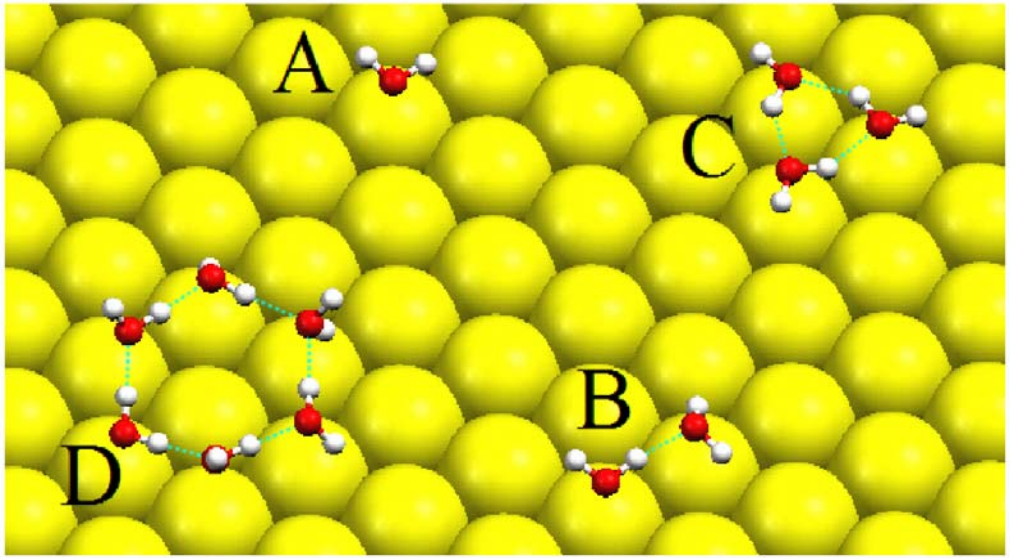

520 meV 433 meV

H-bond: 450 meV (adsorbed dimer)
>>250 meV (free dimer)

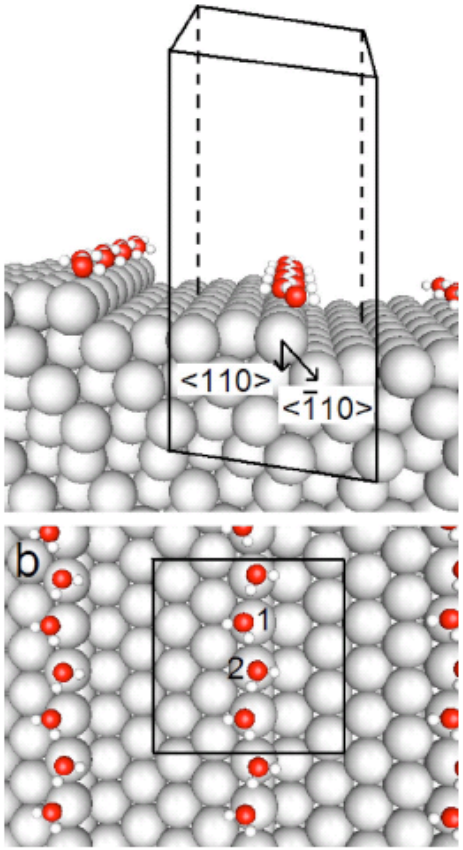

TABLE V. The water monomer and 1D chains adsorbed at the ⟨110⟩/{100} step on the Pt(111) surface, modeled by an unit cell in the (322) surface.

	Monomer		1D chain	
	d_{OPt} (Å)	E_a (meV)	d_{OPt} (Å)	E_a (meV)
H-in	2.22	449	2.42	431
H-out	2.25	426	2.48	385
Mixed			2.45	480
On terrace	2.43	291	2.62, 2.72	246

The 1D water chains at a <110>/{100} step on the Pt (322) surface.

Water bilayer/Pt(111)

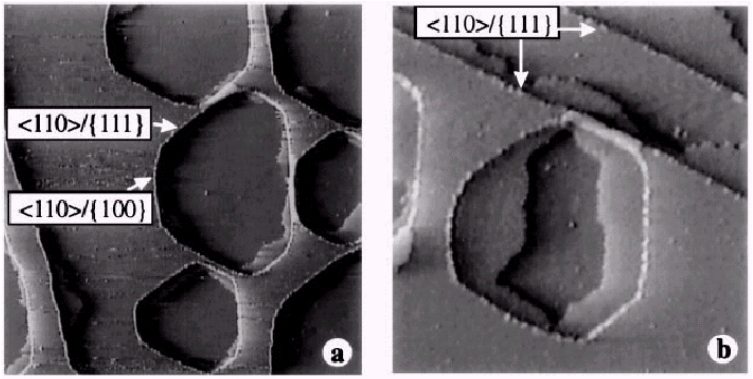

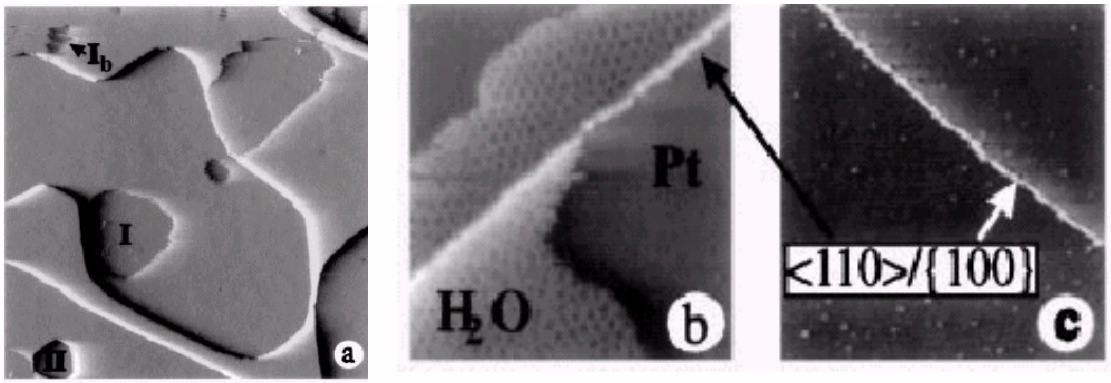

Morgenstern *et al.*, ***PRL*** 77, 703 (1996)

Adsorbed H-up and H-down bilayer with $\sqrt{3} \times \sqrt{3}R30^\circ$ (RT3) reconstruction

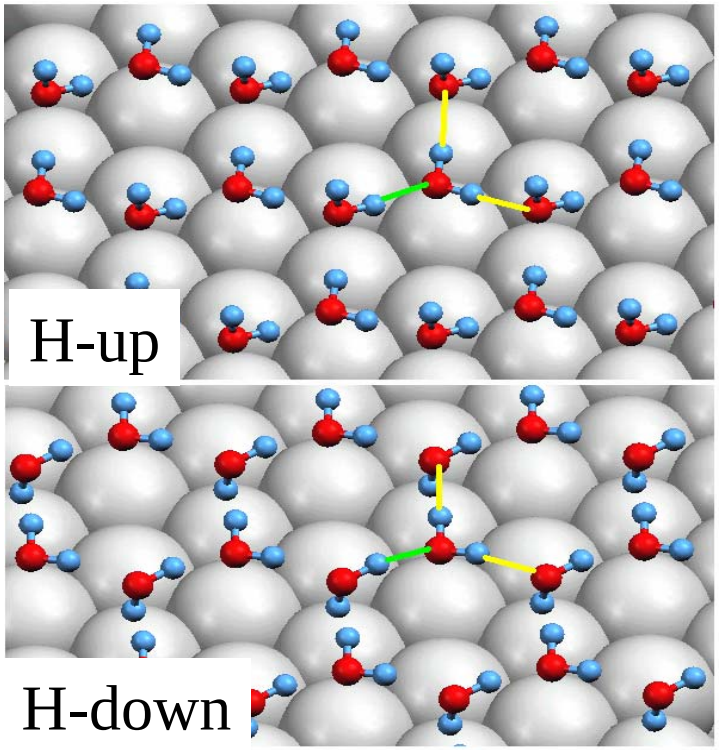

* H-up and H-down close in energy, 522 and 534 meV, whereas half-dissociated layer can be ruled out: E_{ads}/molecule =291 meV;

* Two non-equivalent H bonds;

Vibrational spectra

Translation and rotation

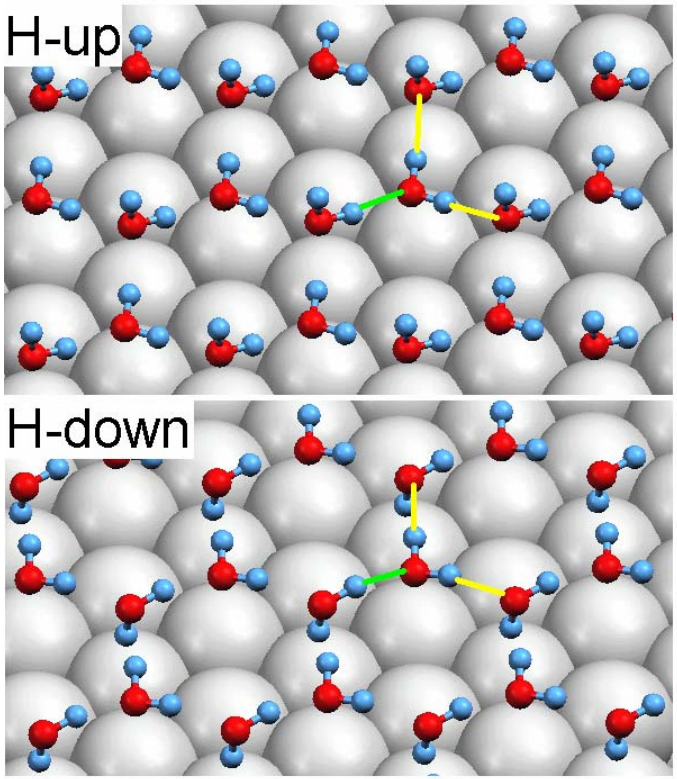

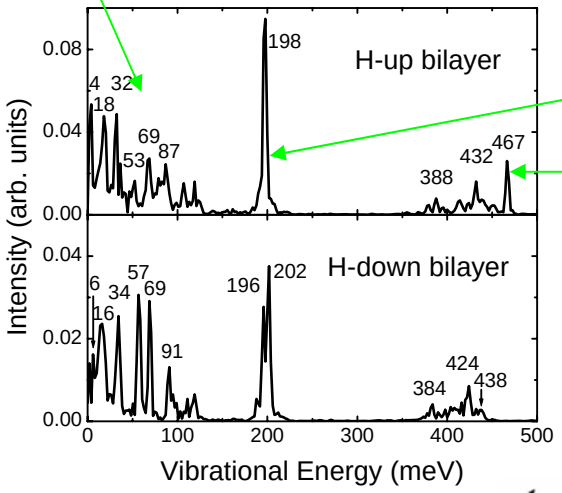

HOH bending

OH stretch

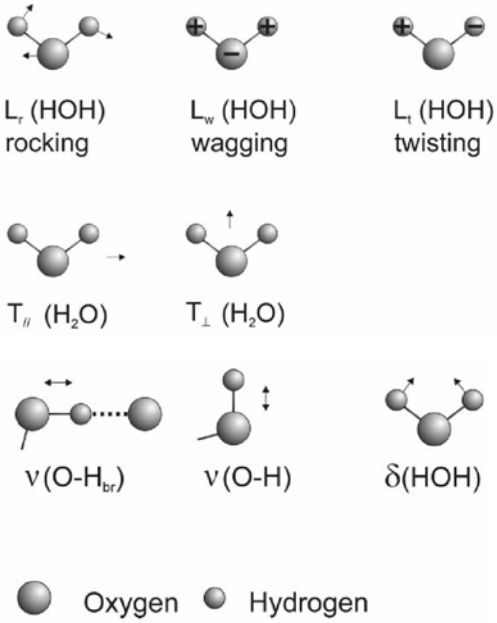

	$T_{//}$	T_2	T_3	L_3	L_4	L_5	δ_a	δ_b	δ_{HOH}	$\nu_{O\text{-}Hb}$	$\nu_{O\text{-}H}$
H_2O	4	16		40	61	89	113	121	190		440
$(H_2O)_2$	8	20	32	44	65	85	105	133	198	347	432,452
H-up	4	18	32	53	69	87	107	119	198	388,432	467
H-down	6	16	34	57	69	91	111	119	196,202	384,424	438
实验	5.85	16.5	33	54	65	84	115	129	201	424	455

Two types of Hydrogen Bonds

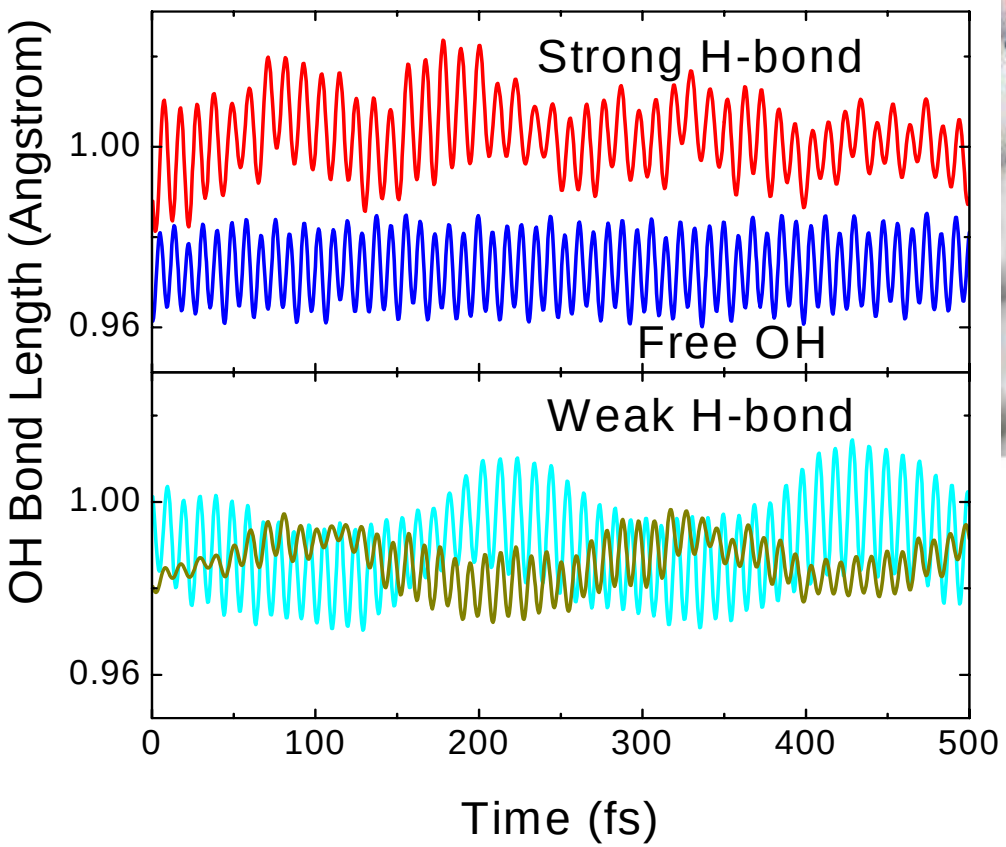

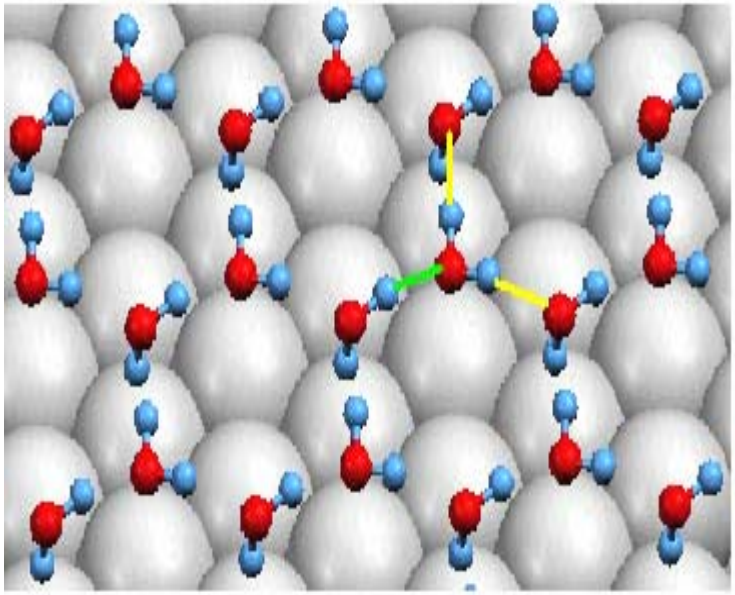

Nature of H-bond at surface

Free dimer

Adsorbed dimer

Strong bond in H-up bilayer

Strong bond in H-down bilayer

Weak bond in H-up bilayer

Weak bond in H-down bilayer

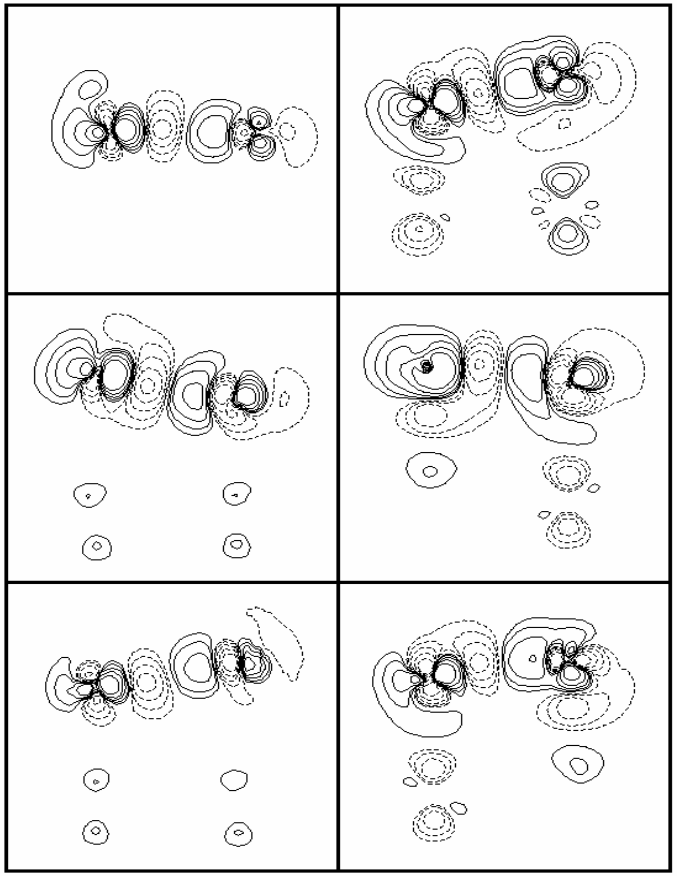

The unit cell and charge density

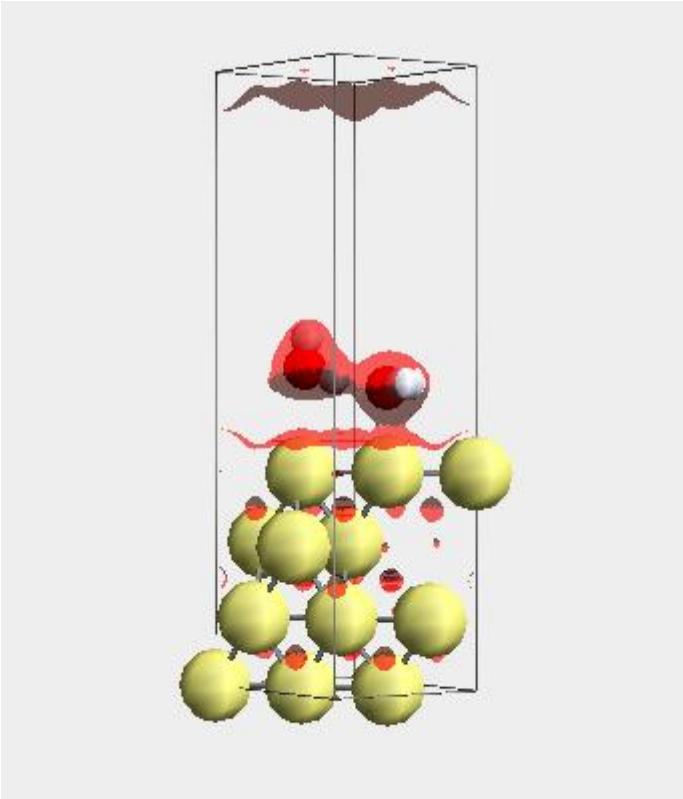

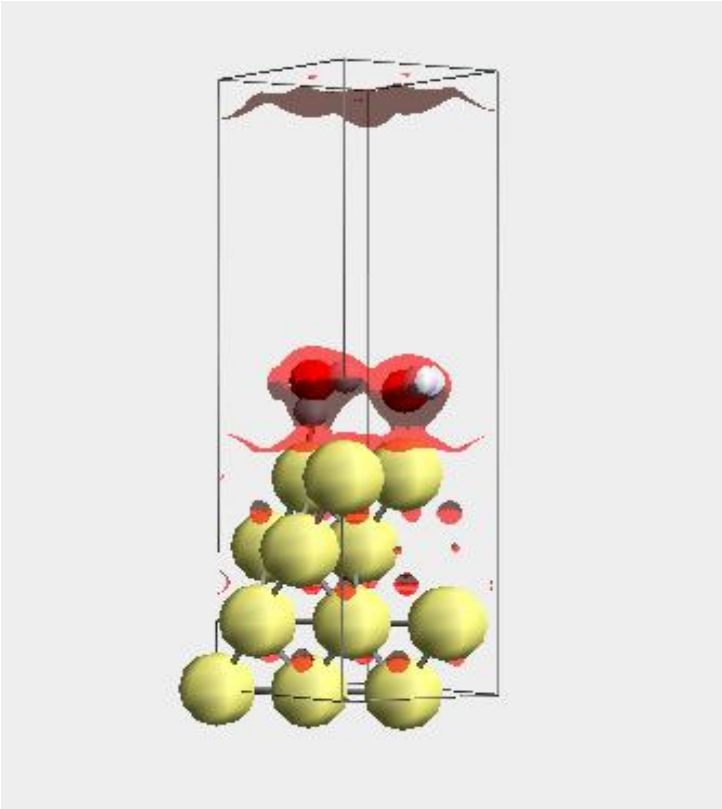

Minimum energy path for H-up flipping to H-down

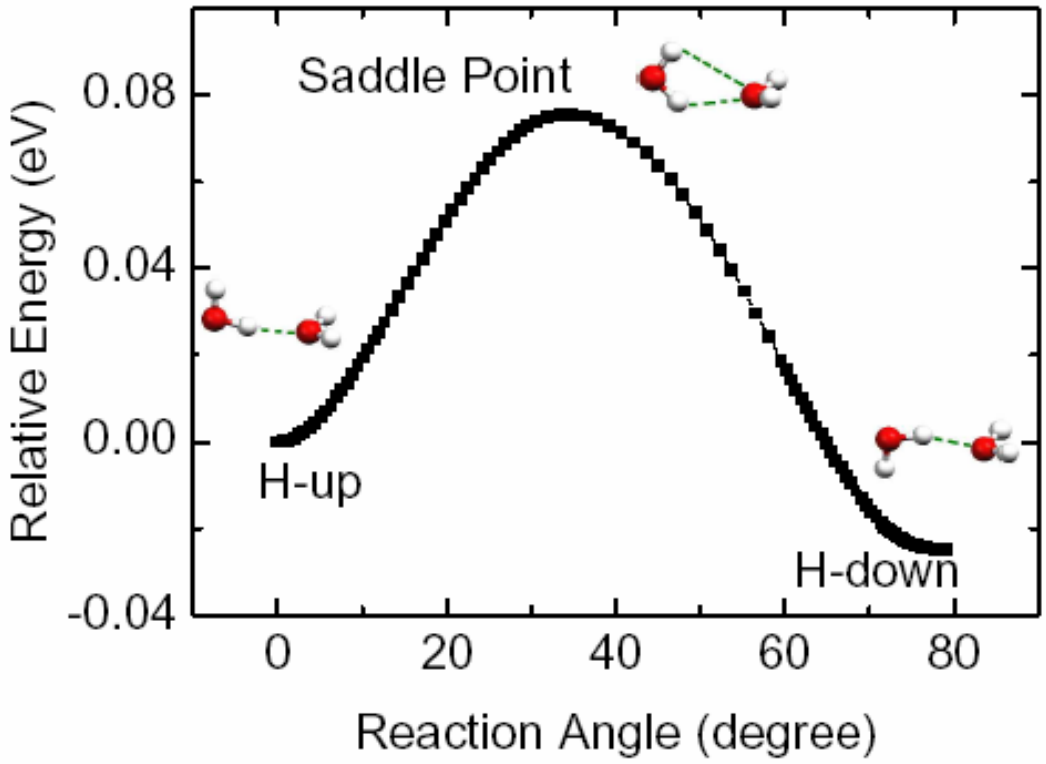

RT3 *vs* RT39, RT37

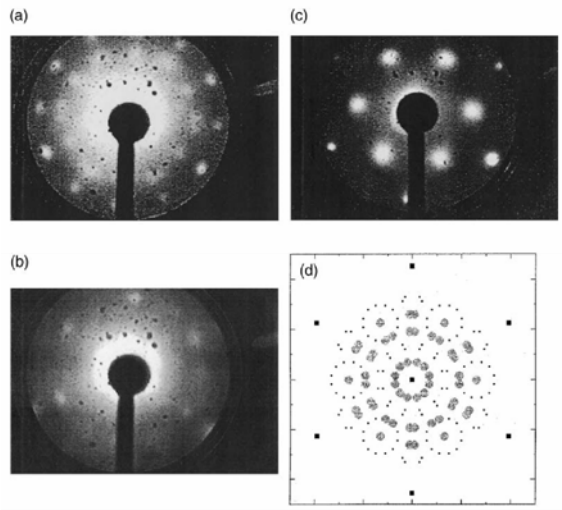

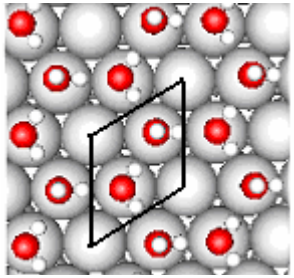

RT3

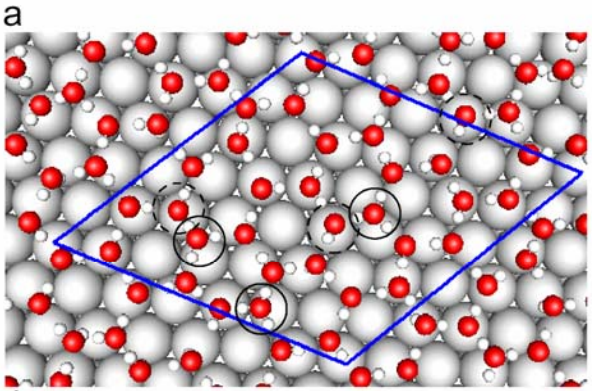

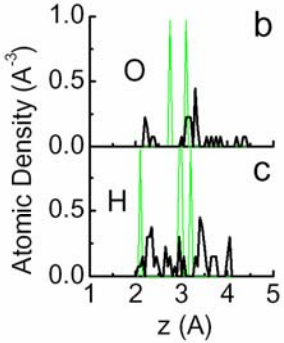

RT39

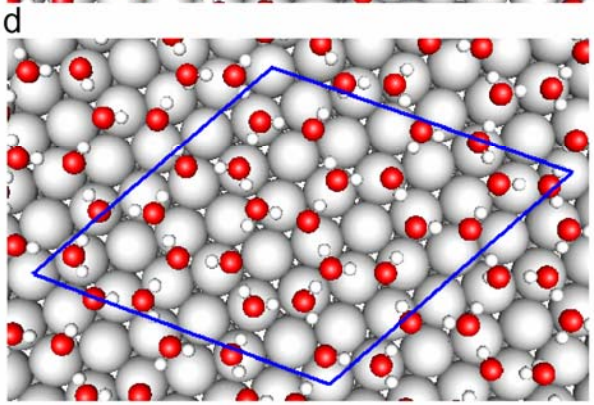

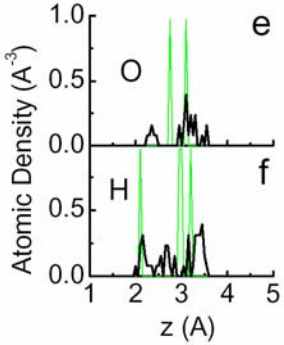

RT37

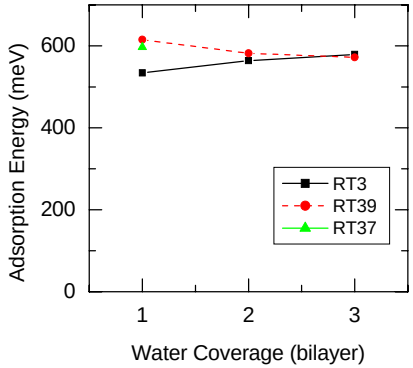

Water on Pt(111)

Ads. species	unitcell	n	E_a	N_{H_2O-M}	N_{HB}	E_{HB}
monomer	3×3	1	304	1	0	–
dimer	3×3	2	433	2	1	258
trimer	3×3	3	359	3	3	55
hexamer	$2\sqrt{3} \times 2\sqrt{3}$	6	520	3	6	368
bilayer	$\sqrt{3} \times \sqrt{3}$	2	505/527	1	3	235
2 bilayers	$\sqrt{3} \times \sqrt{3}$	4	564	1	7	312
3 bilayers	$\sqrt{3} \times \sqrt{3}$	6	579	1	11	303
4 bilayers	$\sqrt{3} \times \sqrt{3}$	8	588	1	15	307
5 bilayers	$\sqrt{3} \times \sqrt{3}$	10	593	1	19	307
6 bilayers	$\sqrt{3} \times \sqrt{3}$	12	601	1	23	320
bilayer	$\sqrt{37} \times \sqrt{37}$	26	597	13	39	297
bilayer	$\sqrt{39} \times \sqrt{39}$	32	615	16	48	309
2 bilayers	$\sqrt{39} \times \sqrt{39}$	64	582	16	112	275
3 bilayers	$\sqrt{39} \times \sqrt{39}$	96	572	16	176	276

Water monomer on different metal surfaces

Substrate	top		bridge		hollow		d_{OH}	∠HOH	θ
	d_{OM}	E_a	d_{OM}	E_a	d_{OM}	E_a			
Ru(0001)	2.28	409	2.55	92	2.56	67	0.981	105.66	16
Rh(111)	2.32	408	2.57	126	2.70	121	0.978	105.95	24
Pd(111)	2.42	304	2.74	146	2.77	130	0.977	105.63	20
Pt(111)	2.43	291	3.11	123	3.12	121	0.978	105.36	13
Au(111)	2.67	105	2.80	32	2.80	25	0.977	105.04	6

Water bilayer on metal surfaces

Surface	Bilayer	z_{OO} (Å)	z_{OM1} (Å)	z_{OM2} (Å)	E_a (meV/molecule)
Ru(0001)	H-up	0.86	2.46	3.42	531
	H-down	0.42	2.69	3.22	533
	half-disso.	0.05	2.09	2.16	766
Rh(111)	H-up	0.79	2.50	3.40	562
	H-down	0.42	2.52	3.12	544
	half-disso.	0.04	2.09	2.16	468
Pd(111)	H-up	0.60	2.78	3.45	530
	H-down	0.36	2.66	3.18	546
	half-disso.	0.07	2.09	2.20	89
Pt(111)	H-up	0.63	2.70	3.37	522
	H-down	0.35	2.68	3.14	534
	half-disso.	0.06	2.12	2.23	291
Au(111)	H-up	0.46	2.90	3.38	437
	H-down	0.29	2.85	3.25	454
	half-disso.	0.14	2.20	2.43	−472

Partial Dissociation Ru(0001)

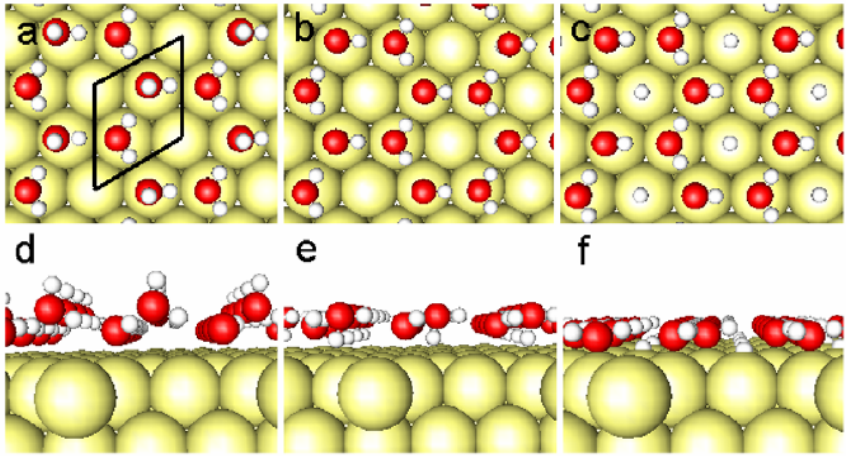

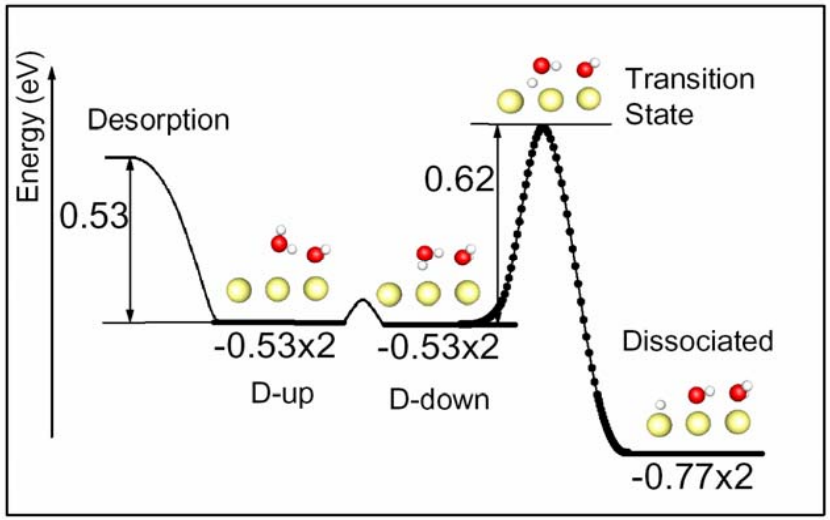

Results

- There exit two types of hydrogen bonds in the water network on Pt, Pd, Rh, Ru, and Au surfaces.

- The OH stretch in the bilayer, which is sensitive to local structures, may provide a general way for recognition of adsorbed water and other hydrogen-bonded species on surface.

- Water adsorption on silica surface:

  Tessellation ice

With <u>Jianjun Yang</u>

PRL 2004; PRB 2005, 2006

Why water and silica?

➢**A simple reason is their importance :**

Over 70% of the earth's surface is covered by water while the crust is dominated by silica (rocks containing SiO_n).

➢**A more technical reason is that the water-silica interaction is ubiquitous and fundamental in natural processes and advanced technological areas:**

Geoscience: water weathers the crusts.

Glass technology and in many other areas of application.

→ Uncover how water-silica interacts is crucial !

Hydroxyls and water layers on silica surfaces

Ambient conditions

Hydroxyl groups have been detected by experiments.

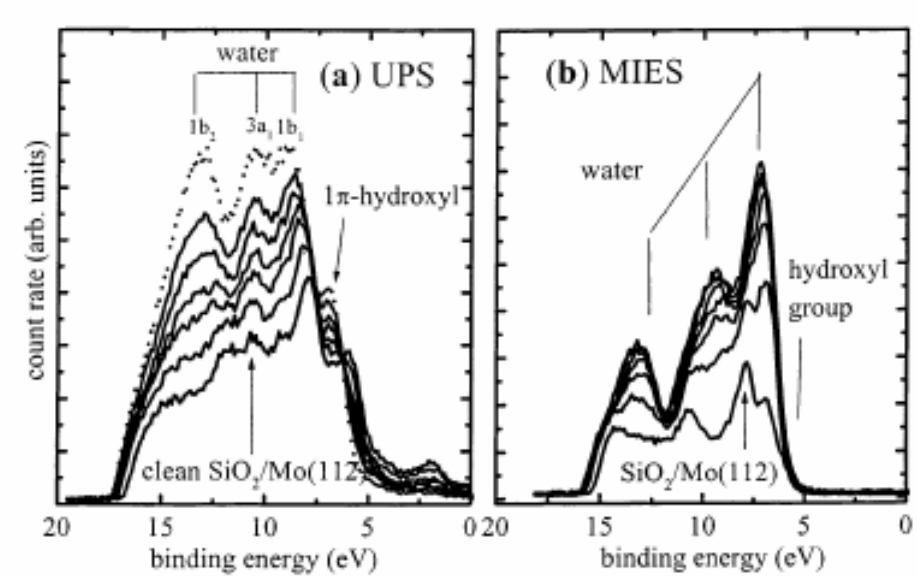

Figure 1. (a) UPS spectra collected from a SiO_2/Mo(112) surface as a function of water exposure at 90 K. (b) MIES spectra collected from a SiO_2/Mo(112) surface as a function of water exposure at 90 K. The UPS and MIES spectra were acquired simultaneously.

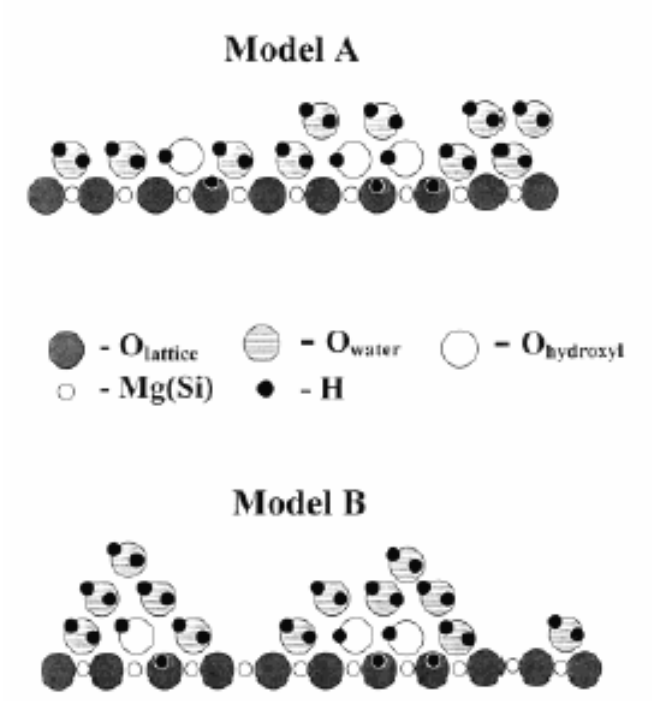

Langmuir, Vol. 19, No. 4, 2003 1141

Typical hydroxyl groups

The presence of hydroxyl groups on silica is important as it impacts the reactivity and performance of the silica surfaces, which are so important both naturally and technologically.

Two typical hydroxyl groups are detected by experiments, the single (Si-OH) and geminal (Si-$(OH)_2$), and some of them form hydrogen-bonding.

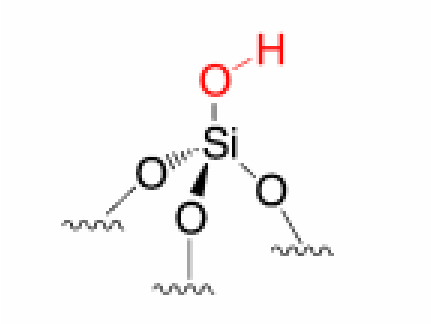

Single hydroxyl

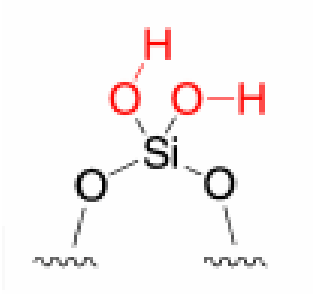

Geminal hydroxyls

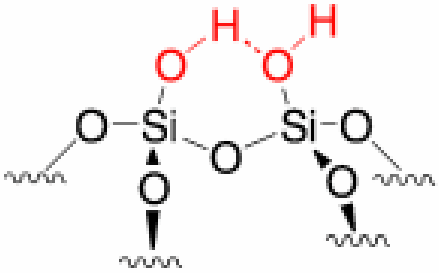

Vicinal hydroxyls

Hydrolysis of silica surfaces

An example by first-principle MD study on cluster model:

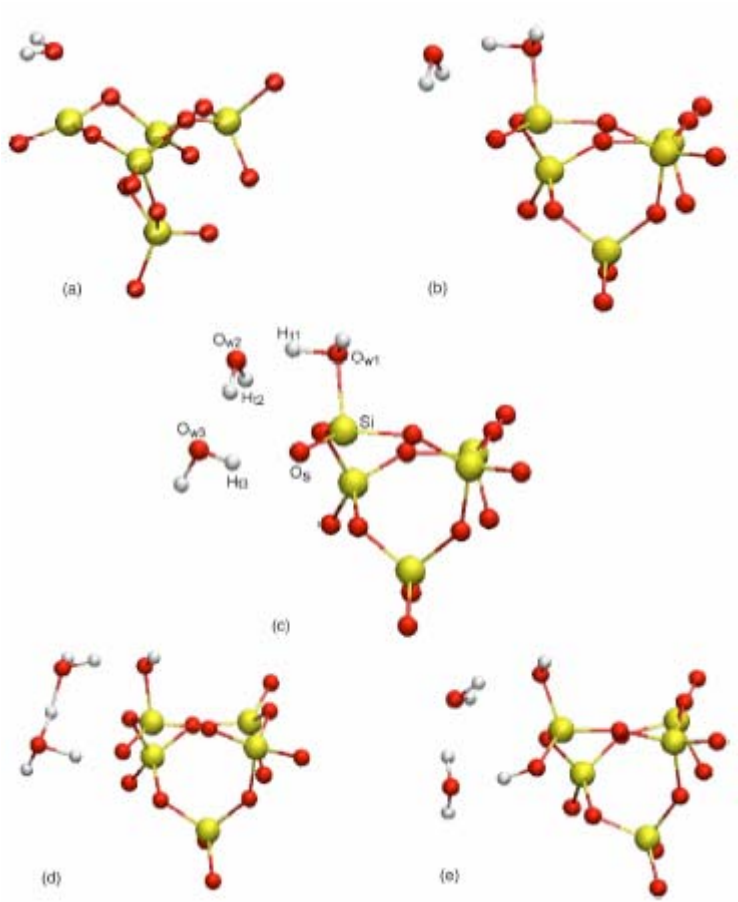

FIG. 2. Hydrolysis process of a three-coordinated silicon atom connected with a one-coordinated oxygen atom (Q_3^1) by water trimer. For clarity, only atoms around the reaction site are shown. Red, yellow, and white spheres indicate O, Si, and H atoms, respectively. (a) A single water molecule is physisorbed on the silicon atom. (b) Two water molecules are adsorbed on the silicon atom. (c) The initial configuration of the system before reaction. (d) and (e) are the structures at 33 fs and 130 fs, respectively.

——— Ma, Foster, and Nieminen

J. Chem. Phys. **122**, 144709 (2005)

Hydrophilic hydroxylated surfaces

Hydroxylated surface → Highly reactive with H_2O moleculars

Experiments show that there is an ordered ice-like structure at water/silica interface .

(PRL 72, 238 (1994); JPC B 109, 16760 (2005))

β-cristobalite (100) and (111), and α - quartz (0001) surfaces are representatives of the hydroxylated silica surface

(see JPC- B 101,3052 (1997))

Hydroxylated surface

Bulk SiO_2

Computational method

Ab-initio calculation:

DFT (density functional theory)

VASP code:

US-PP (ultra-soft pseudo-potential)

GGA (generalized gradient approximation)

Model:

- β-cristobalite (100) and (111) ;
  α - quartz (0001) surfaces
- Slab containing 7~9 atomic layers
- ~10Å of vacuum
- Passivated bottom layer

- ENCUT=350eV
- 2x2x1 k-points grids

A free water molecule :

(OH，∠HOH)	LDA	GGA
E_{cut}=350 eV	(0.973 Å, 105.69°)	(0.973 Å, 104.91°)
E_{cut}=400 eV	(0.975 Å, 105.66°)	(0.973 Å, 104.62°)

Expt: 0.957Å 104.52°

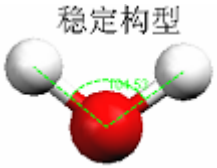

Hydroxylated β-cristobalite surfaces

(100): geminal

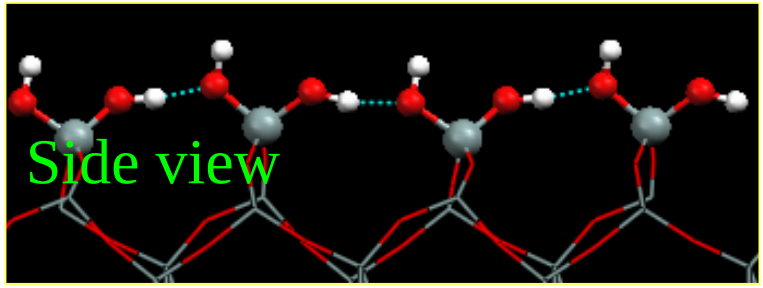

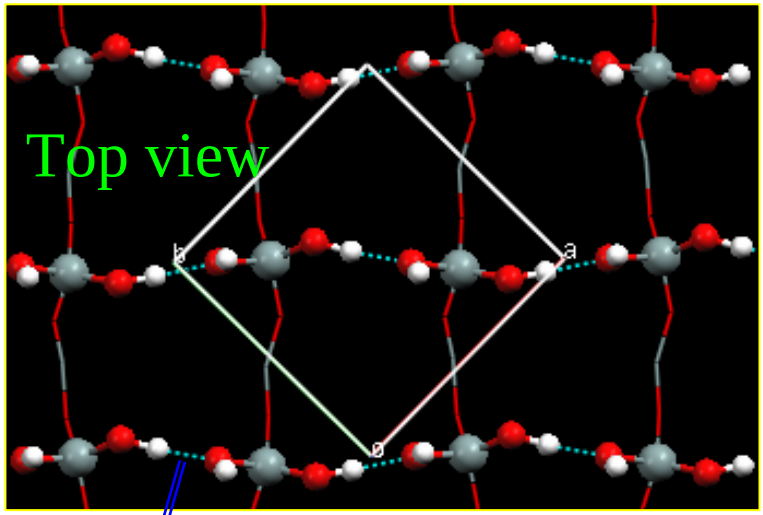

H-bond lengths (O-H):1.644-1.690Å

(111): single

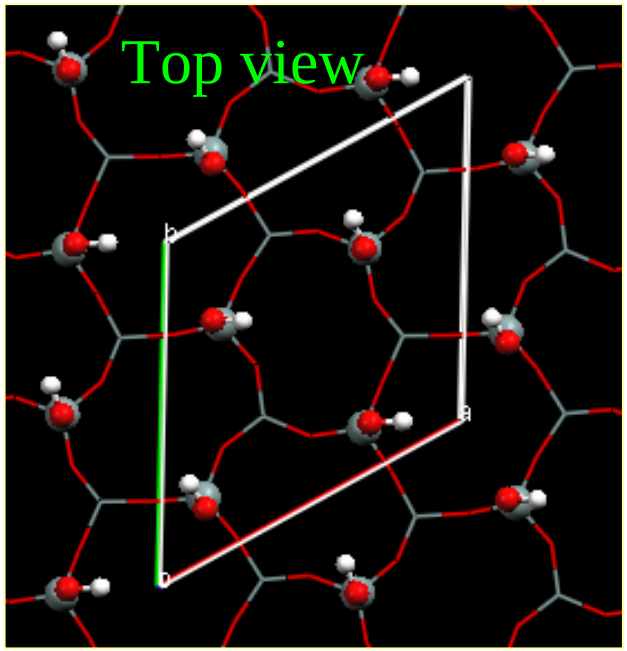

(I) Monomer on β-cristobalite (100) surface

Definition:

H-bond { **O…O < 3.3Å**
H-O…H > 140º

OH bond lengthened: 0.988 (0.973Å)

HOH angle enlarged: 105.1 (104.9º)

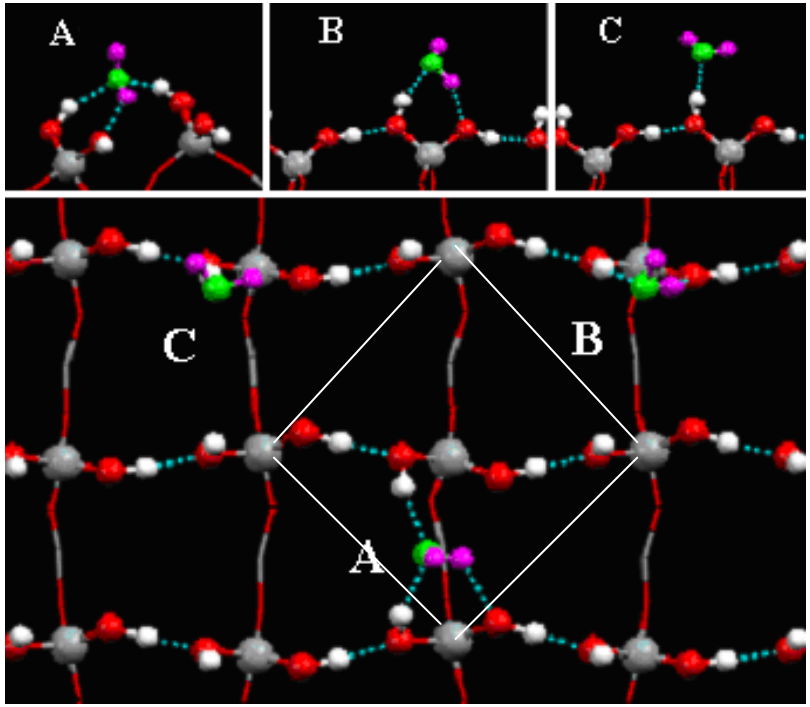

$E_{ads}=\{[nE(H_2O)+E(\text{substrate})]-E(nH_2O+\text{substrate})\}/n$

	N_{HB}	E_{ads} (meV/ H_2O)	d_{OH1} (Å)	d_{OH2} (Å)	∠HOH (º)
A (bridge)	**3**	**622**	0.974	0.988	105.06
B (geminal)	2	508	0.973	0.992	106.03
C (top)	1	339	0.970	0.960	106.12
Free H_2O	—	—	0.973	0.973	104.91

(I) Dimer on β-cristobalite (100) surface

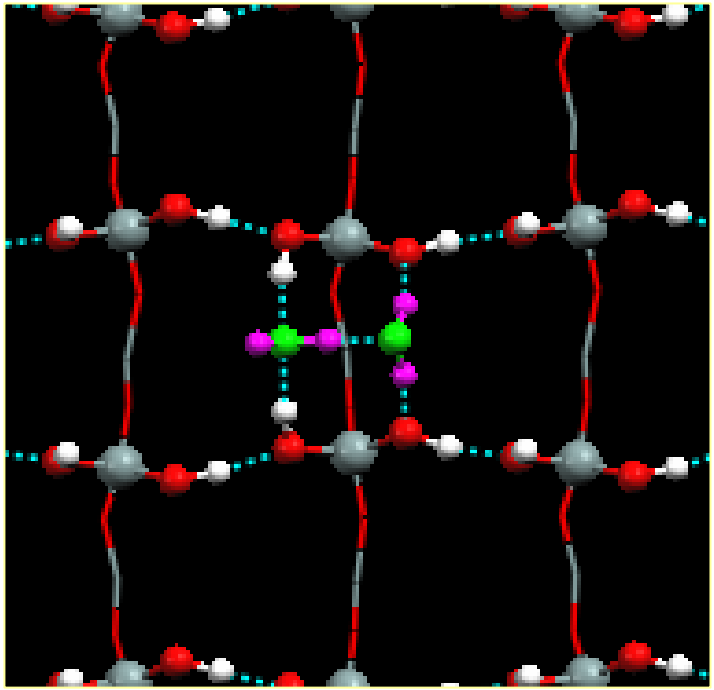

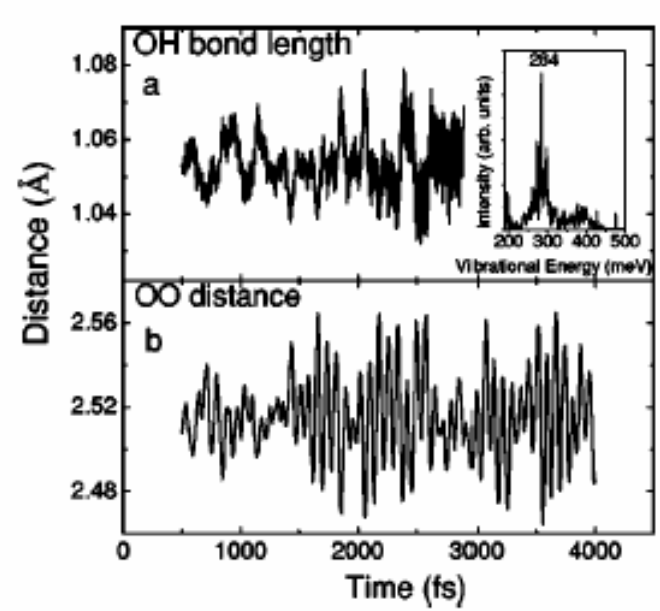

OO distance shortened: 2.53 (2.89 Å)
⟹ **H-bond strengthened**

	translations and librations						δ_{HOH}	$\nu_{O\text{-}Hw}$	$\nu_{O\text{-}H}$
dimer/ β(100)	19		53	69	81	109	197	**284**	414,428,476
H_2O							198		462,478
H_2O (expt.)[a]							198		454,466
dimer	20	34	46	67			198	**442**	462,473,483
dimer (expt.)[b]	19[c]	30[c]	40[c]	65[c]			201	440	450,459,461

(I) Monolayer on β-cristobalite (100) surface

1ML: One hydroxyl adsorbs one water molecule.

Results:

- Forming a 2D H-bonded water network
- Half molecules is parallel and the rest is perpendicular to the surface
- Each H_2O is saturated with 4 H-bonds.

$$1\text{hydroxyl} + 3H_2O$$

⇨ **2D ice layer**

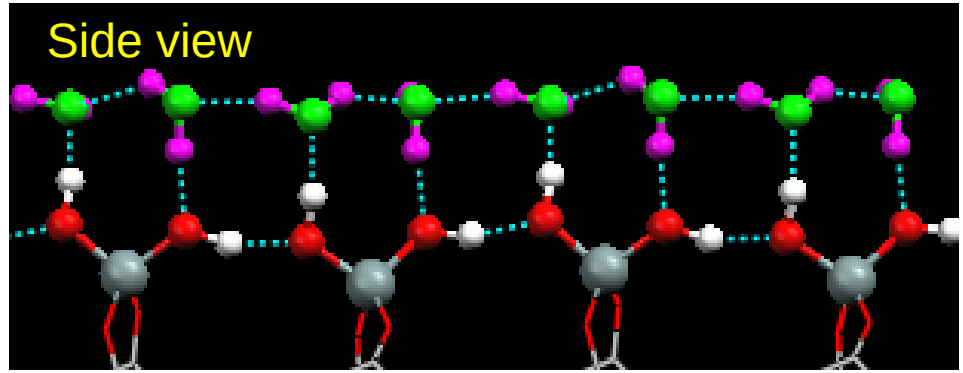

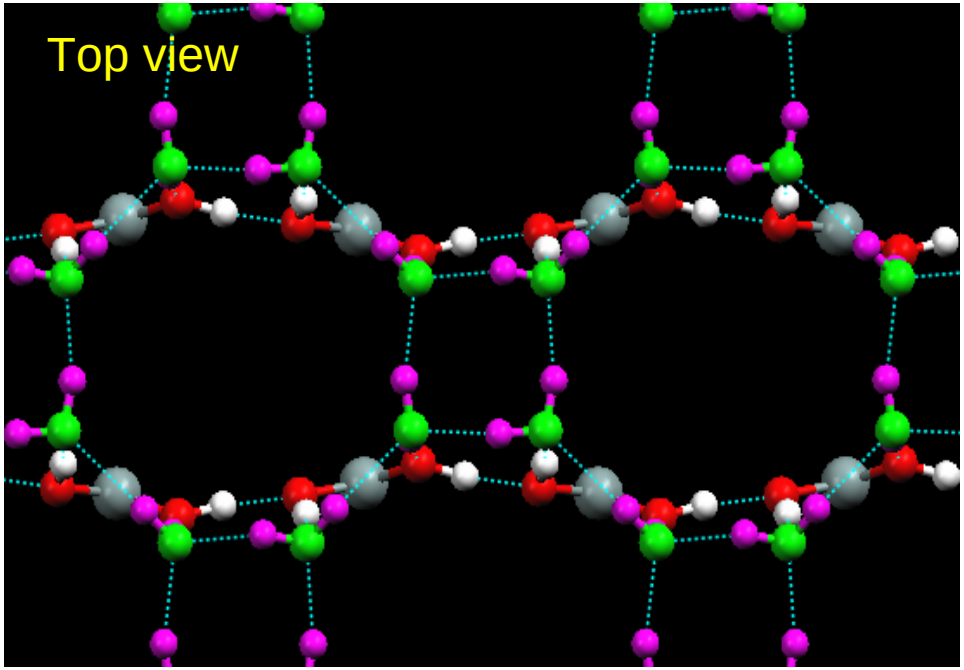

(I) 2D tessellation ice:

Each H_2O is saturated with 4 H-bonds: 1hydroxyl＋3H_2O;
No free OH sticking out of surface

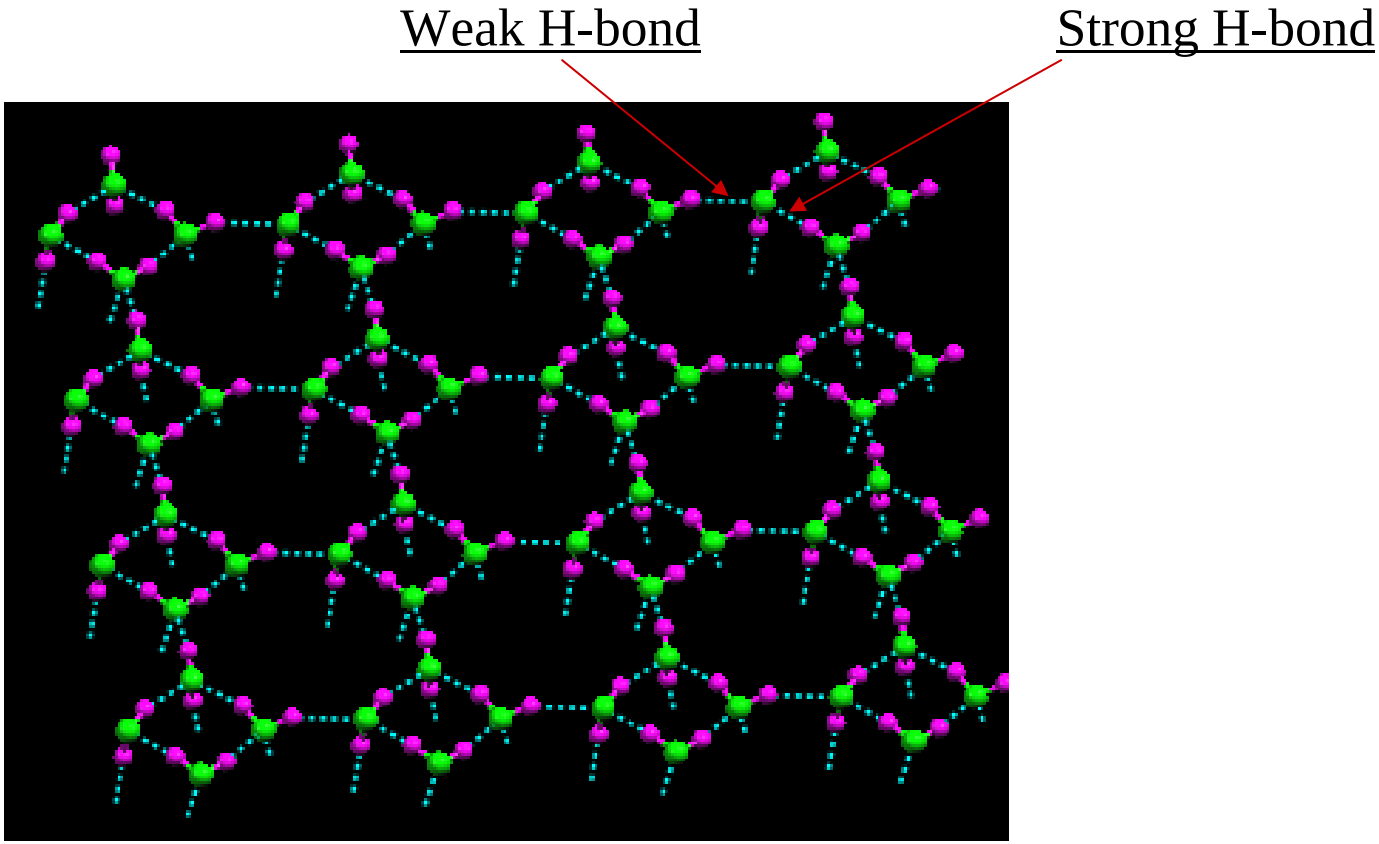

The adsorption energy of the tessellation ice on β-cristobalite (100) is large, 712 meV/H_2O, almost the same as adhesive energy in bulk ice, 720 meV/H_2O. It is stable up to room temperature (300K).

(I) Degenerated 2D ice configurations

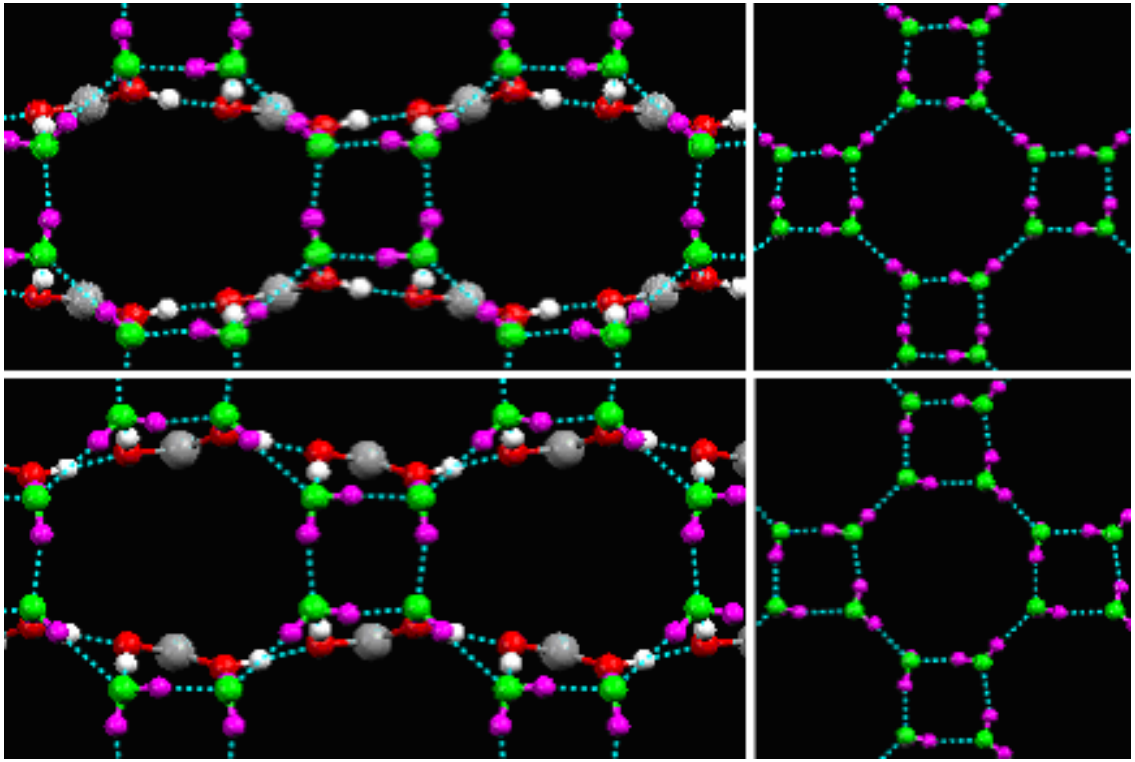

This 2D ice structure can sit on different sites (left panels) with two possible orderings of H-bonds (right panels).

$$\Delta E < 17 meV$$

(I) Vibrational spectrum

(80K;0.5fs;3ps)

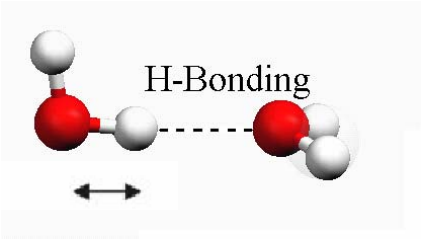

stronger H-bond

→ more red-shifted of OH stretched vibration

→ lower vibration energy

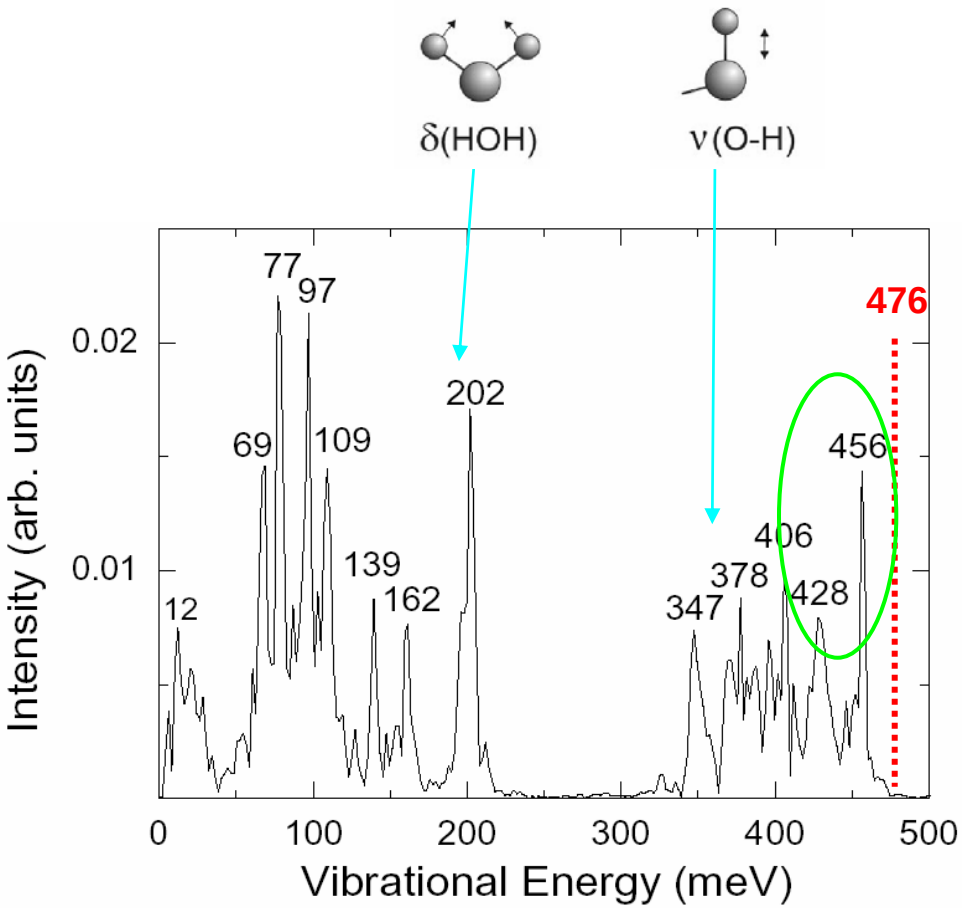

The strong H bond inside the quadrangles: 406 and 428 meV modes;
The weak H bond between the two neighboring quadrangles: 456 meV modes;
The OH stretching: 347 and 378 meV modes;

(I) Isodensity contour plots of difference electron density

free dimer

adsorbed dimer

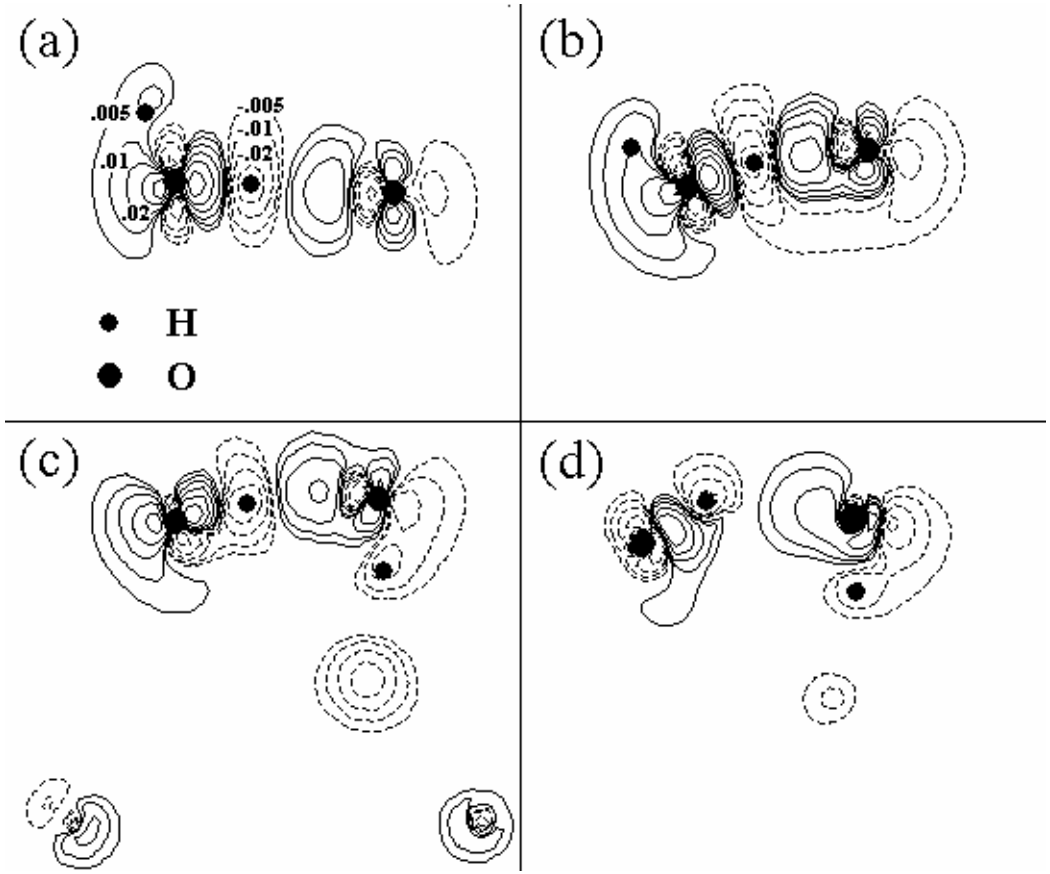

strong HB

in 2D ice

weak HB

in 2D ice

$\Delta\rho = \pm 0.005 \times 2^k$ e/Å^3, for $k = 0, 1, 2, 3 \ldots, 6$

Charge density is plotted along the plane perpendicular to the surface and passing the H-bond we are caring about.

(II) Monolayer on β-cristobalite (111) surface

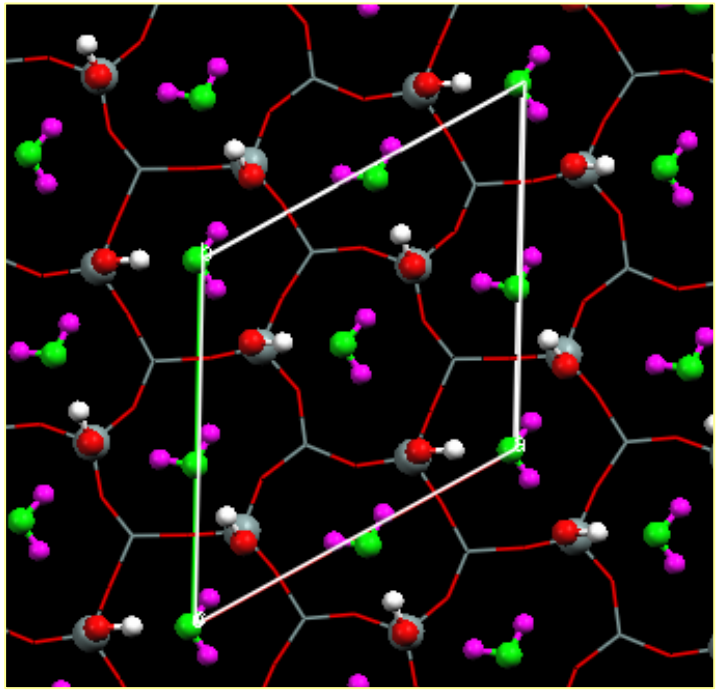

There are four water molecules in the surface cell. The adsorption energy is 701 meV/N_2O.

Because of large distance (about 5Å) between two adjacent single hydroxyls, water molecules can't interact with each other but only H-bond weakly with the surface hydroxyls.

(III) Hydroxylated α-quartz (0001) surface

- geminal hydroxyls
- alternative strong HB (denoted as S) and another weak HB (denoted as W) between hydroxyls

OO distances of 2.73Å and 3.09Å, respectively

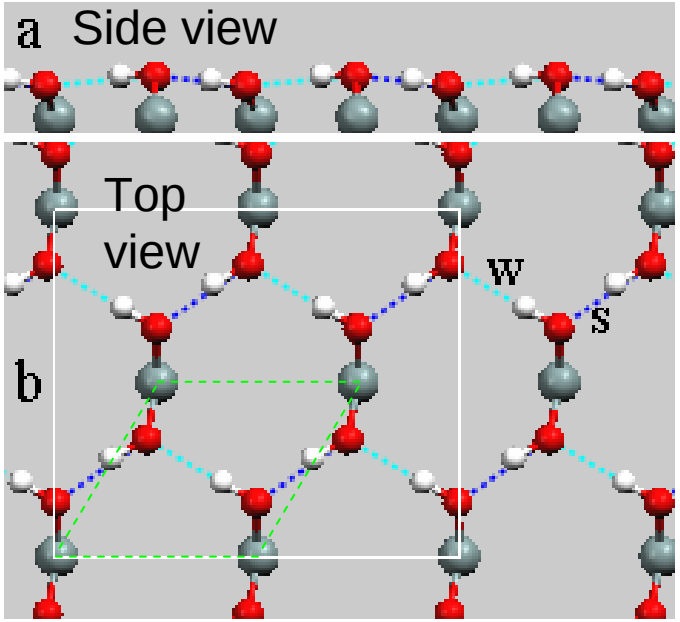

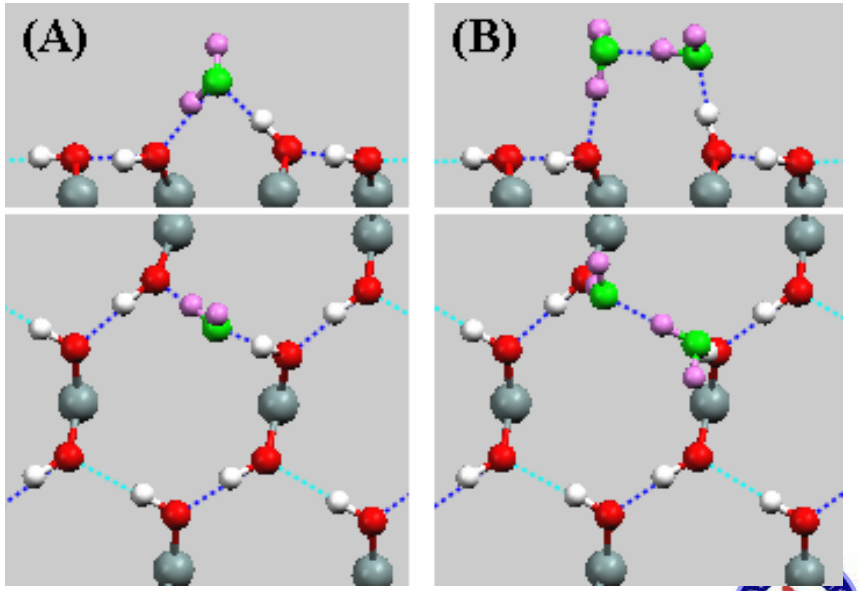

➢ On water adsorption, water-hydroxyl and hydroxyl-hydroxyl interactions compete.

➢Finally, the former wins and weak H-bond between hydroxyls is broken.

(III) Monolayer on α-quartz (0001) surface

* flat bilayer

$d = 0.1$Å——(0.97Å in Ice-Ih)

* two types of H_2O, I and II.

* two types of HBs between molecules

* E_{ads} = 650meV for H-down and 462 meV for H-up bilayer

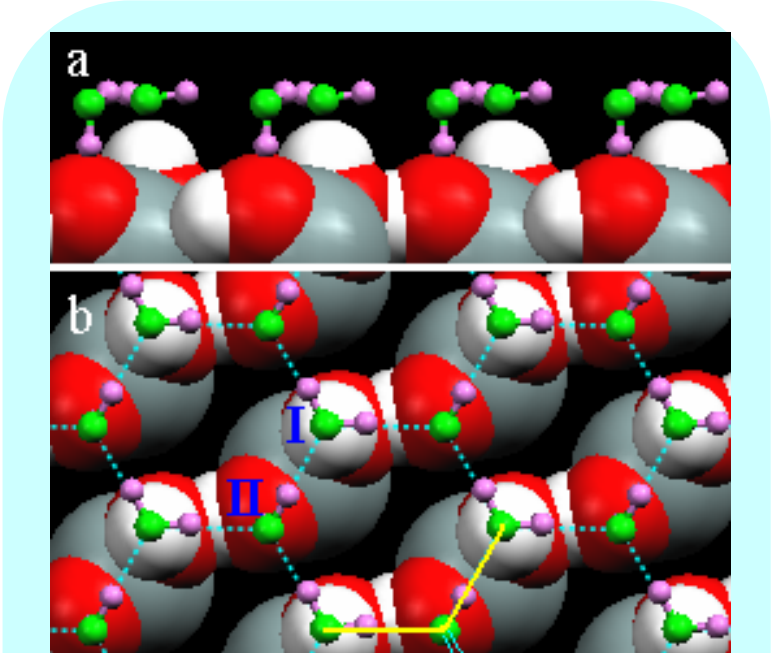

TABLE II. Calculated O-O distances (in Å) of water-water (O_w-O_w), water-surface (O_w-O_s), and hydroxyl-hydroxyl (O_s-O_s) contacts for the ice bilayers on the hydroxylated α-quartz (0001) surface. The O-O distance in the ordinary ice Ih is 2.76 Å.

	O_w-O_w	O_s-O_w	O_s-O_s
Clean surface			2.72, 2.73, 3.09
H-down bilayer	2.77, 2.87	2.67, 2.72	2.55, 2.63, 3.44
H-up bilayer	2.85, 2.87, 2.90	2.74, 3.24	2.54, 2.59, 3.50

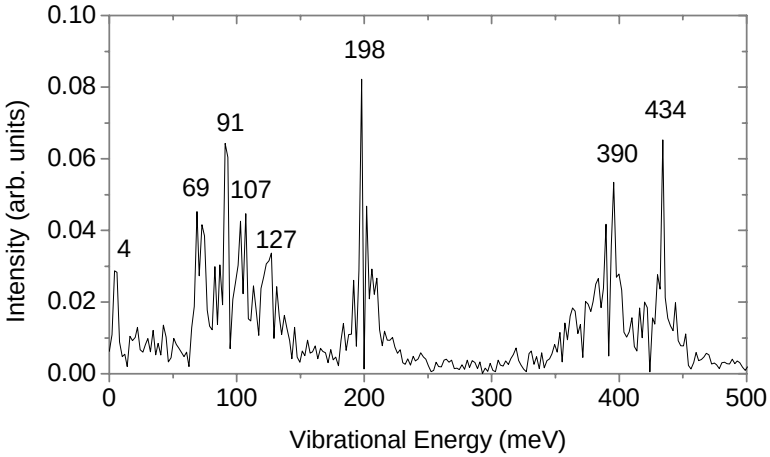

(III) Transition from H-up to H-down

- **thermodynamics**

H-down configuration is favored than H-up one by 0.188eV/H_2O difference in E_a.

- **dynamics** （c-NEB method）

The transition energy barrier from H-up to H-down is very small, 0.035eV per molecule II.

The saddle point occurs at the rotation angle (of molecule II) of 9º。

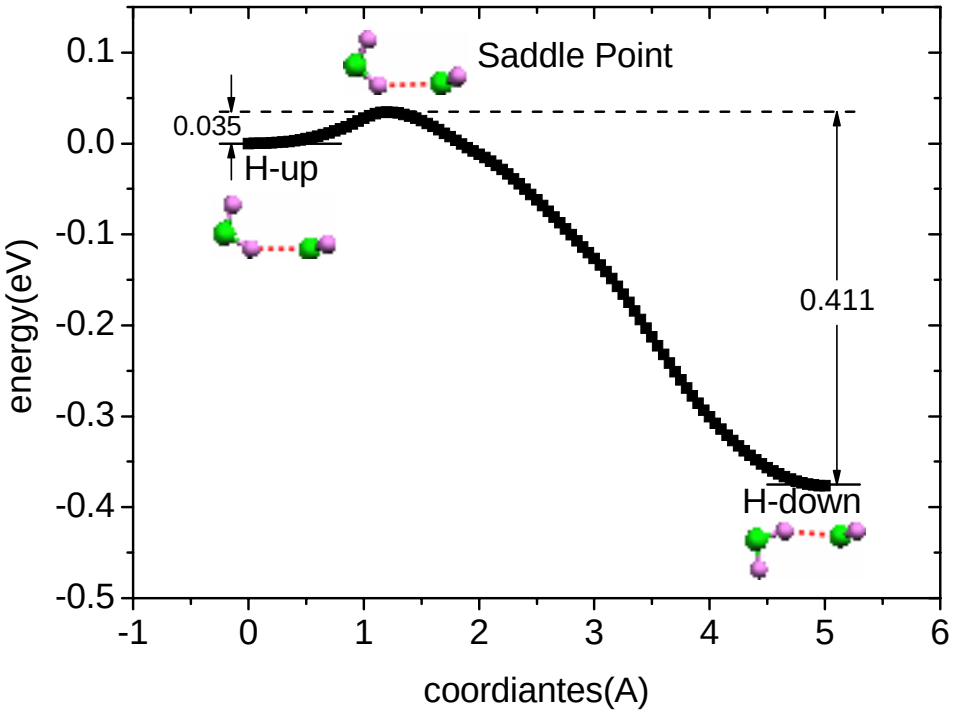

PRL 95, 166104 (2005) PHYSICAL REVIEW LETTERS week ending 14 OCTOBER 2005

Quasi-Ice Monolayer on Atomically Smooth Amorphous SiO_2 at Room Temperature Observed with a High-Finesse Optical Resonator

I. M. P. Aarts,[1] A. C. R. Pipino,[2] J. P. M. Hoefnagels,[1] W. M. M. Kessels,[1] and M. C. M. van de Sanden[1]

[1]*Department of Applied Physics, Eindhoven University of Technology, Eindhoven, The Netherlands*

[2]*National Institute of Standards and Technology (NIST), Gaithersburg, Maryland 20899, USA*

(Received 4 May 2005; published 13 October 2005)

The structure of an H_2O monolayer bound to atomically smooth hydroxylated amorphous silica is probed under ambient conditions by near-infrared evanescent-wave cavity ring-down absorption spectroscopy. Employing a miniature monolithic optical resonator, we find sharp (≈ 10 cm^{-1}) and polarized ($>10:1$) vibration-combination bands for surface OH and adsorbed H_2O, which reveal ordered species in distinct local environments. Indicating first-monolayer uniqueness, the absorption bands for adsorbed H_2O show intensity saturation and line narrowing with completion of one monolayer. Formation of the ordered H_2O monolayer likely arises from H bonding to a quasicrystalline surface OH network.

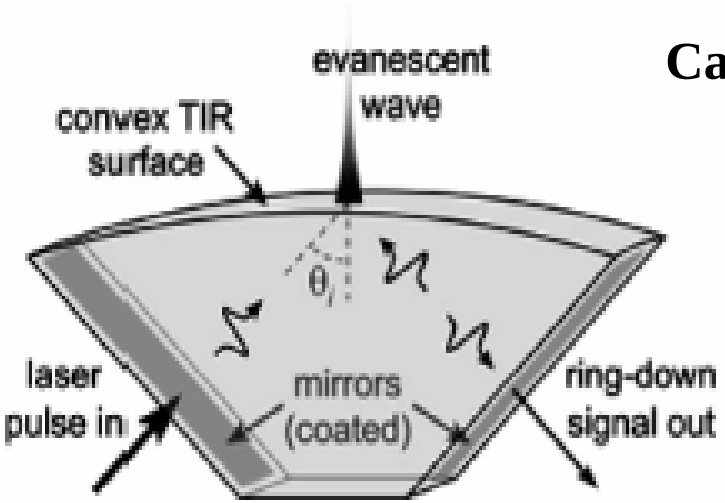

Cavity ring-down spectroscopy (CRDS)

* Ultrapure a-SiO_2: 2X2 cm^2 and thickness of 0.5 cm;
* Probed area: $\pi\sqrt{2}(85 \times 99)$ μm^2;
* Ambient temperature: 22 °C;
* Using the idler of a seeded-tripled-Nd: YAG-pumped optical parametric oscillator operating at 30 Hz, laser pulses (~0.5 mJ/pulse, 6 ns, linewidth < 10 cm^{-1});

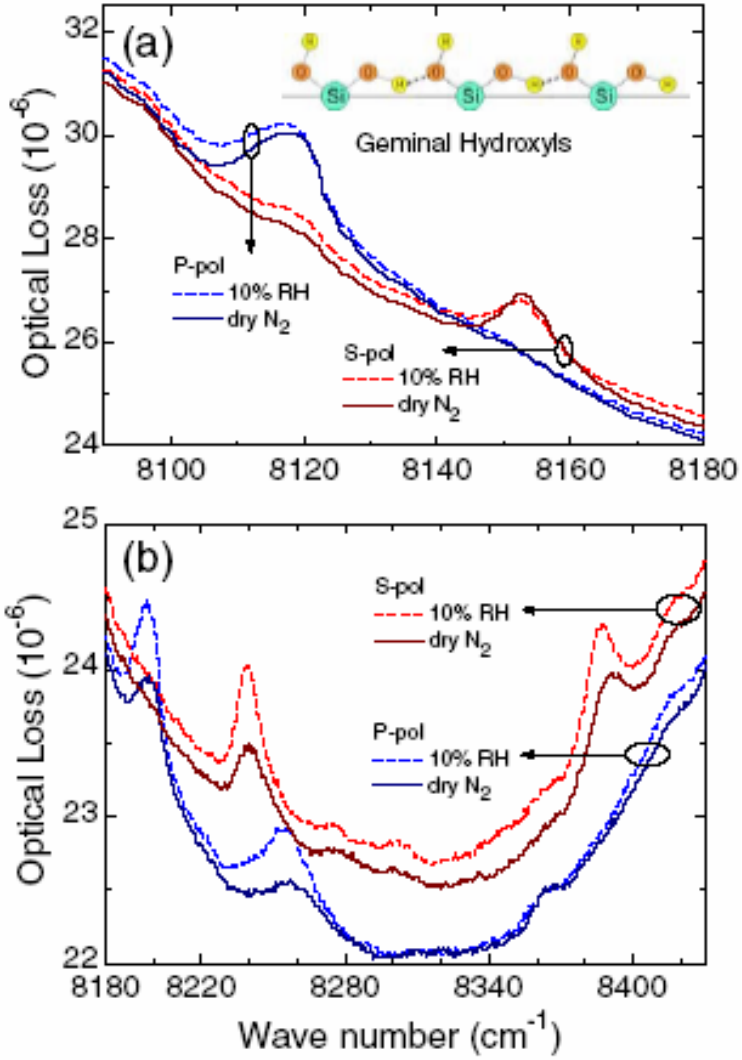

(a) Vibration-combination spectra of a-SiO_2 surface hydroxyls.
Peaks: 8119 and 8154 cm^{-1};

(b) Vibration-combination spectra of adsorbed water.
Peaks: 8199(p), 8241(s), 8260(p) and 8389(s) cm^{-1};

A coverage of ~1 monolayer of water is estimated at 10% RH.

Adsorbed water

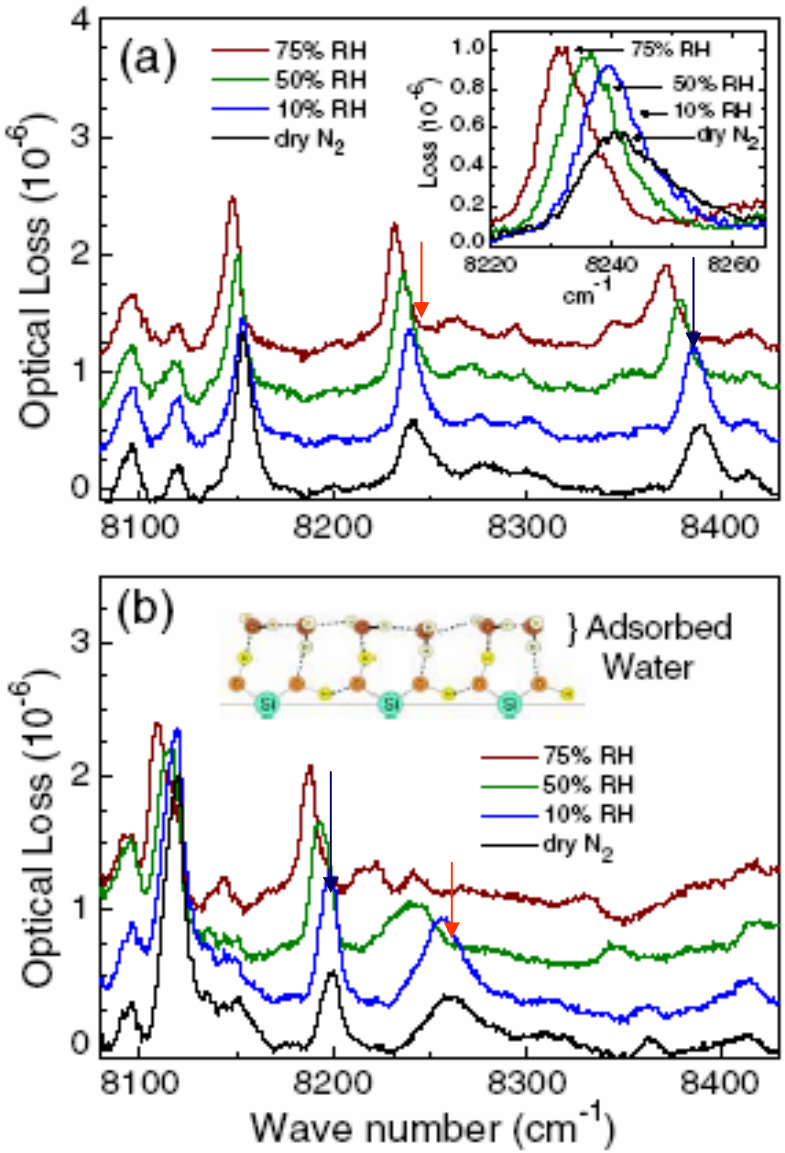

Exp: 2γOH+δOH;

8241(s)/8260(p), 8199(p), 8389(s)

Theo: γOH;

406(degenerate modes), 428, 456

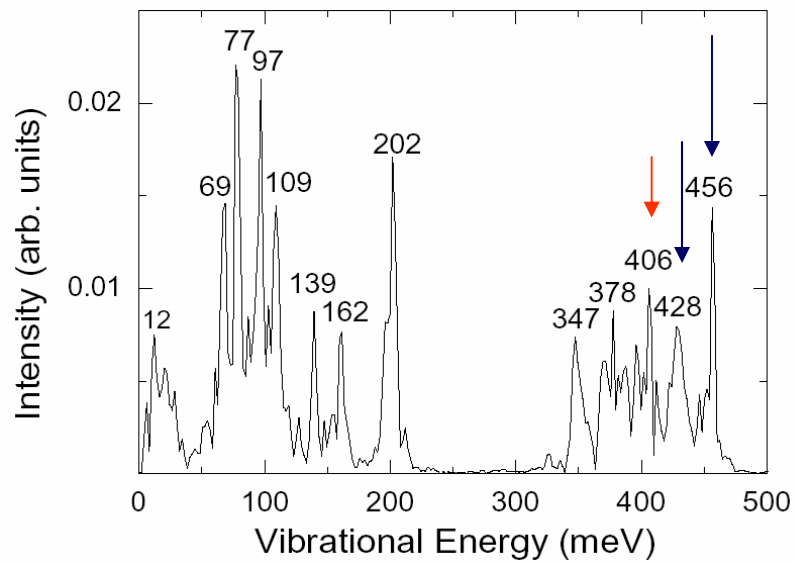

16760 *J. Phys. Chem. B* **2005**, *109*, 16760−16763

Evolution of the Adsorbed Water Layer Structure on Silicon Oxide at Room Temperature

David B. Asay and Seong H. Kim*

Department of Chemical Engineering, The Pennsylvania State University, University Park, Pennsylvania 16802

Received: June 7, 2005; In Final Form: July 7, 2005

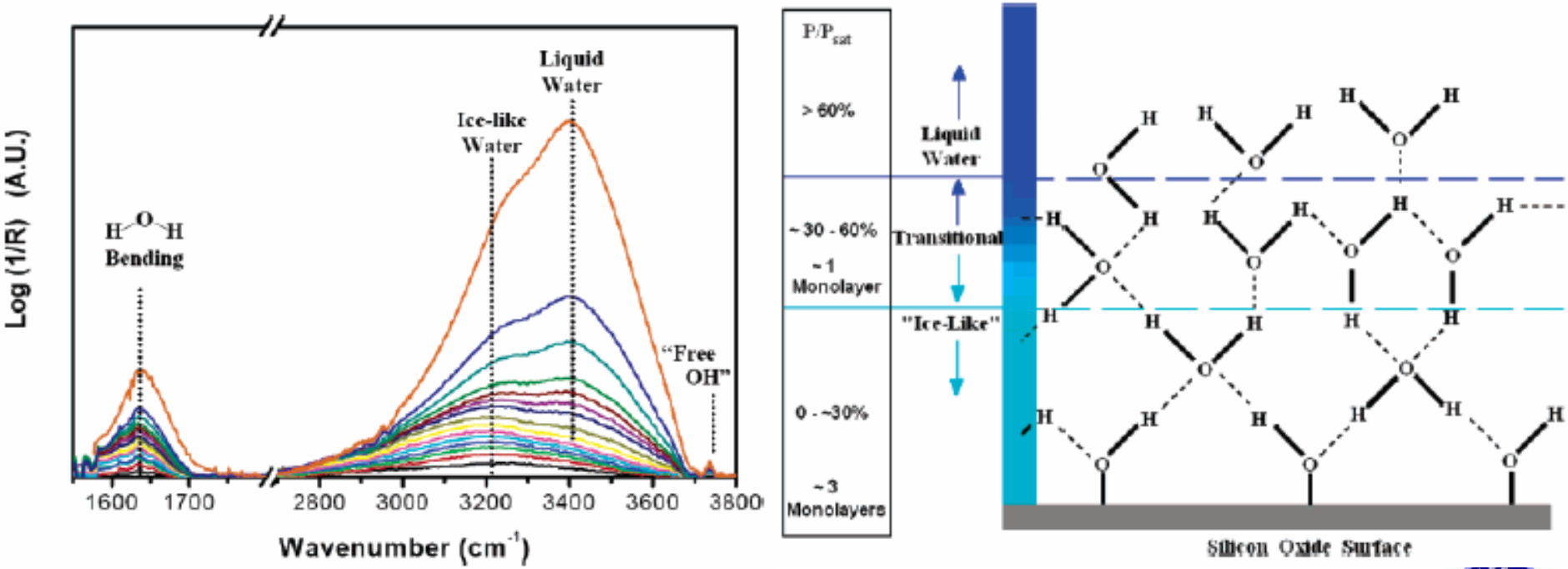

Hydrophilic and hydrophobic behavior

With Sheng Meng & Shiwu Gao

JCP 2003

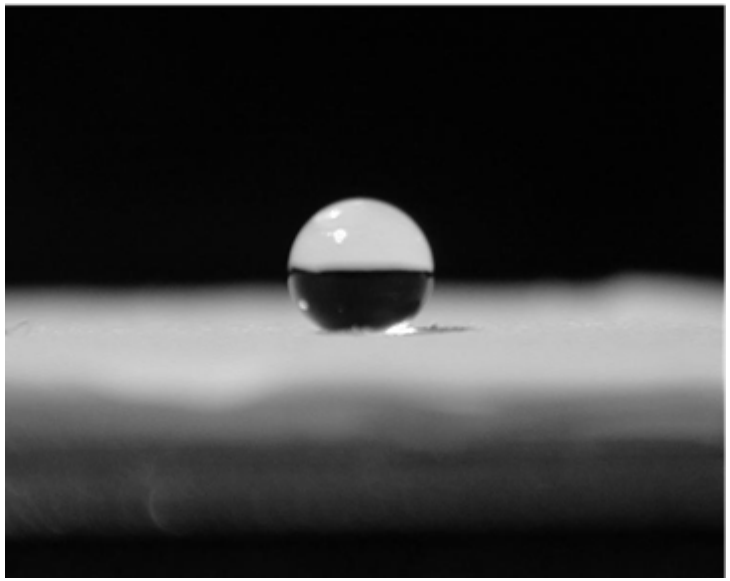

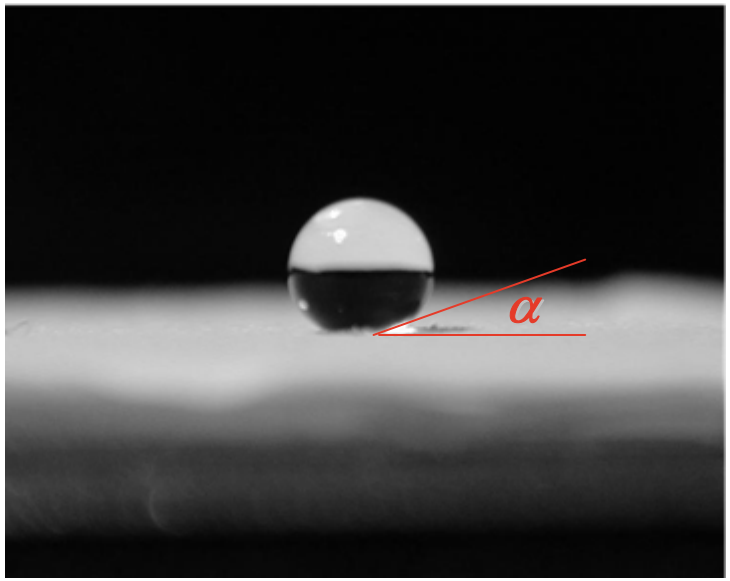

Is this behavior applicable at microscopic level?

Experiments

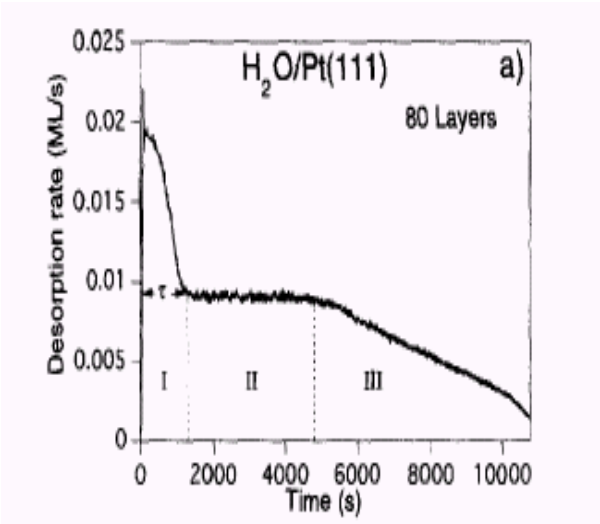

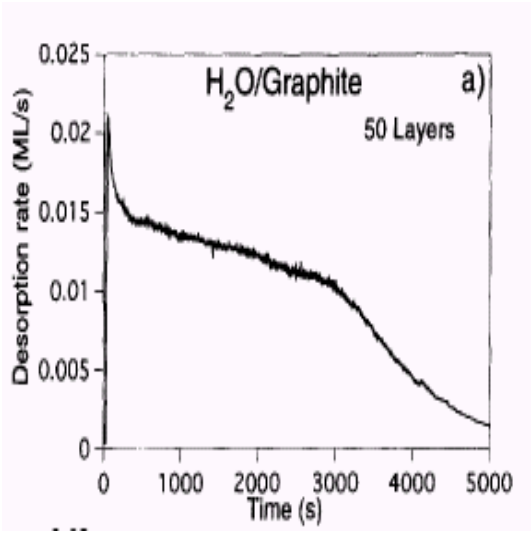

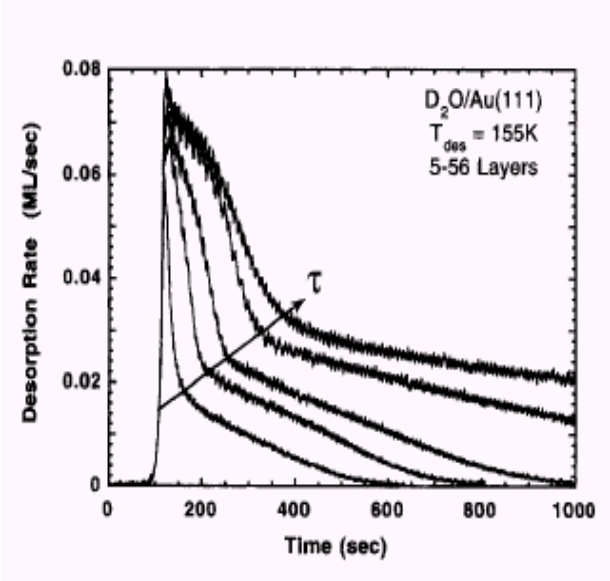

Wetting order:

Pt(111) >Ru(0001) >Cs/graphite >graphite > octane/Pt(111) > Au(111)

Surf. Sci. 367, L13; L19 (1996)

Gold and Platinum in Periodic Table

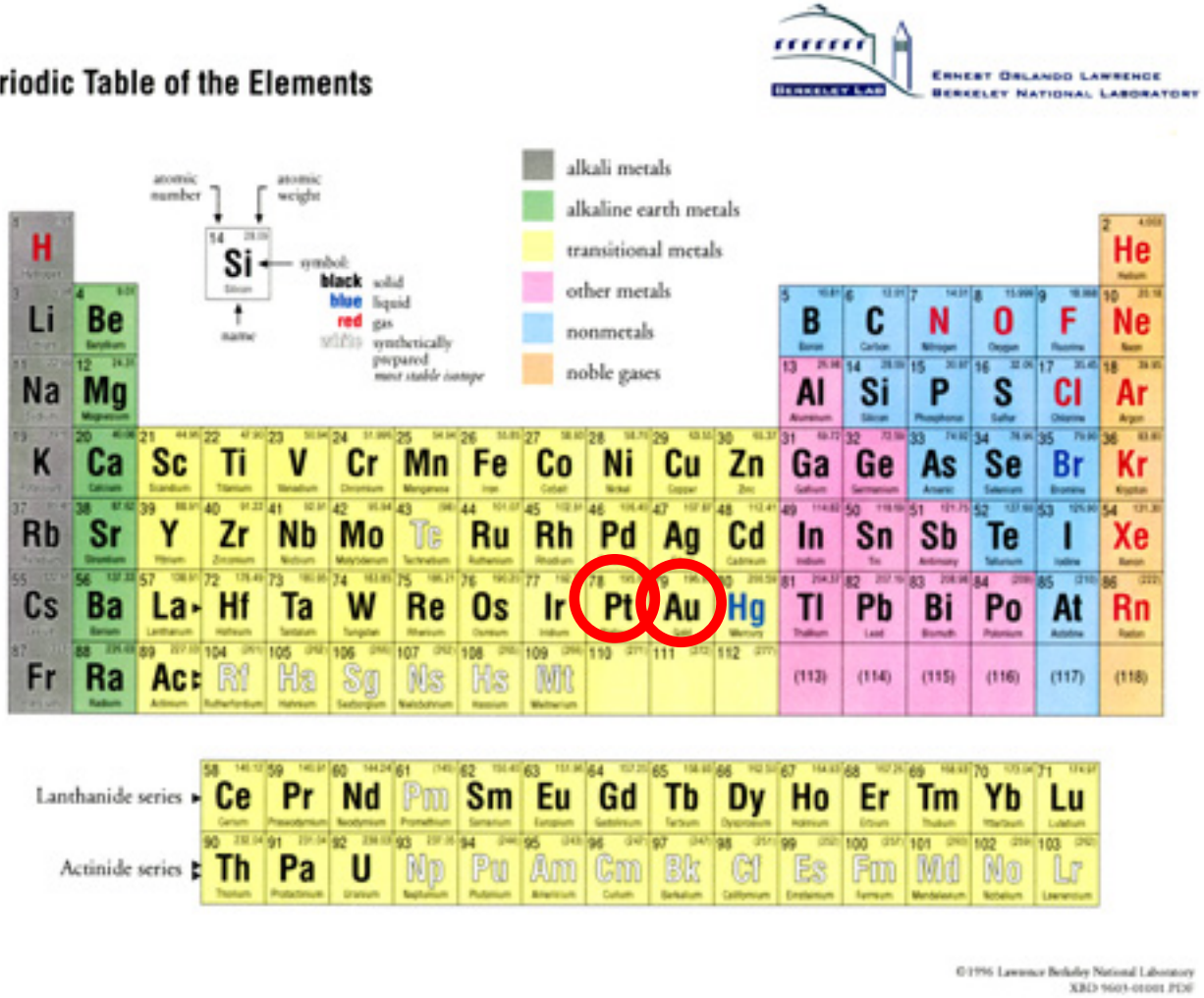

Adsoption Property of Various Water Candidates

Ads. species	Unit cell	n	E_{ads}(Pt)	E_{ads}(Au)	N_{M-H_2O}	N_{HB}	E_{HB}(Pt)	E_{HB}(Au)
monomer	3×3	1	304	105	1	0	-	-
dimer	3×3	2	433	259	2	1	258	308
trimer	3×3	3	359	283	3	3	55	178
hexamer	$2\sqrt{3} \times 2\sqrt{3}$	6	520	402	3	6	368	350
bilayer	$\sqrt{3} \times \sqrt{3}$	2	505/527	437/454	1	3	235	256
2 bilayers	$\sqrt{3} \times \sqrt{3}$	4	564	489	1	7	312	271
3 bilayers	$\sqrt{3} \times \sqrt{3}$	6	579	508	1	11	303	272
4 bilayers	$\sqrt{3} \times \sqrt{3}$	8	588	520	1	15	307	279
5 bilayers	$\sqrt{3} \times \sqrt{3}$	10	593	532	1	19	307	290
6 bilayers	$\sqrt{3} \times \sqrt{3}$	12	601	545	1	23	320	305

Vibrational Recognition

substrate		translations and librations					δ_{HOH}	ν_{O-HB}	ν_{O-H}
Pt	Theo.	18	32	53	69	87	198	388, 432	467
	Expt.[a]	16.5	33	54	65	84	201	424	455
Au	Theo.	17	36			108	201	400,444	455
	Expt.[b]		31			104	205	409	(452)[c]

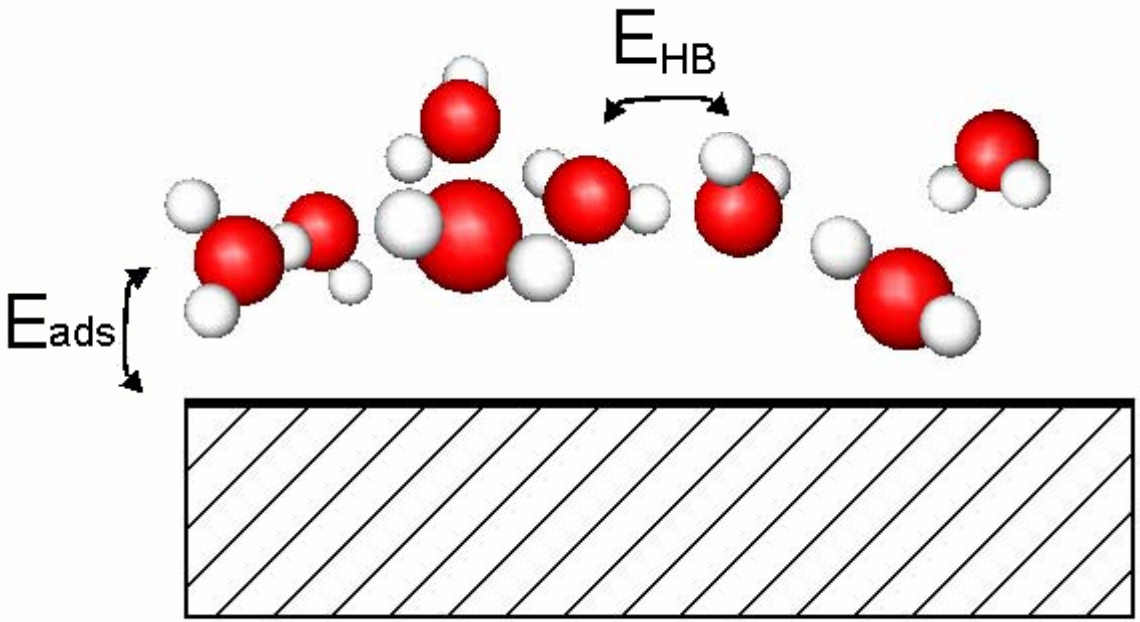
E_{HB}
E_{ads}

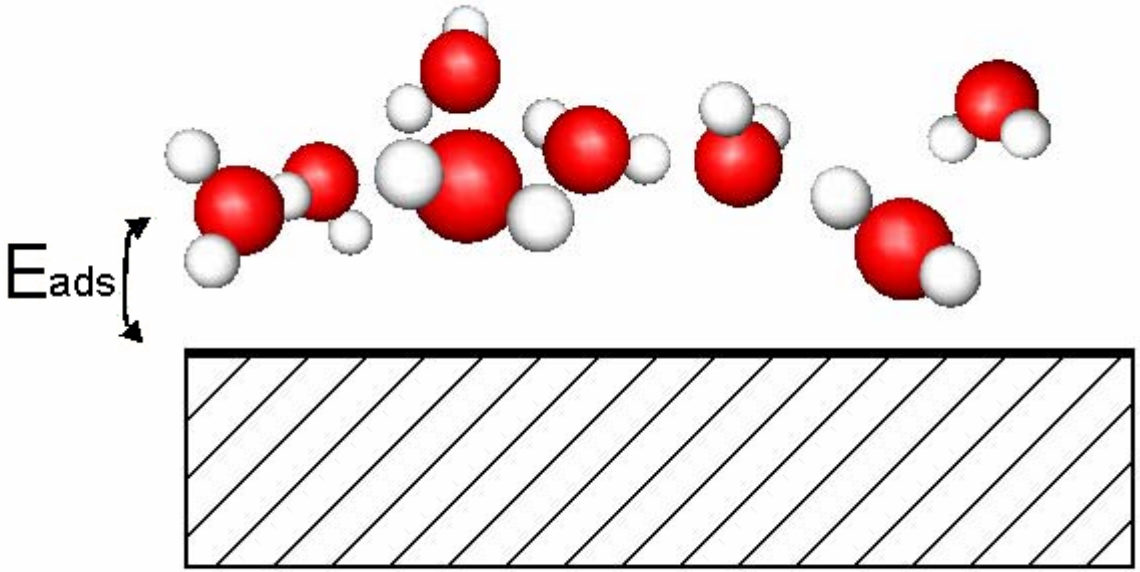
Eads

E_{ads}: the adsorption energy per molecule

$$E_{ads} = (E_{metal} + n \times E_{H2O} - E_{(H2O)n/Metal}) / n$$

Here $E_{(H2O)n/Metal}$ is the total energy of the adsorption system, E_{metal} and E_{H2O} are those for free a surface and a free molecule, respectively, and n is the number of water in the unitcell.

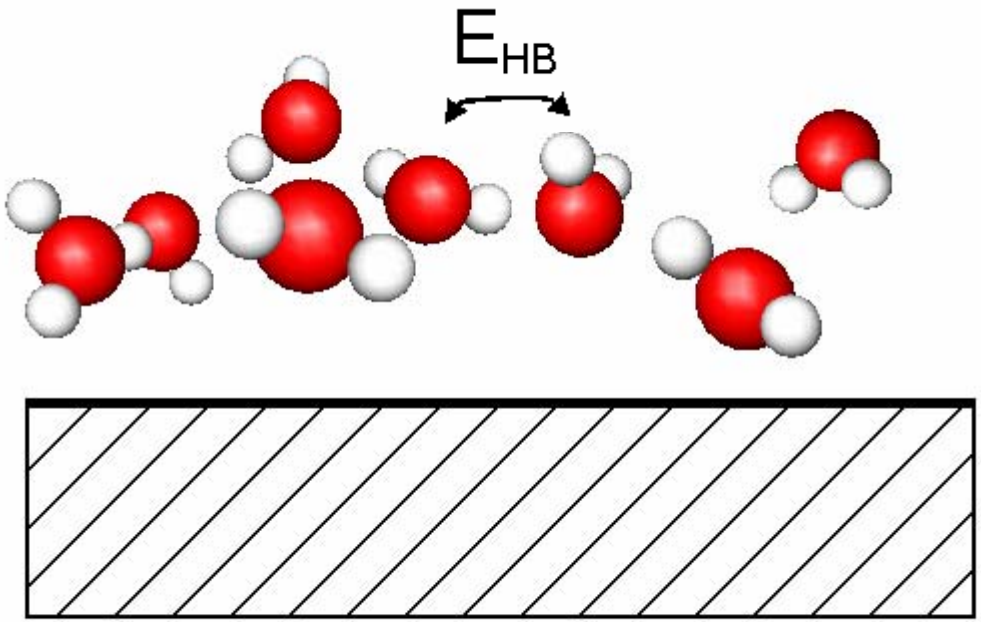
E_{HB}

E_{HB}: the strength of H-bond

$E_{HB} = (E_{ads} \times n - E_{ads}[\text{monomer}] \times N_{M\text{-}H2O}) / N_{HB}$,

for clusters and 1 BL;

or

$(E_{ads}[m\ BL] \times 2m - E_{ads}[(m-1)\ BL] \times 2(m-1)) / 4$,

for m BL, m> 1.

Here E_{ads}[monomer] and $N_{M\text{-}H2O}$ are the adsorption energy of monomer and the number of molecule-surface bonds in the water structures; and E_{ads}[m BL] is the adsorption energy for m bilayers.

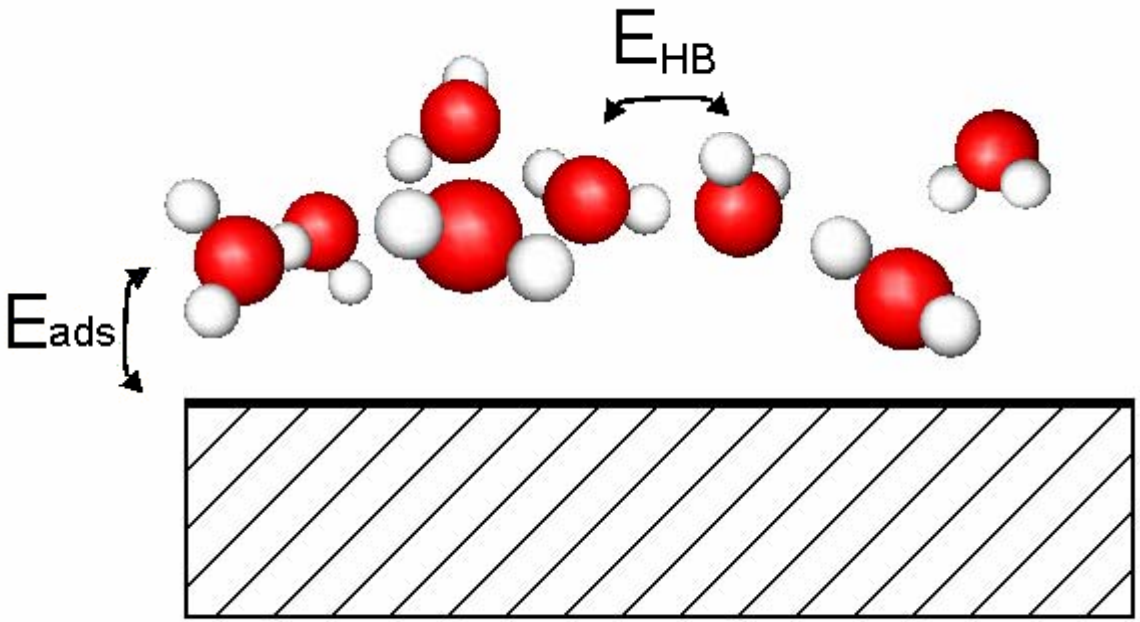

$$w = \frac{E_{HB}}{E_{ads}} = \begin{cases} > 1 & \textit{Hydrophobic} \\ < 1 & \textit{Hydrophilic} \end{cases}$$

Hydrophilic vs. Hydrophobic

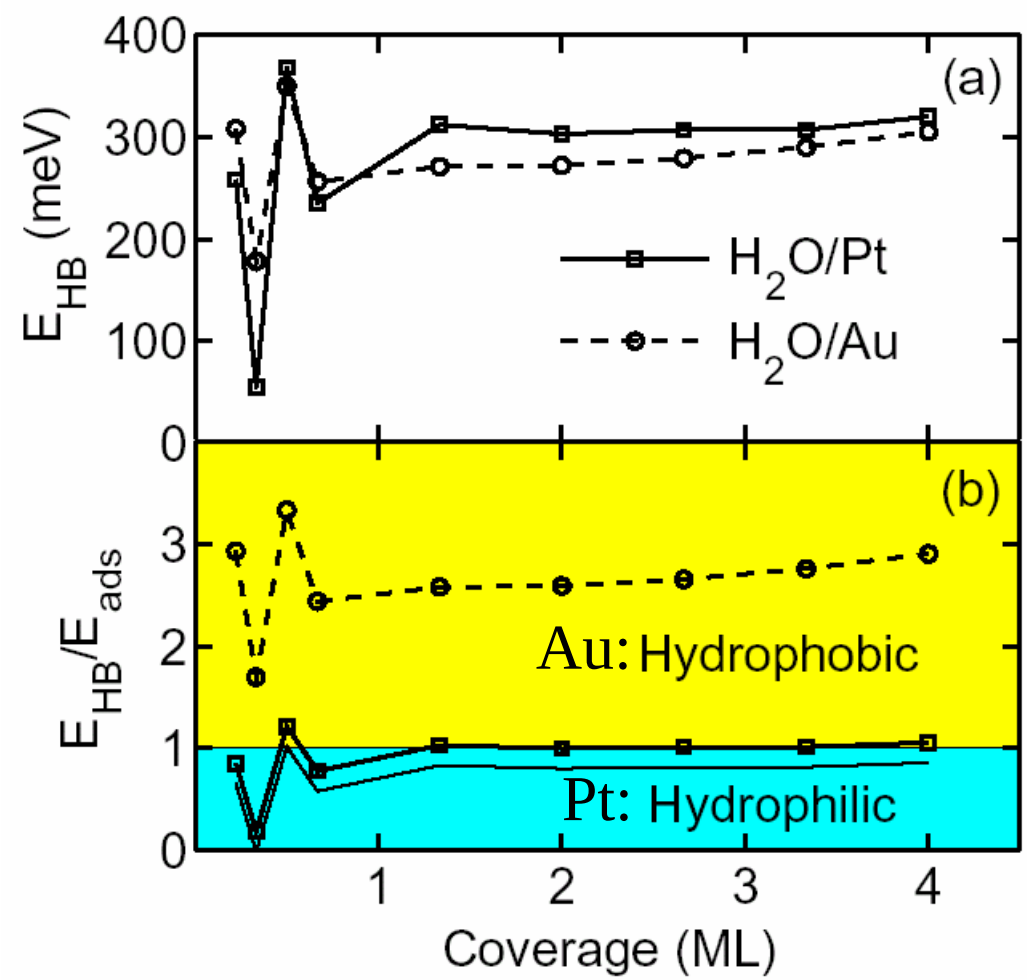

Charge Densities

Pt: d^9s^1
Au: $d^{10}s^1$

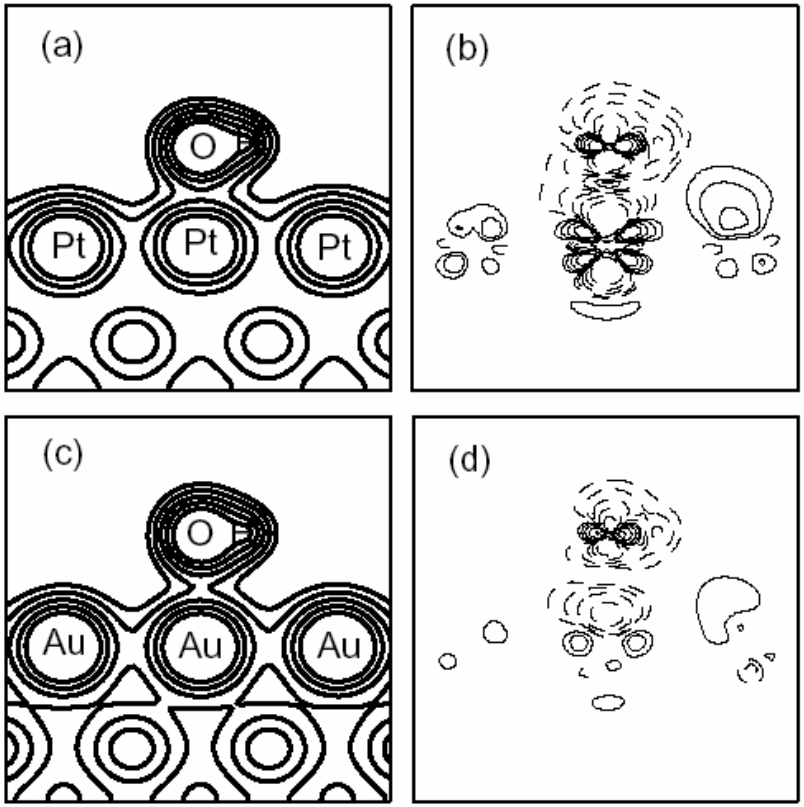

Wetting order

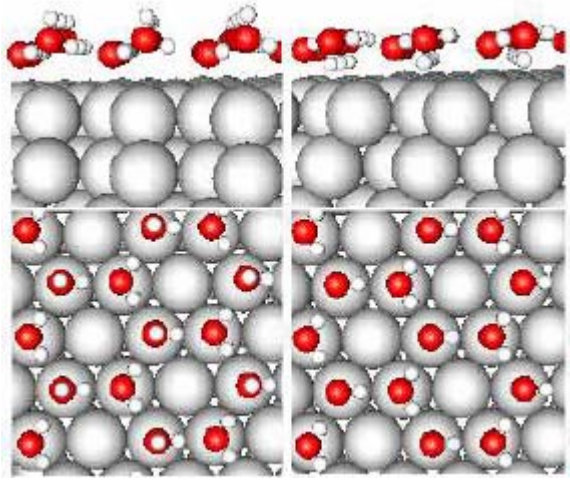

H-up H-down

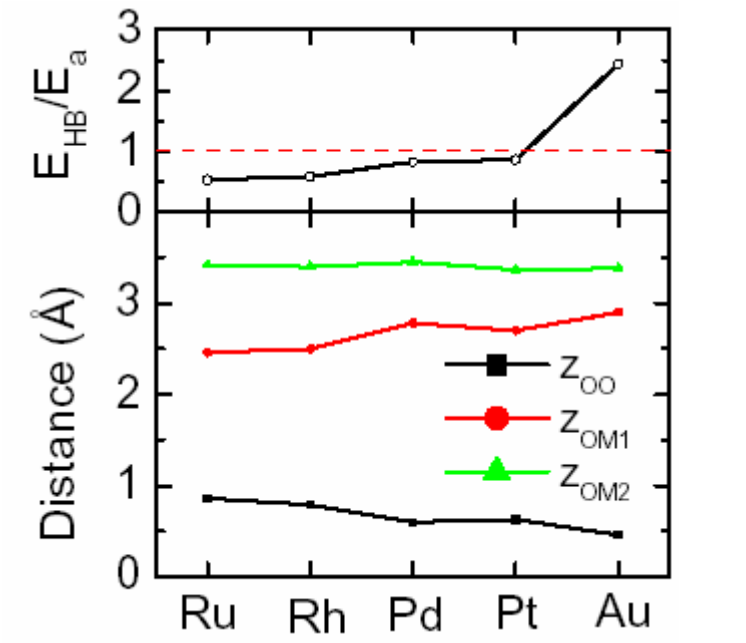

d^7s^1 d^8s^1 d^9s^1 d^9s^1 $d^{10}s^1$

Wetting order:

Ru > Rh > Pd > Pt > Au

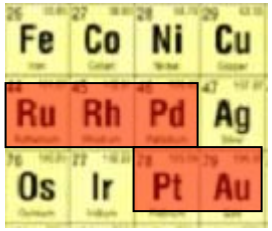

Results

- The hydrophilicity-hydrophobicity can be characterized by the water-surface coupling and the strength of the H-bond at the interfaces;
- The role of d-band of the substracts in participating the interaction upon water adsorption is important.

Water interaction with NaCl:

Adsorption, Dissolution and Nucleation

With <u>Yong Yang</u>

PRB 2006; PRE 2005; JPCM 2006

Water as Solvent:

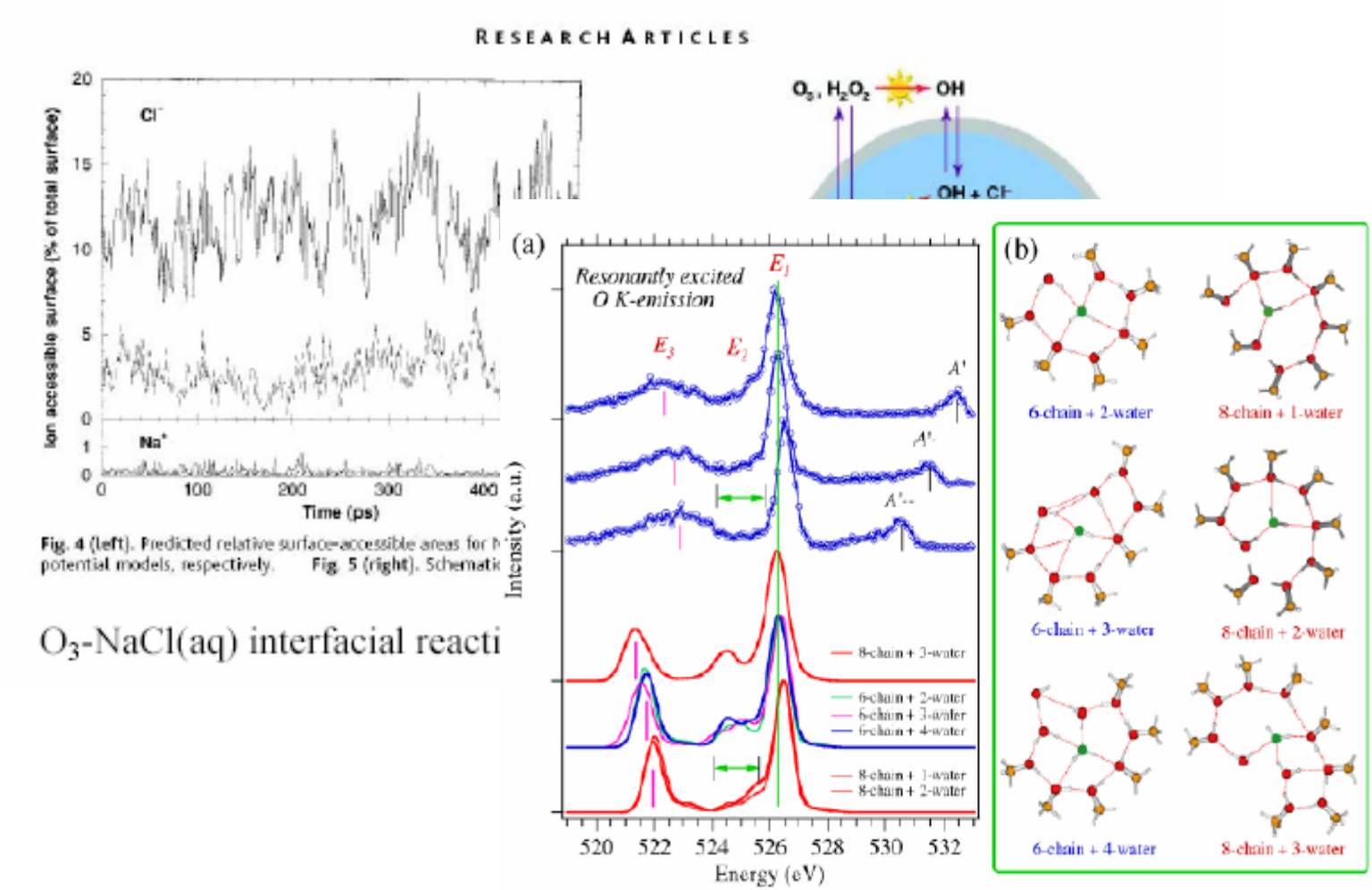

Methanol-Water solution, Guo *et al*, PRL 91,157401 (2003)

NaCl:

One of the most important crystals in daily life.

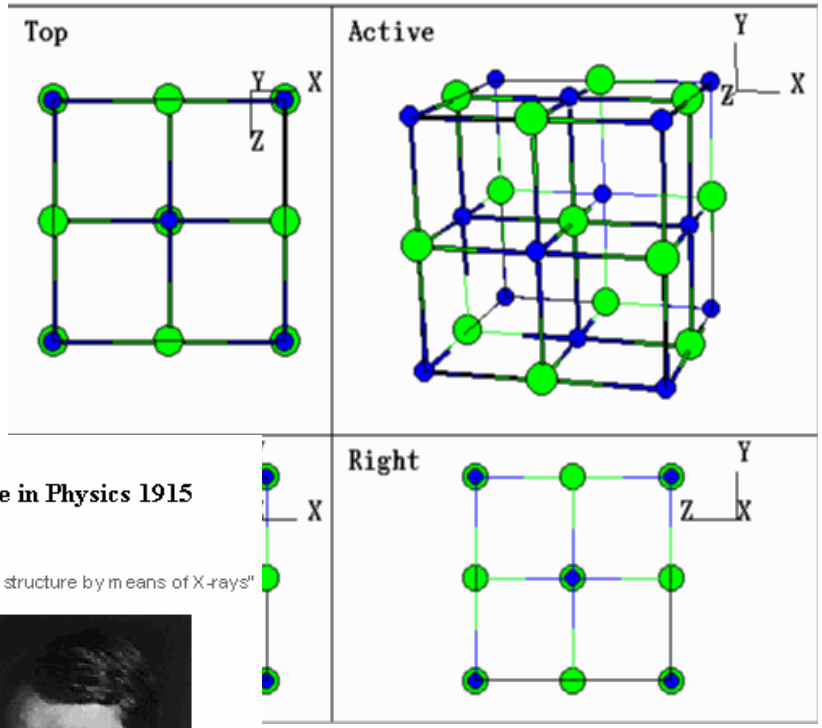

The Nobel Prize in Physics 1915

"for their services in the analysis of crystal structure by means of X-rays"

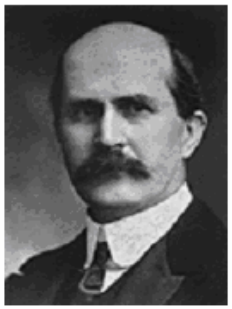

Sir William Henry Bragg

William Lawrence Bragg

NaCl: fcc

Lattice Constant:

5.64 Å (Exp)

5.67 Å (Theo)

OCTOBER 15, 1936 PHYSICAL REVIEW VOLUME 50

Electronic Energy Bands in Sodium Chloride

WILLIAM SHOCKLEY, *George Eastman Research Laboratory of Physics, Massachusetts Institute of Technology*

(Received July 27, 1936)

The Wigner and Seitz method of cellular potentials has been applied to the calculation of wave functions in NaCl. A renormalized Hartree field has been used around the Cl and the Prokofjew field around the Na. The relative heights of the potentials are determined by use of Madelung's number. The problem of joining the functions at the cell boundaries has been treated by the Slater method of fitting ψ and ψ' at midpoints. For the outer Cl electrons a reasonable approximation is to join at Cl−Cl midpoints only. This gives rise to a face-centered lattice for which solutions of the Slater conditions have been found by Krutter. Several new solutions have been derived which allow fairly accurate energy contours in momentum space to be drawn for the Cl $3p$ band. If the joining is made at Cl−Na midpoints alone, a large number of unsatisfactory zero-width bands arise. When both Cl−Cl and Cl−Na midpoints are used, the boundary conditions can be treated only for special cases. For these they are consistent with the Cl−Cl solutions. Several attempts to calculate the ultraviolet absorption frequency are described and the difficulties involved are discussed.

I. INTRODUCTION*

THERE has been a great advance in the calculation of wave functions in solids in the last four years. The initial impetus was derived from the contributions of Wigner and Seitz.[1] From a consideration of the Pauli principle they concluded that an electron in a monovalent metal

* The writer is indebted to Dr. Seitz for discussions of this paper and that by Douglas H. Ewing and Frederick Seitz. The viewpoints of the two papers differ in that the ionic picture of the lattice has been adhered to in this paper and no attempt to obtain a self consistent field has been made.

[1] Wigner and Seitz, Phys. Rev. **43**, 804 (1933).

What happens when water meets NaCl?

H_2O monomer on NaCl (001)

The most stable configuration

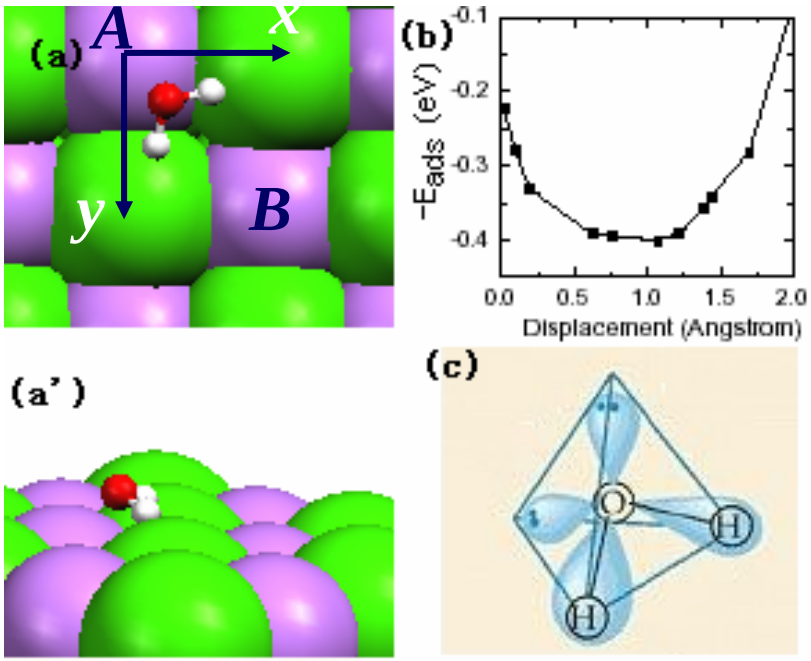

E_{ad} = 0.401 eV

α = -27°

ΔO_{xy} = 1.1Å

H_2O monomer on NaCl (001)

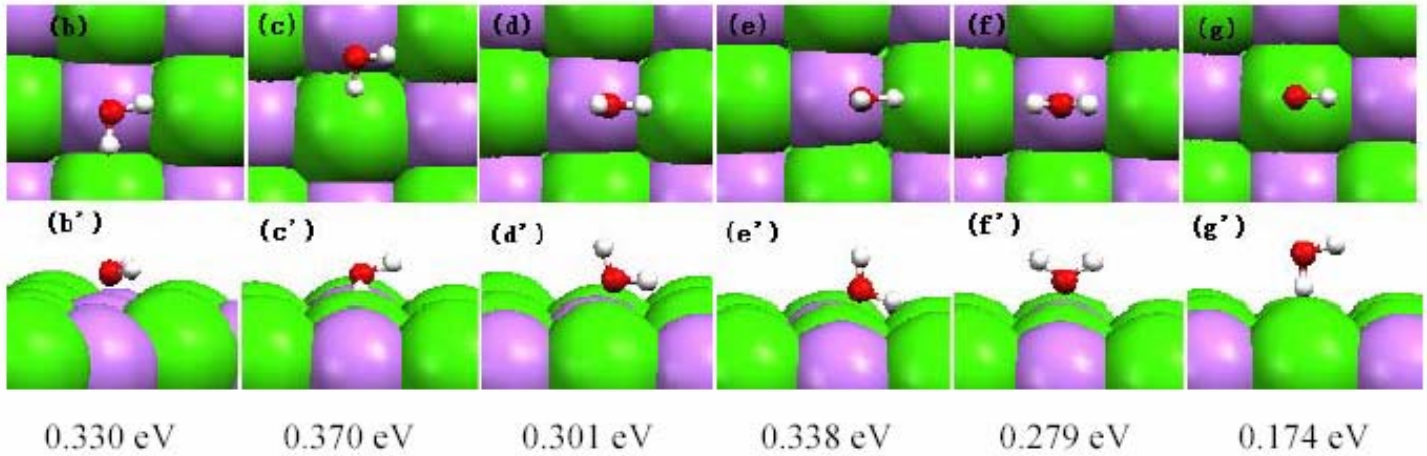

Bond strength: O - Na > H - Cl

Adsorption energy: lying > standing

H_2O monomer on NaCl (001)

Vibrational recognition of 3 typical configurations

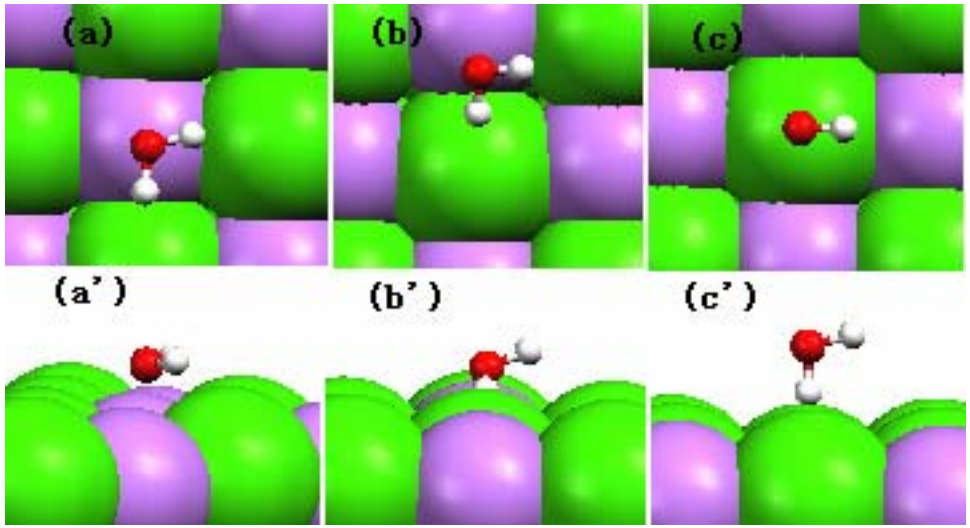

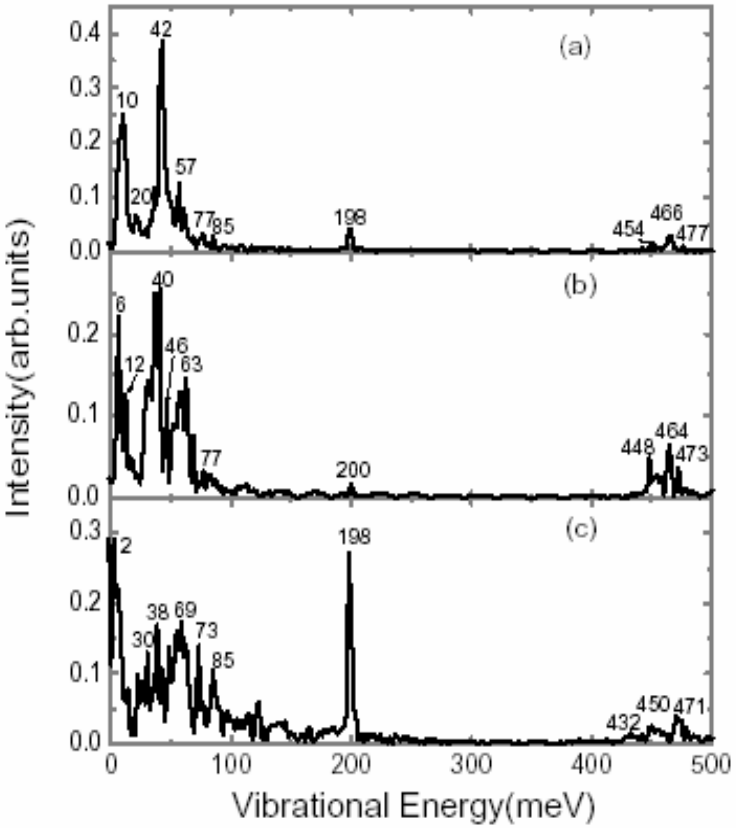

Strength of H-Bond:

(a) < (b) < (c)

H_2O dimer on NaCl (001)

The most stable water dimer on NaCl (001)

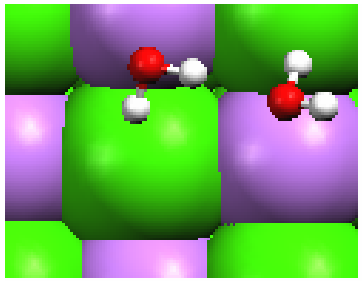

proton donor: $d_{H_2-Cl} = 2.388\,\mathring{A}$ $d_{O-Na} = 2.430\,\mathring{A}$

proton acceptor: $d_{H_2-Cl} = 2.218\,\mathring{A}$ $d_{O-Na} = 2.917\,\mathring{A}$

hydrogen bond: $d_{H\ldots O} = 1.973\,\mathring{A}$ $d_{O\ldots O} = 2.873\,\mathring{A}$

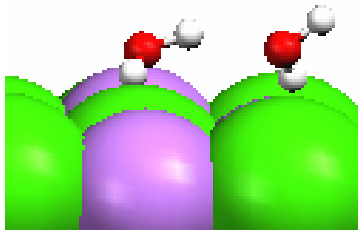

$E_{ads} = 0.819$ eV

$E_{H-Bond} = 0.203$ eV

$E_{sw} = 0.616$ eV

For two free water molecules, $E'_{ads}=2\times0.401=0.802$eV.

H_2O dimer on NaCl (001)

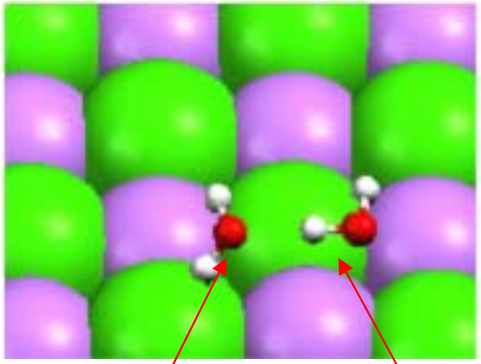

$E_{ads} = 0.402$ eV $E_{H-Bond} = 0.178$ eV $E_{sw} = 0.224$ eV

proton donor: $d_{O-Na} = 3.056 Å$

proton acceptor: $d_{H_1-Cl} = 2.201 Å$

hydrogen bond: $d_{H\cdots O} = 1.774 Å$ $d_{O\cdots O} = 2.758 Å$

H acceptor H donor

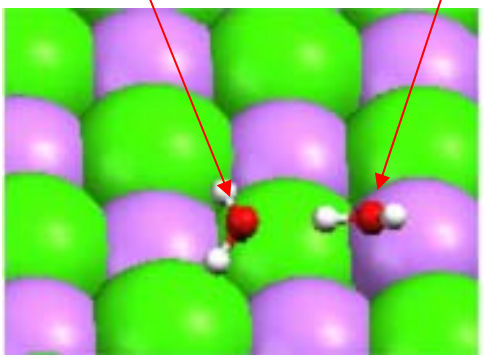

$E_{ads} = 0.569$ eV $E_{H-bond} = 0.227$ eV $E_{sw} = 0.342$ eV

proton donor: $d_{O-Na} = 2.545 Å$

proton acceptor: $d_{H_1-Cl} = 2.241 Å$

hydrogen bond: $d_{H\cdots O} = 1.848 Å$ $d_{O\cdots O} = 2.838 Å$

The strength of H-bond is affected by E_{sw} of H donor

1 ML H_2O on NaCl (001)

E_{ads}=0.394eV

E_{ads}=0.387eV

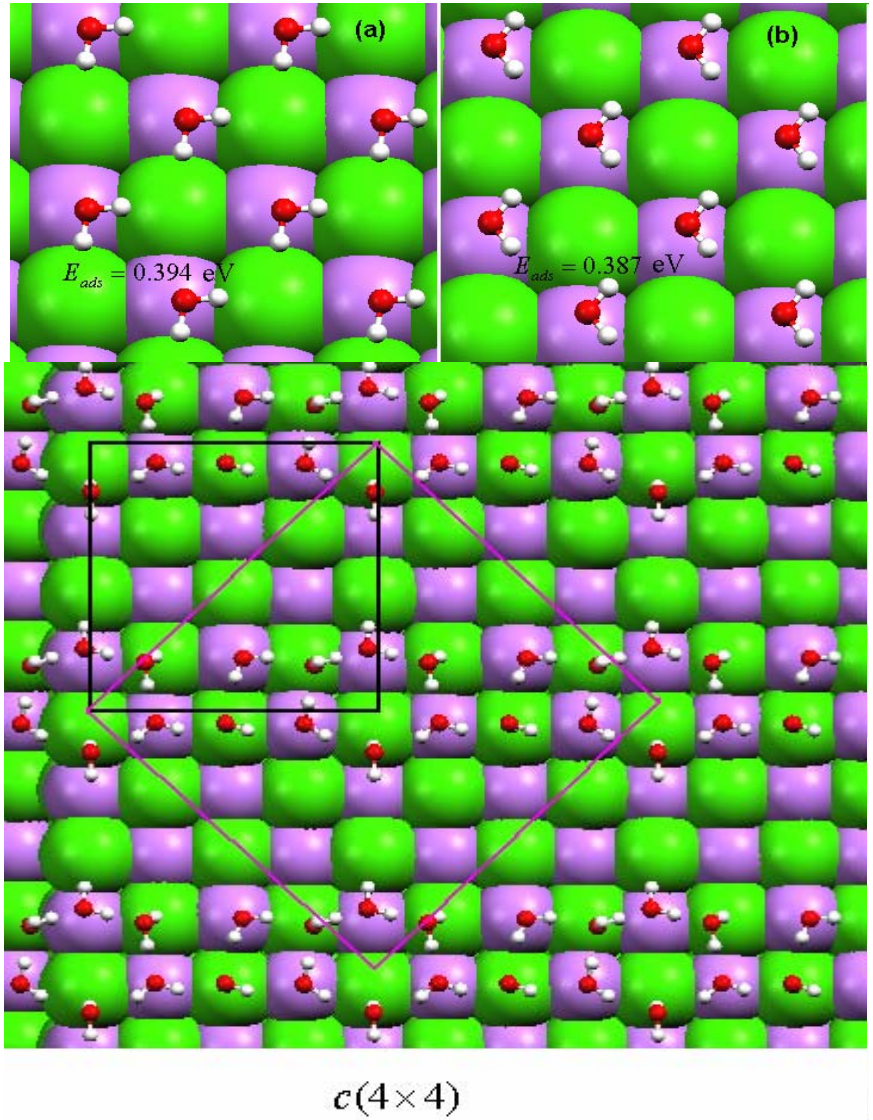

E_{ads}=0.347eV

E_{ads}=0.477eV

Start from (d), MD at 80 K get to (e) ,(f)—H-Bond Ring, newly predicted for 1 ML H_2O on NaCl (001).

E_{ads}=0.519eV

E_{ads}=0.500eV

1.5 ML H_2O on NaCl (001)

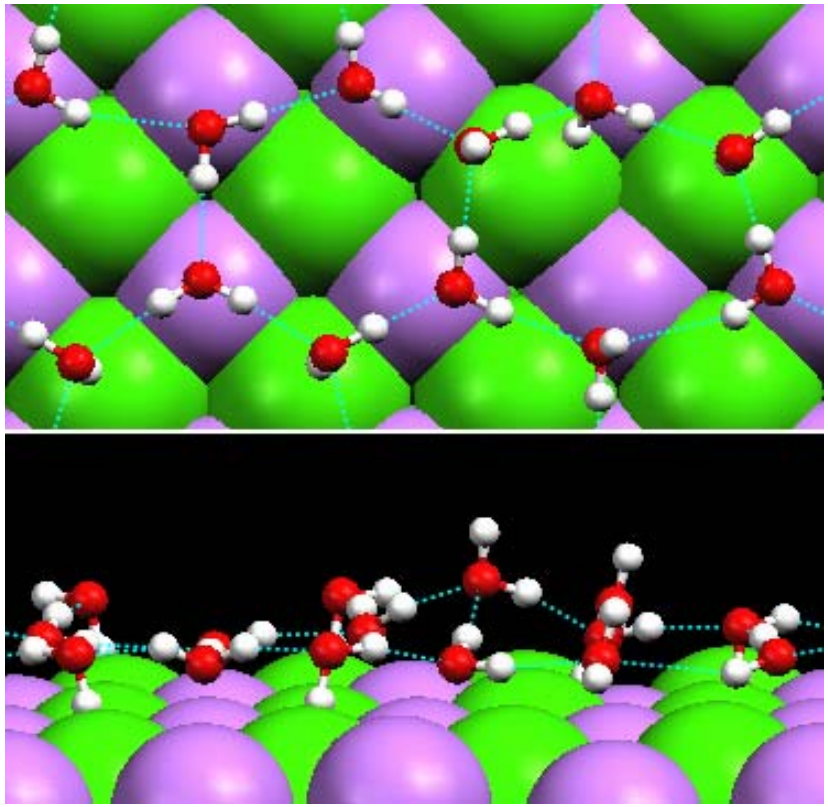

Hexagonal water ring with trilayer in (001) direction

2 ML H_2O on NaCl (001)

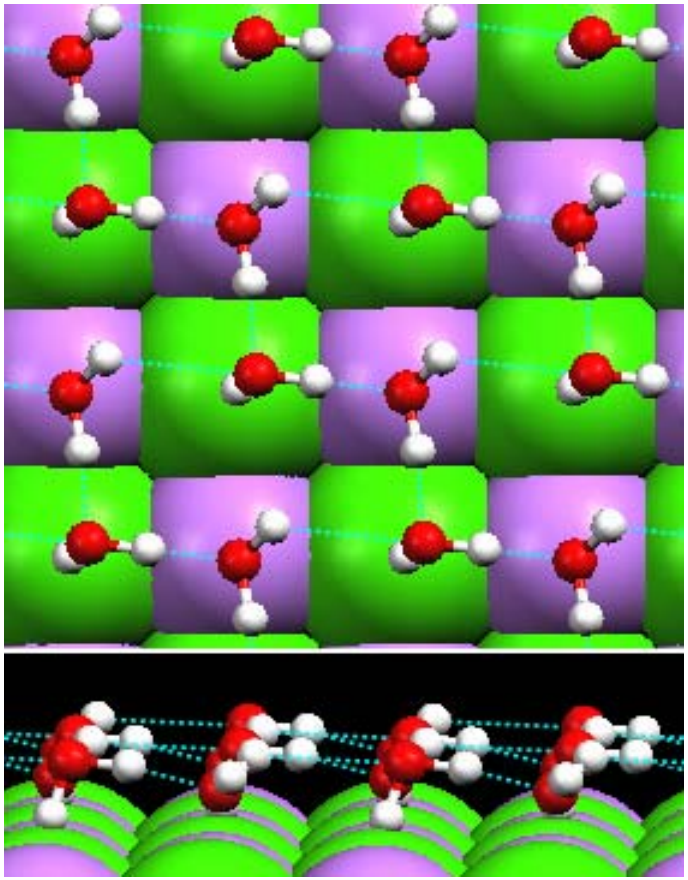

Bilayer, 2D ice-like

Comparison of E_{ws} and E_{ww}

The water-surface interaction E_{ws} is decreased with coverage.

The water-water interaction E_{ww} is increased with coverage.

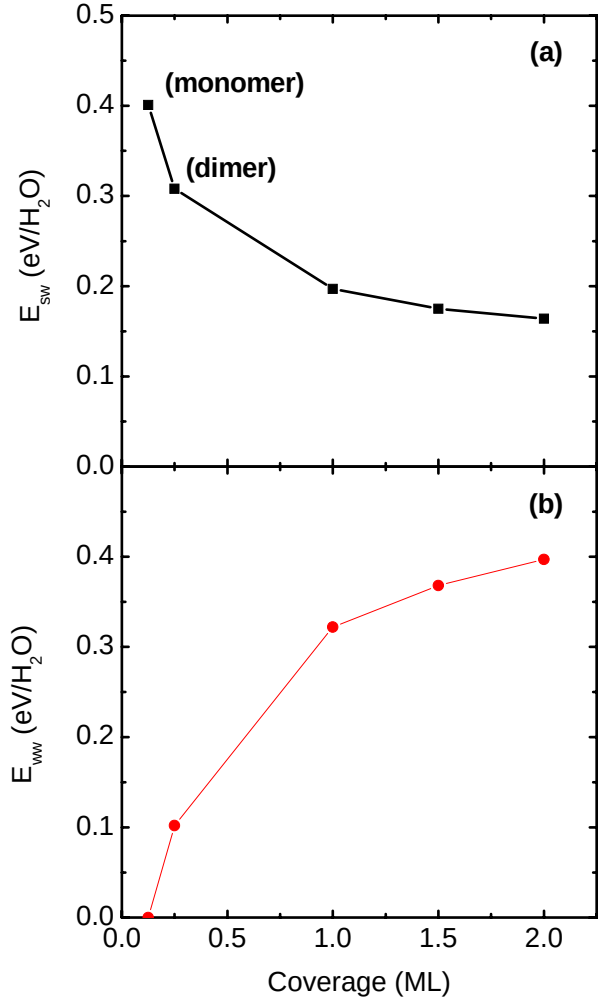

For $\theta \geq 1$ ML, $E_{ww} \geq E_{sw}$, which indicats NaCl(001) surface is a hydrophobic-like surface.

Summery

A H_2O monomer, where O is near Na and H adjacent to Cl, tends to lie on NaCl (001) surface with a tilted dipole plane.

The hydrogen bond affects the adsorption of a H_2O dimer significantly.

For 1 ML, 1.5 ML, and 2 ML H_2O on NaCl (001), the water-surface interaction is reduced, while water-water interaction is enhanced with the increase of water coverage.

Dissolution

From *ab initio* calculations, at least six water molecules are needed to dissolve a NaCl pair.

Side view

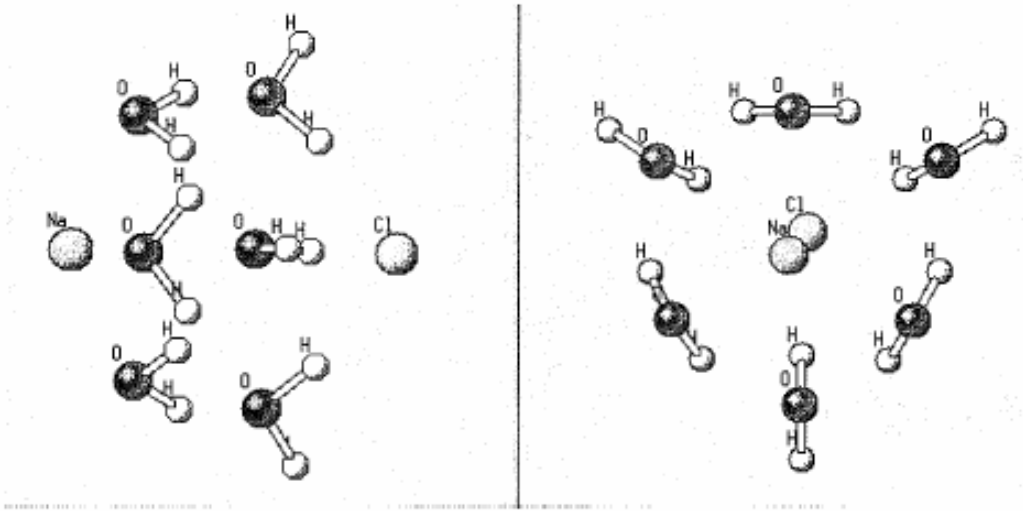

Top view

How about a nanocrystal ?

Dissolution

- Classical MD performed by AMBER package with TIP3P model.
- System investigated: 625H_2O (liquid state) + 32NaCl.
- NTP: ~350 K, ~1 bar.

Size of unitcell :
27.86Å×27.88Å ×27.50Å

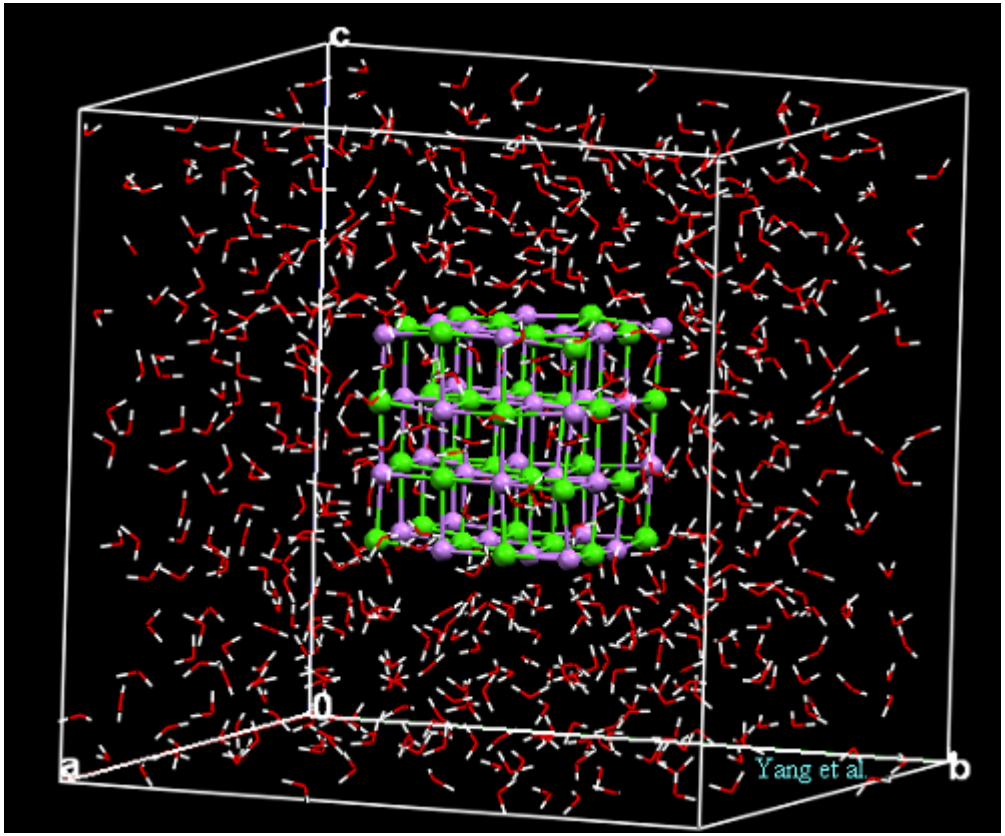

Cl^- Na^+ H_2O

Before Dissolution

Radial distribution of water around nanocrystal

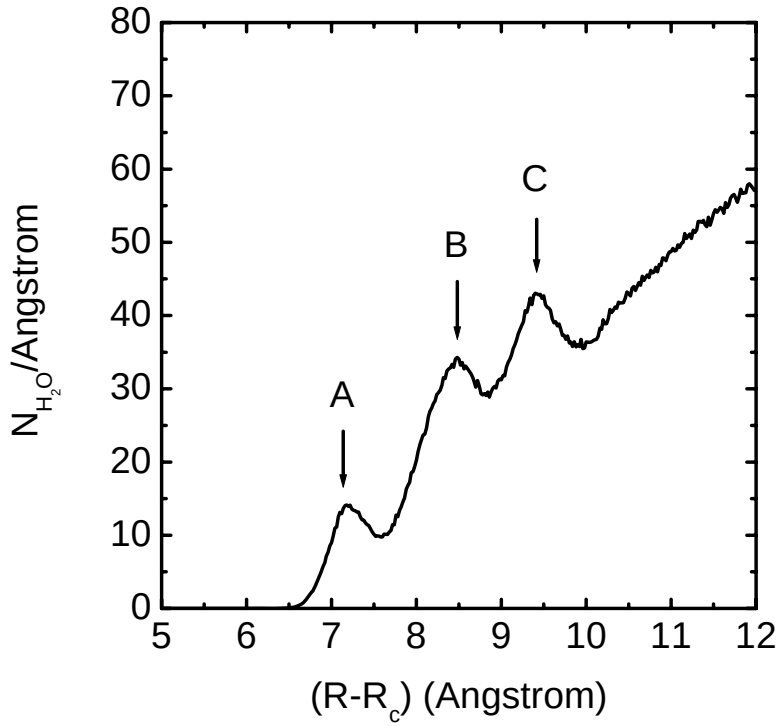

A: (100) faces, B: edge sites, C: corner sites

Dissolution sequences:

Cl^-, Na^+, Cl^-, Na^+…

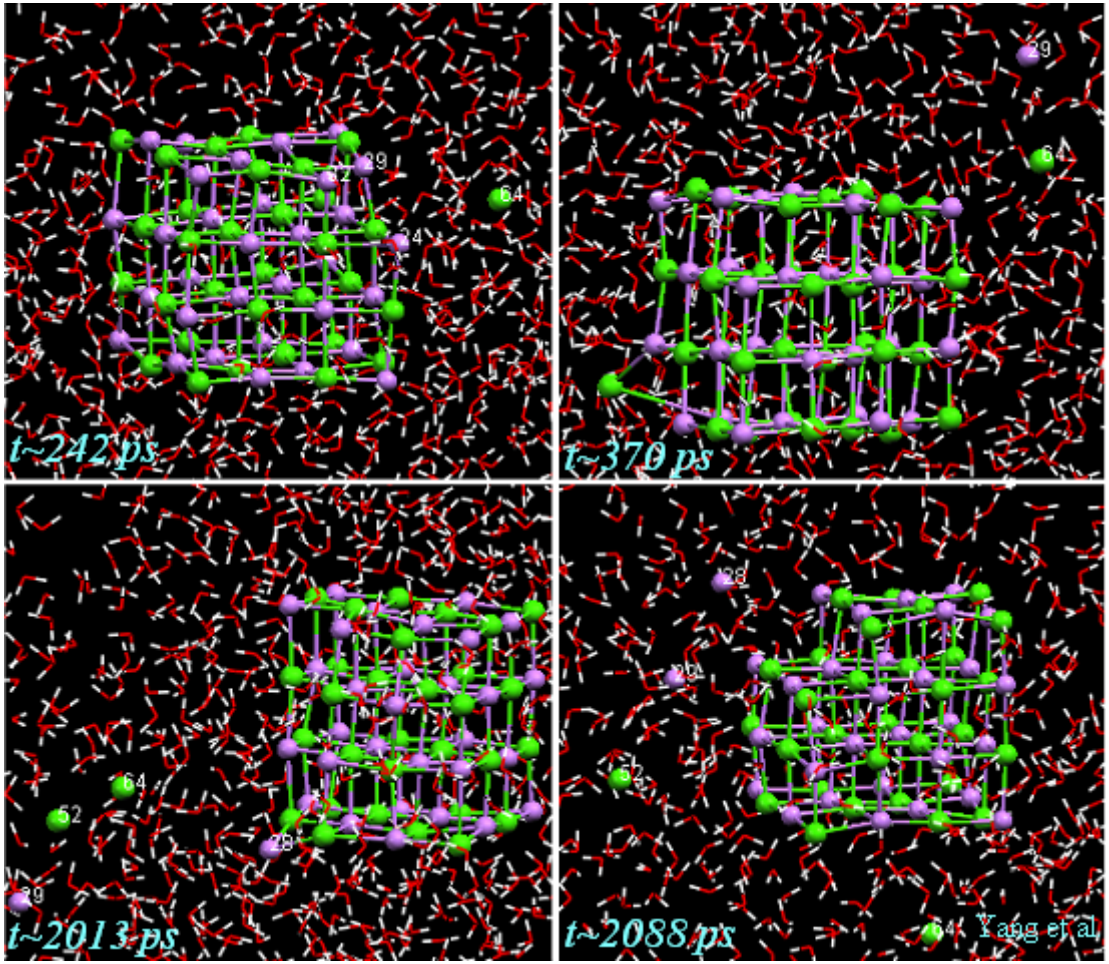

Superscripts:

1~32 for Na^+

33~64 for Cl^-

Role of water & dissolution pathway

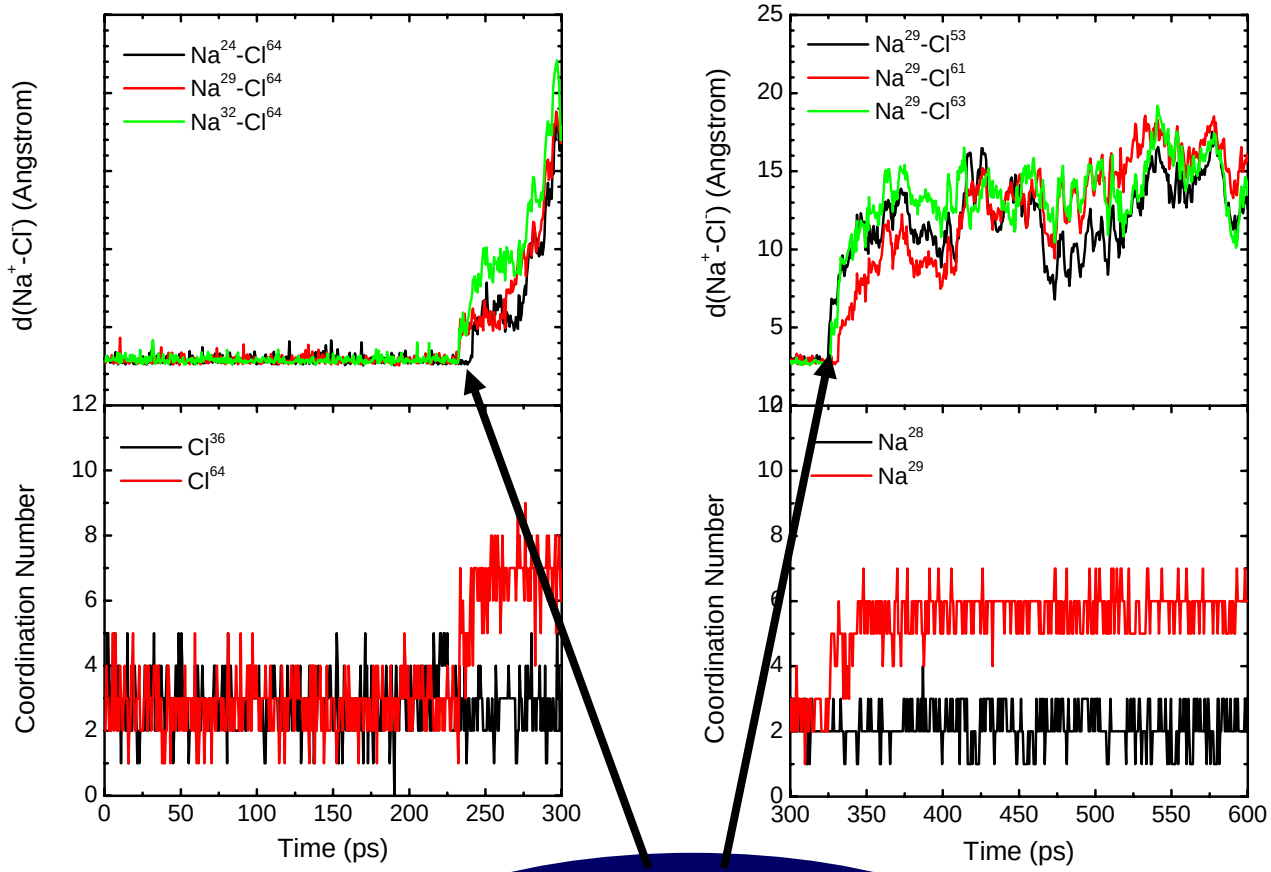

Breaking two of the three ionic bonds simultaneously !

Pathway

Site and orientation selection in the early stage of dissolution: corner sites, $[11\bar{1}]$ direction.

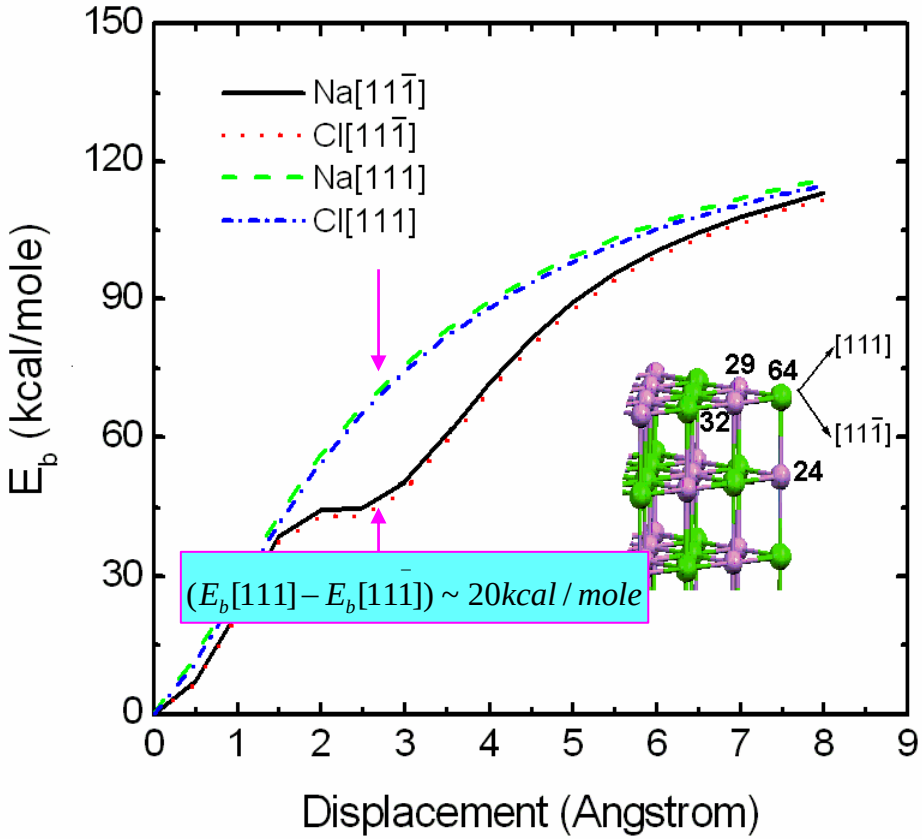

Kinetic Energy Distribution

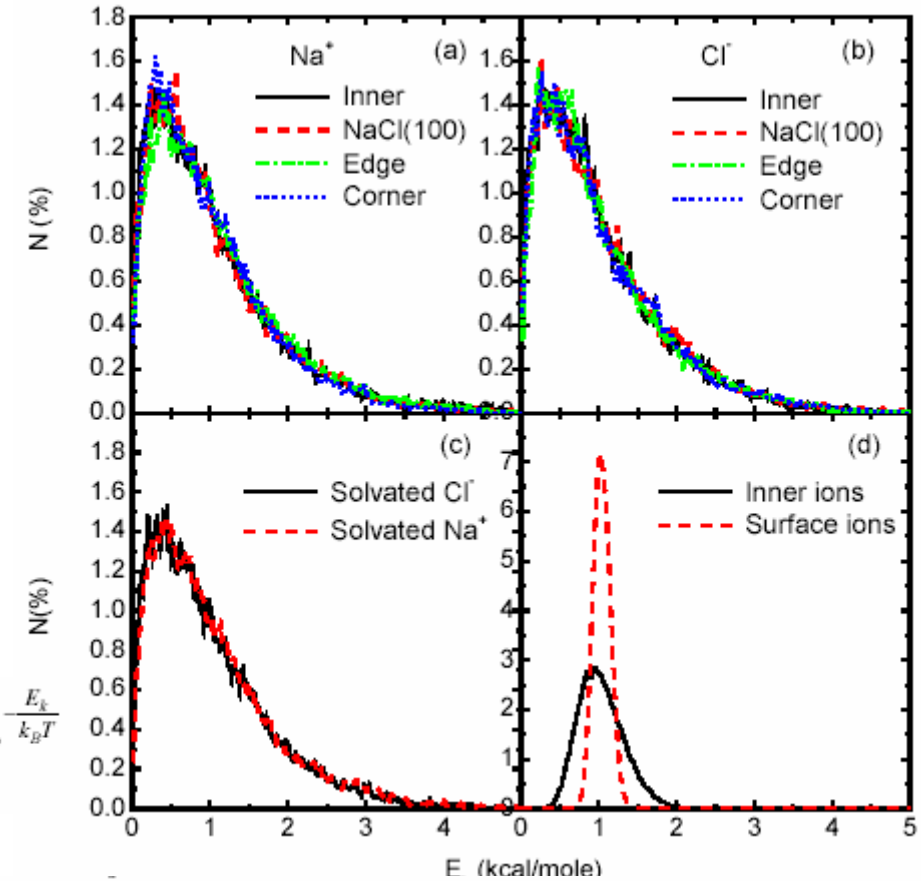

$$p_1(E_k) = 2\pi\left(\frac{1}{\pi k_B T}\right)^{\frac{3}{2}} \sqrt{E_k} \cdot e^{-\frac{E_k}{k_B T}}$$

$$p_n(E_k) = A^n \frac{\sqrt{\pi^n}}{2^n \Gamma(\frac{3}{2}n)} E_k^{\frac{1}{2}(3n-2)} e^{-BE_k} = \frac{1}{\Gamma(\frac{3}{2}n)} \left(\frac{1}{k_B T}\right)^{\frac{3n}{2}} E_k^{\frac{1}{2}(3n-2)} e^{-\frac{E_k}{k_B T}}, \quad (n>1)$$

Why does Cl^- dissolve prior to Na^+ ?

* The difference of dissolution barrier (E_b + $E_{hydration.}$) is very small. (Cl^- slightly lower than Na^+).

* Local density of water around the ions is the key factor.

Hydration structures

Hydration structures of Na^+, Cl^- ions : Radial Distribution Functions (RDFs).

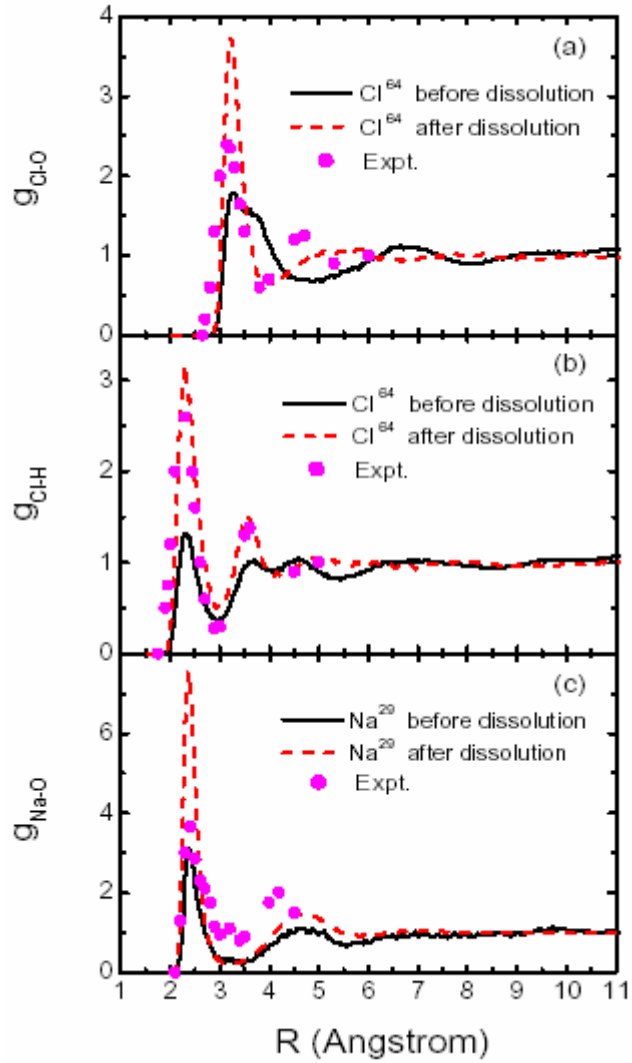

Summery

- The atomic process of NaCl dissolution in water shows a sequence of Cl^-, Na^+, Cl^-, Na^+…
- The process starts from the corner sites and prefers in the $[111]$ direction.
- The local structure of water molecules around the Na^+, Cl^- ions plays important role in the early stage of dissolution.
- The kinetic energy distribution of a group particles is independent of bonding environment, but dependent on the temperature and the number of particles.

A typical example: NaCl

- **Spontaneous nucleation of NaCl in supersaturated solution — irregular shape, Na^+ serves as center of stability in early stage.**

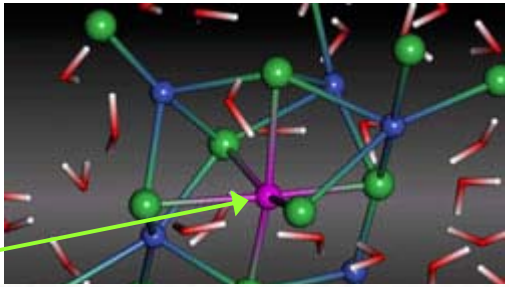

- **A more important case: Nucleation at solid-liquid interface**

Nucleation

Classic MD simulation in AMBER 6.0 package.

A five-layer NaCl (001) slab with 160 NaCl units.

At room temperature, in the supersaturated salt solution:

$$N_{NaCl} : N_{H2O} \sim 1 : 9.$$

The system was equilibrated at ~ 300 K for at least 300 ps with harmonic restraints applied on the Na+, Cl- solutes, before running.

NTP: 300 K, 1 atm.

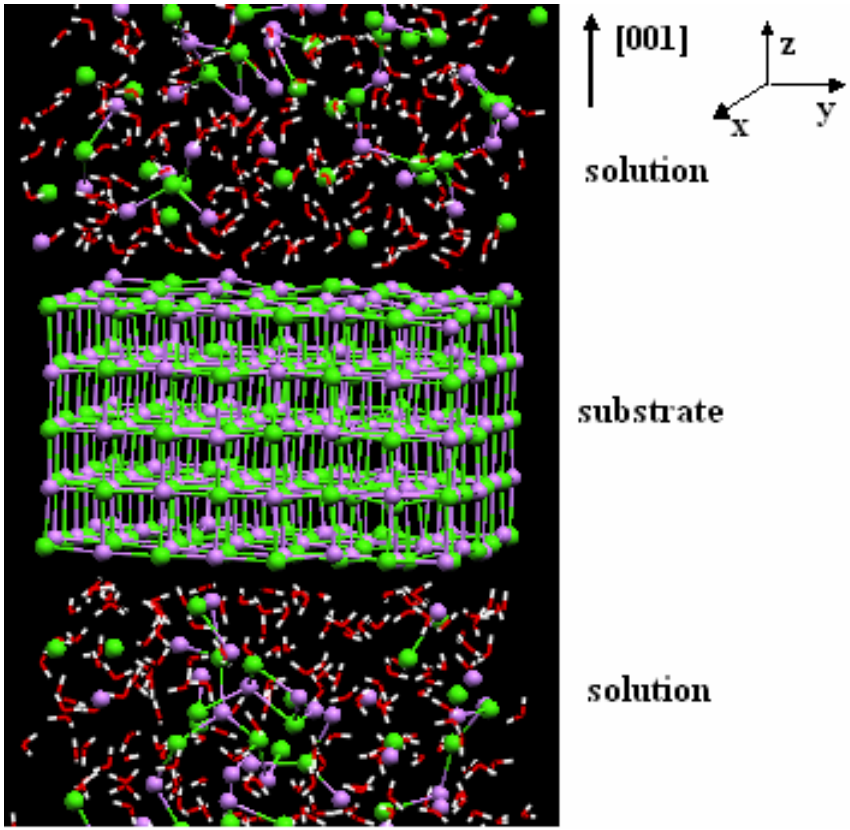

Na^+ Cl^- H_2O

Critical size

$$\Delta G(n) = n\Delta\mu + \gamma A$$

Bulk term

Surface term

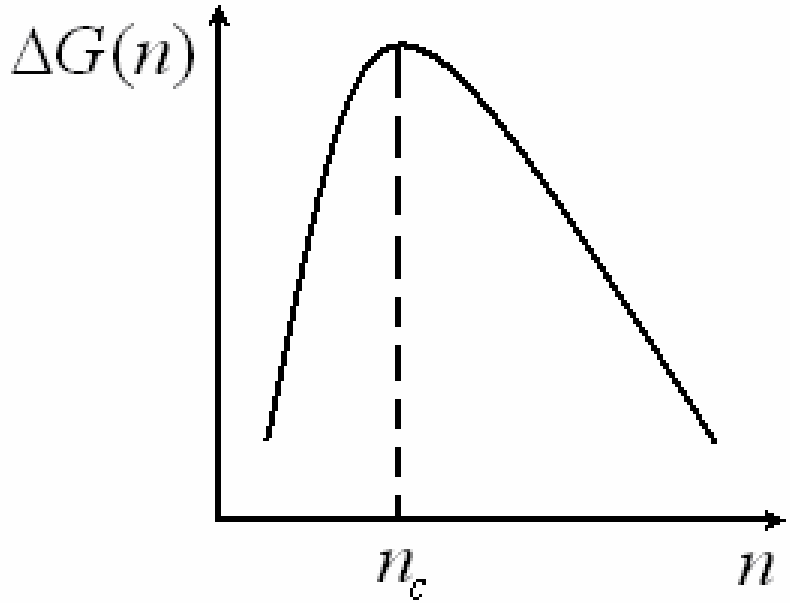

***N* > *n*$_c$,**

Island growth!

Critical size

By statistical analysis, the critical size is found to consist of two atoms: one Na^+ and one Cl^-.

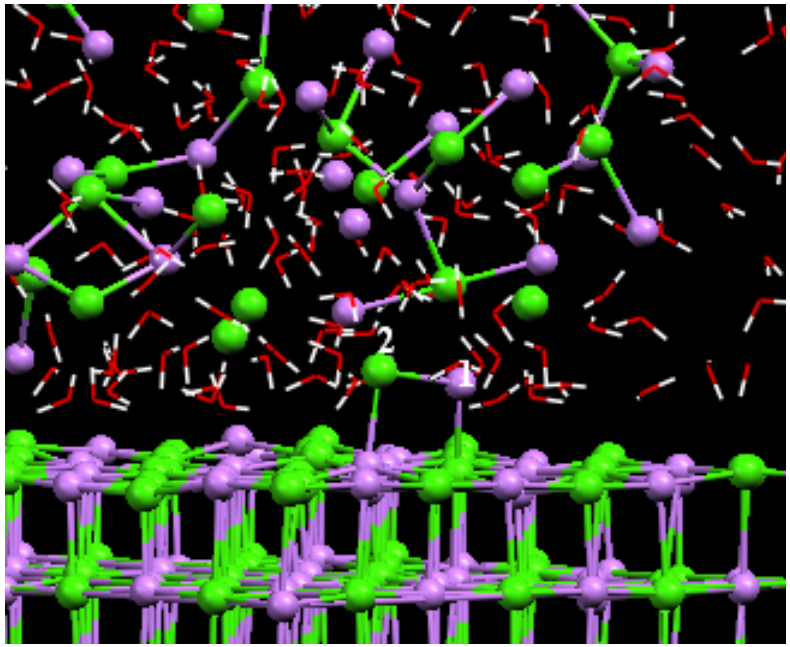

All the trajectories with different initial configurations and velocities were simulated for 1.2 ns

Growth modes

1. Frank-van der Merwe: Layer By Layer

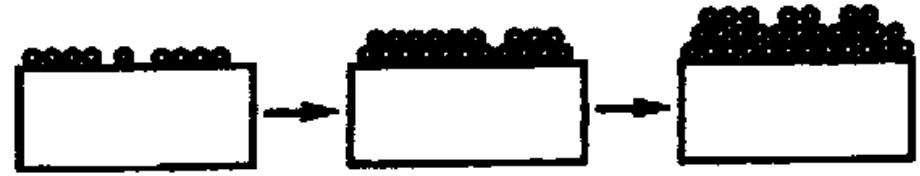

2. Volmer-Weber: 3D

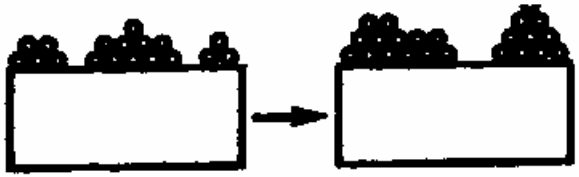

3. Stranski-Krastanovs

At the water-NaCl(001) interface, NaCl growth takes a 3D growth mode.

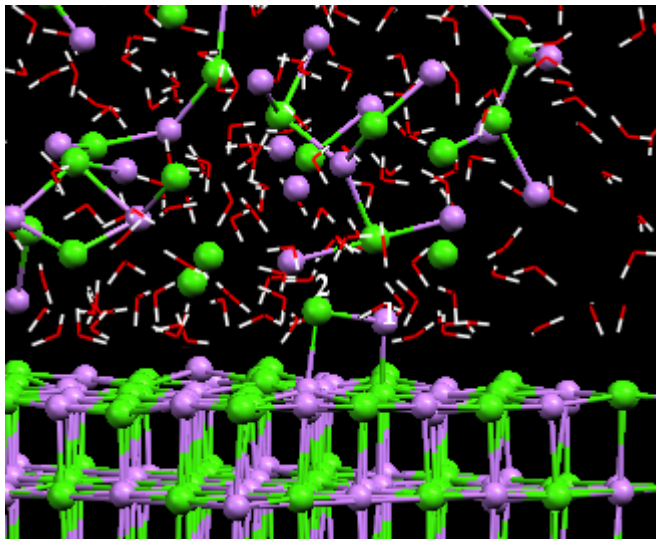

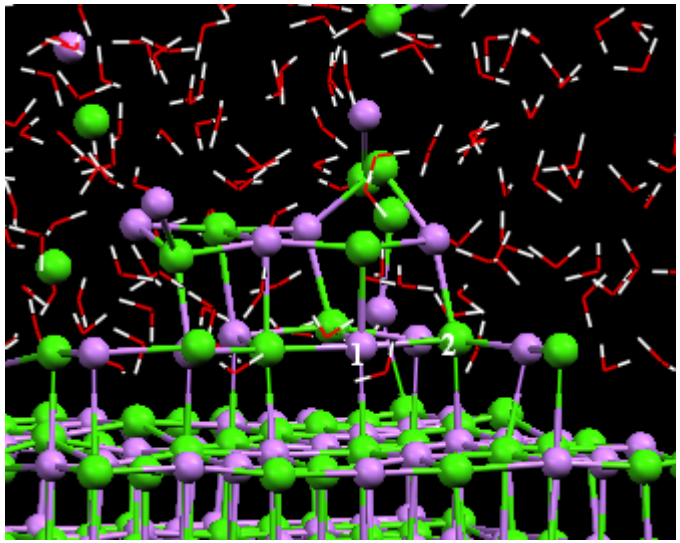

A positively-charged surface is found at early stage.

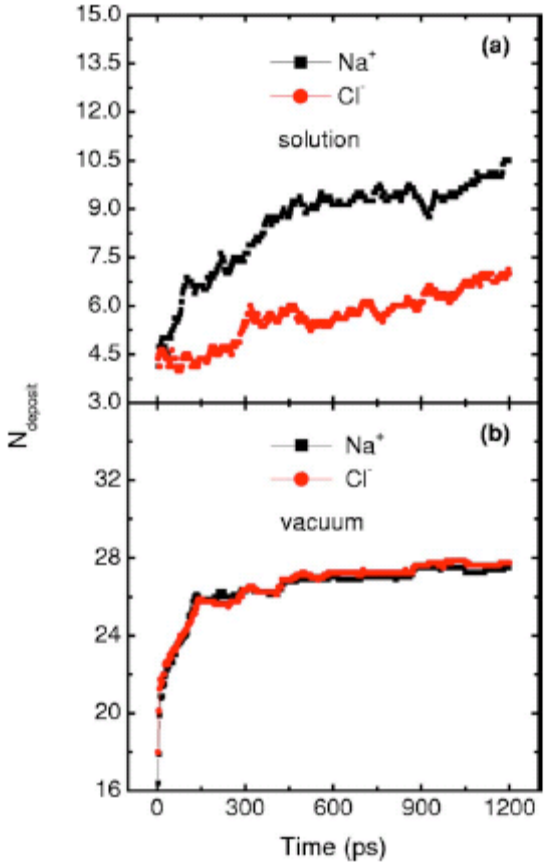

“New” driving force for nucleation !

Role of water

1. Why 3D growth at interface ? (2D growth in vacuum)

2. Why do Na^+ and Cl^- show different deposition rate?

A relative stable water network occurs at the interface !

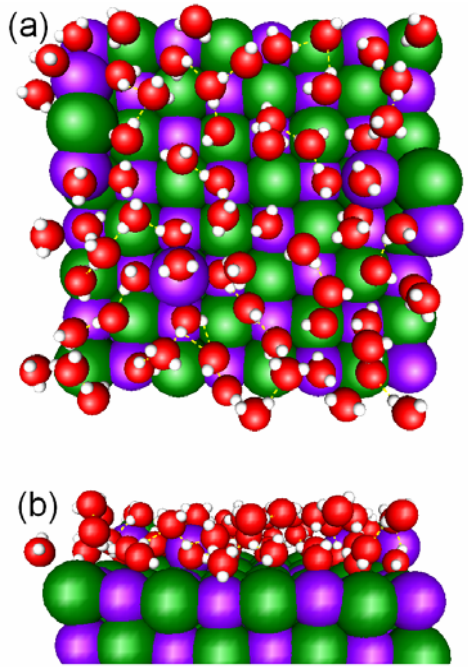

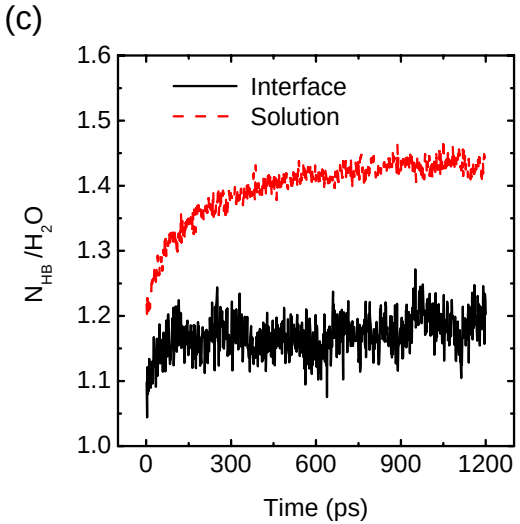

* Water network results in the surface charge.

$Na^+(aq) \longrightarrow H_2O$ — Cl^- (substrate) **Easy (H-Cl weak bond)**

$Cl^-(aq) \longrightarrow H_2O$ — Na^+ (substrate) **Hard (O-Na strong bond)**

Based on our *ab initio* calculation for water monomer on NaCl (001), we found the averaged resident time of the water molecules on the top sites of surface Na^+ is about 8.95 ps, while the averaged resident time of the ones on the top sites of surface Cl^- is about 4.12 ps.

Different deposition rate !

* Water network tunes the growth mode :

- Na^+ and Cl^- ions diffuse in surface plane.
- 3D growth at interface !
- Steps and defects in a crystal.

Summery

- The critical size of NaCl nucleation on NaCl (001) surface is a Na^+-Cl^- pair in the supersaturated salt solution.
- A stable water network is formed at interface.
- Due to the presence of the water network and the effect of the hydration force at the interface, the stable nuclei on NaCl surface contain more Na^+ ions than Cl^- ions, and the growth of the nuclei at the water-NaCl (001) interface takes a 3D islanding mode.
- The charged surface induces a new driving force to the nucleation.

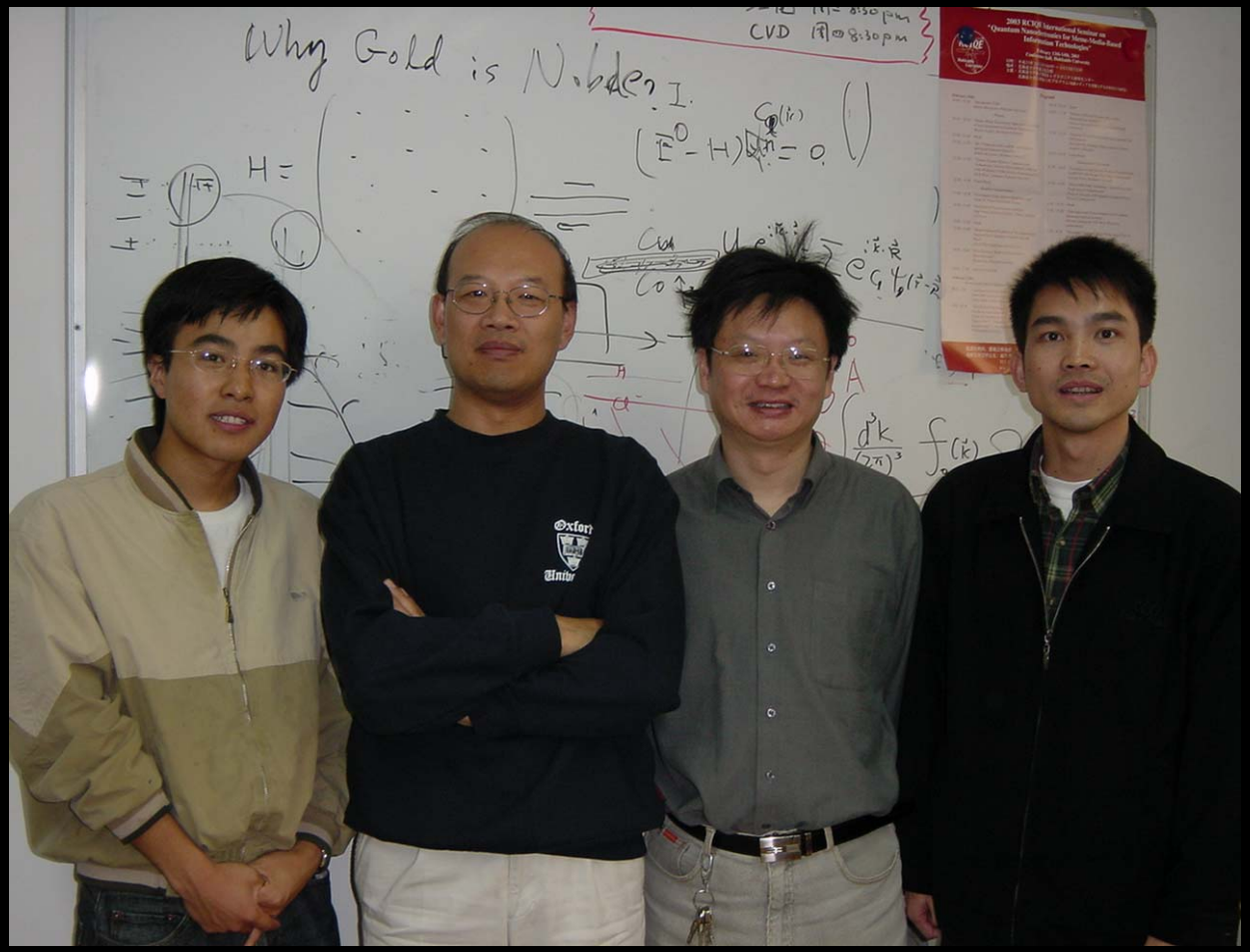

J. Chem. Phys. 119, 7617(2003)
Phys. Rev. Lett. 89, 176104(2002)
Phys. Rev. Lett. 91, 059602(2003)
Phys. Rev. Lett. 92, 146102(2004)

Shiwu Gao


Thank you !

Enge (E.G.) Wang's group in IOP/CAS, Beijing

(August, 2007)

Research in this group is focused on the study of the macroscopic property and microscopic behavior of surface-based nanostructures controlled by chemical and physical events. The approach is a combination of atomistic simulations and experiments. There are five staffs, E.G. Wang, Shuang Liu, Xuedong Bai, Wenlong Wang, and Wengang Lu. The areas of current interest include:

1) Novel formation and decay mechanism of nanostructures on surface;

2) Water in a confined condition, such as on surface, between interfaces, inside nanotube;

3) Covalently bonded light-element nanomaterials, such as the development of nanocones, polymerized carbon-nitrogen nanobells, aligned nanohelices and single-walled boron-carbon-nitrogen nanotubes.

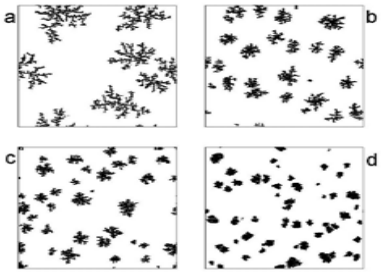

Surfactant-Mediated Epitaxy
Phys. Rev. Lett. (1999)
Phys. Rev. Lett. (2004)

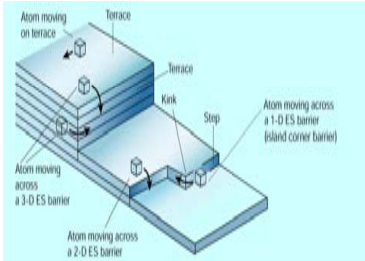

ES Barrier Controlled Growth
Phys. Rev. Lett. (2001)
Phys. Rev. Lett. (2002)
Science (2004)

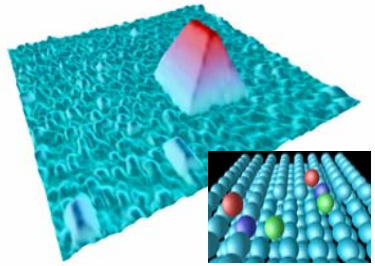

Adatom Upward Diffusion
Phys. Rev. Lett. (2003)
Phys. Rev. Lett. (2004)

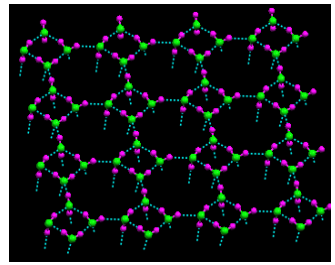

Ice Tessellation
Phys. Rev. Lett. (2004)
Phys. Rev. B (2005)

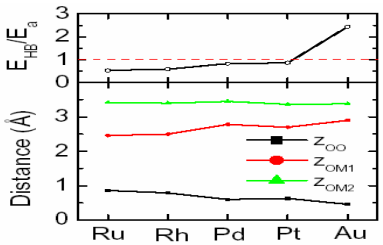

Hydrophilicity
J. Chem. Phys. (2003)
Phys. Rev. B (2004)
Phys. Rev. Lett. (2002)

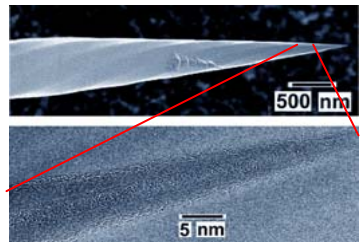

Nanocones
Science (2003)
Science (2004)
JACS (2006)

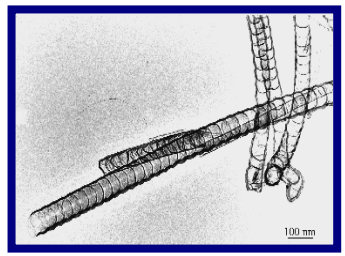

Nanobells
Appl. Phys. Lett. (1999)
Appl. Phys. Lett. (2000)
Appl. Phys. Lett. (2001)

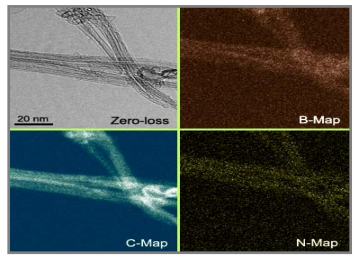

BCN SWNT
JACS (2006)
JACS (2007)

吴克辉 (Tohoku)

吴　静 (Maryland)

马旭村 (MPG)

郭建东(ORNL)

钟定永(Muenster)

李茂枝(Ames Lab)

张广宇 (Stanford)

支春义 (NIMS)

历建龙 (UT Austin)

肖文德 (EMPA)

许　智 (IoP)

朱文光 (Harvard)

张立新 (NREL)

孟　胜 (Harvard)

杨建君 (Saskatchewan)

于迎辉 (NIMS)

杨　勇 (Tohoku)

郑客飞 (Parma)

郭东辉 (Hokkaido)

江　颖 (UC Irvine)